Application of a Hydrological Model for Predicting River Ice Breakup

by

Genevieve Brown

A thesis
presented to the University of Waterloo
in fulfillment of the
thesis requirement for the degree of
Master of Applied Science
in
Civil Engineering (Water)

Waterloo, Ontario, Canada, 2019

AUTHOR'S DECLARATION

I hereby declare that I am the sole author of this thesis. This is a true copy of the thesis, including any required final revisions, as accepted by my examiners.

I understand that my thesis may be made electronically available to the public.

Abstract

In cold regions, the breakup of river ice can be a significant event, resulting in flooding and damage to communities. Given the severity of such events, it is desirable to be able to predict the timing and severity of breakup. Limited progress has been made on forecasting breakup as no deterministic model of the breakup process and ice jam formation exist. Current tools for predicting breakup rely on developing a relationship between the previous winter conditions and the current spring conditions, with the understanding that a large runoff with a thick ice cover has the potential for a more severe breakup than if ice has had time to melt. These tools are largely empirical, statistical, or soft computing methods which rely on historical data sets of discrete observations to relate the complex relationship between climate and hydrology to breakup conditions and are limited by access to the extensive data required.

Within the current prediction methods, the application of hydrological models for predicting breakup is limited. Hydrological models can address some of the limitations of current tools, as they are able to simulate the relationship between climate and hydrology which has a strong influence on the breakup period. Additionally, hydrological models may be more practical in regions with limited data, as they can simulate variables of interest instead of relying on historical data.

This thesis demonstrates how a hydrological model can be used to predict breakup, through the coupling of a 1D river ice model with a hydrological model. Emphasis is placed on the development of the hydrological model to ensure that it provides realistic results throughout the basin.

The Liard basin, a large river basin, in northern Canada is used as a case study. A thorough calibration strategy, based on an iterative, multi-objective approach is used in the development of the model. The final model exhibits strong performance in both calibration and validation throughout the basin. A simple 1D river ice model is coupled with the hydrological model.

The hydrological model can forecast the timing of breakup well based on the timing of the initial rise in the hydrograph. Breakup severity is predicted using a simple threshold model based on ice thickness, flow, and accumulated shortwave radiation. The prediction method was applied to an independent location as verification of the methodology with promising results.

Acknowledgements

I would first like to thank my supervisor, Dr. James Craig, for his guidance and support over the course of my studies. I am grateful for all of the opportunities that he has been able to provide to further my work.

I would also like to thank Anna Coles, Ryan Connon, and Shawne Kokelj from the Government of the Northwest Territories for their support and enthusiasm for the Liard basin model. I also wish to thank Jennifer Nafzinger from the Government of Alberta for providing guidance and expertise on the subject of river ice.

My graduate degree would not have been successful without the help and encouragement from all of my colleagues in Dr.Craig's and Dr.Tolson's research groups. As well, I need to thank all my friends in Waterloo, old and new, who have made a second degree in Waterloo so enjoyable. Finally, I need to thank my family for their continued love and support.

Table of Contents

List of Figures

List of Tables

Chapter 1
Introduction

1.1 Overview

The breakup of river ice is a significant event in cold regions which can cause flooding and damage to communities. In Canada, the formation of ice jams resulting from the breakup period have been recorded across the country. The stages associated with breakup and ice jam formation are often significantly higher than the stages associated with open water flow and can occur quite rapidly. Given the damage that the breakup of river ice can cause, it would be useful to be able to forecast both the timing and severity of the breakup period.

Current prediction tools are generally based on the concept that a more severe breakup will occur when there is high runoff with a thick or strong ice cover than if the ice cover has had time to gradually melt. The tools rely on correlating discrete observations that describe the antecedent winter conditions and current spring conditions with breakup severity. As a result, they tend to rely on large historical data sets and tend to be site specific. In general, there is low confidence in the predictive abilities of current tools due to high false positive rates or unreported prediction rates.

Hydrological models are a common tool used to forecast open water flooding but have had limited application to predicting flooding during breakup. Hydrological models may be able to address some of the limitations of current tools as they can simulate the complex relationship between climate and hydrology which influences the breakup period. Additionally, they may be more practical in a setting where limited observation data exists as the variables of interest are simulated. A hydrological model used for the purpose of predicting breakup may require additional calibration objectives beyond matching streamflow to ensure it is fit for its purpose.

This thesis demonstrates how a hydrological model could be used to predict river ice breakup through the coupling of a 1D river ice model with a hydrological model. Emphasis is placed on the development and calibration of the hydrological model and the applicability of the model and prediction process to regions with limited data. The Liard basin, a large river basin in northern Canada, is used as a case study.

1.2 Objectives

The primary objective of this thesis is to demonstrate how a hydrological model can be used to predict river ice breakup This will require a 1D river ice model to be coupled with a hydrological model to determine:

- Timing of freeze up
- Ice growth and decay
- Breakup timing and severity

The development of the model will focus on being applicable to data sparse regions in Canada.

The secondary objective of the thesis is the development of a robust hydrological model of the Liard River basin in northern Canada. In addition to acting as a platform for the development of the river ice model, the model is also motivated by the need for a flood forecasting model for the Government of the Northwest Territories in the Liard basin. Beyond this thesis, the model will also be used to test improved conceptual models of wetland systems, taking into consideration permafrost thaw. Therefore, development of the model will focus on producing results which are valid and realistic.

1.3 Thesis Organization

The thesis is organized into several chapters, with the first chapter providing the introduction. The subsequent chapters are as follows:

Chapter 2 – Background

Chapter 2 provides a general overview of river ice processes and current methods used in predicting breakup. This is followed by an introduction to hydrological models and the motivation behind using hydrological models to forecast river ice breakup. Finally, an overview of the Liard basin is given.

Chapter 3 – Methods

Chapter 3 describes the river ice model to be coupled with the hydrological model. This includes determining freeze up timing and simulating thermal ice growth and decay. This is followed by a description of the methodology for determining breakup timing and severity. Data sources used to validate the river ice processes are summarized.

Chapter 4 – Hydrological Model Development

Chapter 4 describes the development of the Liard basin model including data sources, model discretization, model structure, and calibration procedure. This is followed by a discussion on the results of the hydrological model and a comparison to existing models of the same basin. The focus of results in this chapter is on the hydrological model function without the river ice processes.

Chapter 5 – Results and Discussion

Chapter 5 provides the results of integrating a river ice model into the Liard hydrological model for forecasting breakup. Specific results related to freeze up timing, thermal ice growth and decay, and breakup timing and severity are discussed. An independent case study is introduced and tested in this chapter.

Chapter 6 – Conclusions

Chapter 6 summarizes the research and provides future directions for this research.

Chapter 2
Background

In order to understand the motivation and the need to forecast river ice breakup with the help of hydrological models, it is necessary to have a basic understanding of both river ice and hydrological processes and models. The following section describes basic river ice processes from initiation of ice cover to breakup and formation of ice jams. An overview of current river ice breakup prediction tools and their limitations is discussed. This is followed by a discussion of hydrological models, their current applications to river ice problems and how they could be applied to breakup prediction. Finally, the Liard basin, used here as a case study, and its characteristics are introduced.

2.1 River Ice

2.1.1 Ice Formation

Formation of river ice is first initiated when water temperature is at or below 0°C. The rate of cooling in the river is a function of the net energy flux:

$$Q_{Net} = Q_{SW} + Q_{LW} + Q_H + Q_{LE} + Q_G$$

where Q_{Net} is the net energy flux [MJ/m^2/d], Q_{SW} is the net shortwave radiation flux, Q_{LW} is the net longwave radiation flux, Q_H is the sensible heat flux, Q_{LE} is the latent heat flux and Q_G is heat inputs from groundwater inflows and the river bed. Unlike lakes, where thermal gradients can exist, the turbulent flow within a river ensures that the water column temperature is generally well mixed.

A stable ice cover will first form as border ice in calm, slow flowing areas along the edge of a river. Within the main channel, super cooling of turbulent water will result in the formation of small ice particles, about 1-5 mm in diameter, known as frazil ice. The continued generation of frazil ice will eventually cause frazil to aggregate into larger floes and pans. In areas where the river constricts, the floes and pans will reach a concentration that results in the formation of a stationary ice cover. Incoming ice floes and pans will accumulate on the upstream edge allowing freeze up to continue upstream. The accumulated ice cover may go through a process where it collapses, thickens, and shortens depending on the mechanical strength of the ice cover, which can result in accumulated thicknesses of several meters (She, Hicks, & Andrishak, 2012).

2.1.2 Ice Growth and Decay

Once a consolidated ice cover has formed, ice will grow or recede as a function of the balance of heat fluxes at the air-ice interface and at the ice-water interface.

At the air-ice interface, the energy flux is controlled by the surface energy balance. The presence of snow over the ice can create an insulating layer due to its reduced thermal conductivity when compared to ice. The weight of snow can also cause the ice and snow layers to submerge below the water surface resulting in the formation of slush and "white-ice" on top of the ice layer (Ashton, 2011).

Within the ice, the heat flux is controlled by 1D heat conduction; an energy balance leads to the following governing equation for temperature in the ice:

$$\rho_i c_i \frac{\partial T_i}{\partial t} = \frac{\partial}{\partial z}\left(k_i \frac{\partial T_i}{\partial z} + \varphi\right)$$

where T_i is the temperature of the ice [°C], ρ_i is the density of the ice [kg/m^3], c_i is the specific heat capacity of the ice [J/°C], k_i is the thermal conductivity of the ice [W/m/°C], and ϕ is an internal heat source [W/m^2]. The internal heat source is typically caused by shortwave radiation transmission into the ice and snow layers. Unlike longwave radiation in which absorption occurs in a thin layer at the surface, shortwave radiation can be transmitted within the ice and snow layers, causing internal warming and melt. This internal melt is important during the breakup period, as it decreases the internal strength of the ice, potentially advancing the onset of breakup (Prowse, Chew, & Demuth, 1990).

At the bottom of the ice, the energy flux is based on convective heat exchange with the river. The convective heat exchange is thought to be considerable in the decay of ice in the spring due to the rise in water temperature (Prowse & Marsh, 1989).

Beyond thermal growth and decay, other ice processes can occur throughout the winter depending on the river size and type, climate, and hydrological regime, resulting in a highly variable ice cover. For example, frazil ice can continue to accumulate on the underside of a surface ice cover causing the formation of hanging dams. Anchor ice, in which a mass of ice develops on a fixed object in the river, can also occur. Aufeis, a process in which water is forced

to the ice surface through cracks, can cause ice to accumulate to significant thicknesses of many meters (Turcotte & Morse, 2013).

2.1.3 Breakup

The breakup of ice cover can be generally classified into two types: thermal breakup and mechanical breakup. Thermal breakup is a result of increased heat transfer in spring causing river ice to essentially melt in place. During thermal breakup, the ice cover can decay from the surface due to atmospheric heat fluxes and at the bottom due to heat flux from the water. The atmospheric heat flux tends to dominate the decay process, although water temperatures close to 0°C can still result in a considerable heat flux. In some cases, the heat flux from the water has been recorded to be up to 40% of the atmospheric heat flux, i.e. about 30% of the total incoming melt energy (Prowse & Marsh, 1989).

Mechanical breakup is caused by an increase in streamflow which can occur due to a mid-winter melt event or spring freshet. Before the ice can fully melt due to energy inputs, the increased flow results in the formation of longitudinal and transverse cracks within the ice cover, reducing the ice cover to a series of ice sheets (Beltaos, 1990). The ice blocks and slabs are then transported downstream by the current. Mechanical breakup carries greater risk as it can lead to the formation of ice jams and flooding (Beltaos, 2003).

Breakup can be thought of as the combined result of “driving” and “resisting” factors (Beltaos, 2008; Turcotte & Morse, 2015). Driving factors are those which “drive” the breakup of ice like increased hydrodynamic forces where as resisting factors “resist” breakup like the strength of the ice cover. The direct driving and resisting factors are a result of many indirect factors, which are primarily controlled by the climate, hydrology, and physical characteristics of a watershed. For example, shear forces (driving forces) are a function of river discharge which in turn is influenced by the winter snowpack, rain, the heat flux controlling snowmelt, and watershed properties like contributing area and gradient. Resisting factors, like the ice cover strength, is influenced by winter weather conditions, the timing of freeze up in the fall and the spring energy flux.

As with other ice processes, there can be variability in breakup timing and magnitude along a single river due to differences in climate and channel morphology. Breakup does not necessarily

proceed in a linear fashion from the headwaters to the outlet but can be staggered with breakup of downstream reaches occurring prior to breakup of upstream reaches (Jasek, 2003).

2.1.4 Ice Jam Formation

Ice jams, initiated by the mechanical breakup of a river, can form if the conveyance of ice sheets and blocks within the river is impeded. This typically occurs due to morphological transitions or structures within the river, like sharp bends, narrow reaches, or bridges.

Once a jam forms, the jam will evolve depending on several factors including flow, and channel and ice properties. A surface jam, in which a single layer of ice floes forms on the water surface, can occur at low velocities (Beltaos, 1995). The externally applied forces (e.g. friction force between the ice and riverbank, drag on ice cover by flowing water etc.) and inter-floe forces caused by the accumulation of floes will increase until the jam collapses or reconfigures. A thickened jam occurs as a result of this collapsing and reconfiguration. Jams can also evolve into hanging dams when slow flow allows for a large level of deposition underneath the jam. Finally, jams can become "grounded" when the thickness of the jam completely blocks the river depth, resulting in flow only moving through internal voids within the jam.

2.1.5 Flooding

The formation of an ice jam can cause significant flooding and damage to communities and infrastructure. Ice jam flooding has been recorded throughout Canada, from the Northwest Territories (Prowse, 1988; Stanley & Gerard, 1992; Watson, Hicks, & Andrishak, 2009) to New Brunswick (Beltaos & Burrell, 2002; Hicks, McKay, & Shabayek, 1997; Tang & Beltaos, 2008). The damage which results from ice jam flooding can be quite severe due to physical impacts from the ice and the increased river stages.

Flooding from ice jams can be the result of the backup of water behind a jam or from the jam releasing suddenly, causing a flood wave to propagate downstream. In some cases, like in the Peace-Athabasca delta, flooding occurs as a combined result of the two processes, with surges from upstream jams triggering downstream breakup and subsequent jams (Beltaos, Prowse, & Carter, 2006).

The presence of an ice jam can cause the upstream river stage to increase significantly when compared to similar flows under open water conditions. For example, Prowse (1988) studied

jams at the confluence of the Liard and Mackenzie rivers in the Northwest Territories from 1978 to 1984 and concluded that the river stages upstream of a jam were approximately 4 to 8 m above those which would result from a similar discharge under open water conditions. The significant increase in river stage behind the jam is caused by the increased hydraulic resistance from the roughness of the underside of the jam and a decrease in cross-sectional area available for flow due to the submerged thickness of the jam. To be able to pass the incoming flow against the increased resistance, the upstream river stage increases substantially.

Flooding can also occur through the release of an ice jam, creating a wave which moves downstream. These dynamic waves are also commonly called surges or "javes". The waves move at high velocities (often greater than 5 m/s) and can cause a rapid rise in water levels downstream (Beltaos, 1990; Beltaos & Krishnappan, 1982; Jasek, 2003). For instance, Hutchison and Hicks (2007) recorded a rise of 4 m in 15 minutes on the Athabasca River upstream of Fort McMurray.

If there is no ice cover downstream of the ice jam when it releases it is considered an unimpeded ice run (Jasek, 2003). Unimpeded ice runs often occur at a sharp bend or constriction in the river. In these cases, the river has broken up in a "non-sequential" manner, with any ice that existed downstream having melted or moved further downstream prior to the formation and release of the jam. If there is an intact ice cover downstream the ice run is considered impeded. The release of these ice jams is typically caused by a combination of the weakening downstream ice cover and increased downstream forces (i.e. increased discharge).

2.2 Forecasting

Forecasting plays an important role in the overall preparation for flood events. By providing warning of future events, the government and public can take measures to reduce damages and impacts. Under open water conditions, it is common for forecasts to rely on hydrological models which predict streamflows given the watershed's properties, weather forecasts, and upstream flow measurements. An effective model should be able to accurately predict both the flow and timing of flood events with model outputs being used to inform decision making. An awareness of the associated uncertainty of the model forecast can help further understand flood risk (Toth et al., 2000).

In comparison to the significant research and development related to forecasting open water flooding (Beven et al., 1984; Campolo et al., 1999; Cloke & Pappenberger, 2009; Nash & Sutcliffe, 1970; Toth et al., 2000), limited progress has been made on forecasting floods related to river ice breakup. In practice, forecasting jurisdictions rely heavily on the past experience and knowledge of breakup and ice jams within a watershed and real time observations of ice conditions and river gauges (Beaton et al., 2017; Beltaos et al., 2012; Lindsey & Johnson, 2017). Given the severity of flooding and the short time scale at which events can occur, it would be useful to have an accurate and reliable forecasting model to help inform flood preparedness.

To date, forecasting tools related to breakup and ice jams have focused on two different objectives. The first group of tools attempts to forecast if a jam will occur during breakup or provide a qualitative risk of flooding likely associated with that seasons' breakup. The second group of tools are based on forecasting the flooding that occurs once a jam has formed. As described in Section 2.1, flooding from ice jams either occurs from the back up of water behind the jam, from a released surge, or a combination of the two. Available forecasting tools have primarily focused on predicting the future river stage behind an ice jam (Beltaos et al., 2012; Brayall & Hicks, 2012; De Coste et al., 2017; She & Hicks, 2006; Stanley & Gerard, 1992; Warren et al., 2017). While progress has been made in simulating the flood wave from a jam release, these models have not yet been applied to in forecasting mode (Beltaos & Krishnappan, 1982; Blackburn & Hicks, 2003; Hicks et al., 1997; She & Hicks, 2006). These types of models are generally based on detailed understanding of river hydraulics and ice dynamics and mechanics. They require significant data, including detailed bathymetric data, ice thickness data, and surveyed jam profiles. Given how quickly flooding can occur from ice jams and the lack of this data in practice, these tools provide less advance warning than the tools used to forecast breakup and subsequent flood severity. The following section will focus primarily on the former group, tools used to forecast breakup severity and the formation of ice jams.

2.2.1 Current Prediction Tools

Forecasting the timing and severity of river ice breakup is useful for being able to predict the likelihood of ice jam formation and prepare for subsequent flooding. Prediction methods for ice jams and breakup are closely linked since there is no analytical model to describe the breakup process or the development of an ice jam. In many cases, the forecasting of breakup is

synonymous with forecasting ice jam flood risk due to the high annual frequency of ice jams at the rivers of interest once breakup has occurred (Mahabir, Hicks, & Fayek, 2006; Turcotte & Morse, 2015). A severe breakup corresponds to a higher likelihood of ice jam formation and subsequent flooding.

Forecasting approaches for breakup and ice jam flood risk rely heavily on empirical and statistical methods such as threshold models, regressions, and soft computing methods (e.g. fuzzy regression, neuro-fuzzy methods). These approaches generally are informed by variables that describe the antecedent winter conditions and spring thaw conditions with the understanding that high runoff when there is still a thick ice cover results in a higher risk of a severe breakup and ice jam formation than if the ice has had time to melt gradually.

Threshold models are based on correlating the severity and timing of breakup or flood risk with exceedances of river ice and watershed thresholds (Shaw et al., 2013; Shulyakovskii, 1963; Stanley & Gerard, 1992; Turcotte & Morse, 2015). These types of models are trained using historical data from the location of interest. The variables used as input to threshold models are those which provide an indication of the driving and resisting forces. For example, a threshold-based forecast of breakup timing and intensity on the Montmorency River was based on discharge, 24 hour rain, 24 hour air temperature, cumulative freezing degree days, and cumulative thaw degree days (Turcotte & Morse, 2015). Generally, models are applied simply by the determined threshold value or some combination of values has been exceeded. In the case of Wuebben & Gagnon (1995), variables with a high correlation to ice jamming were given a corresponding positive value whereas those with low correlation were given negative values. The overall sum of the values indicated the ice jam flood potential, with values greater than one indicating a higher risk for ice jam potential. Threshold models are attractive for forecasting since they are easy to use and typically rely on readily attainable data for the watershed of interest. However, these models tend to be extremely site specific as the thresholds only apply to the site where they were developed. Beltaos (2008) attempted to reduce the site specific issue through the use of a more conceptually based model. However, this model required inputs like channel curvature which may not be easily attainable. Threshold models also require adequate historical data to determine the threshold criteria. Some models also explicitly incorporate the julian date and therefore are only specific to spring breakup and cannot forecast mid-winter

events (Shaw et al., 2013). Additionally, given the somewhat arbitrary selection of variables, some models can produce results with no statistically significance difference between threshold values that forecasted jam and no jam conditions (White, 2003).

Regression models are based on predicting a variable or outcome based on a combination of variables. Similar to threshold models, input variables used in the regressions are indicators of the severity of winter and spring melt. Regression models can address some of the subjective and site specific methodology used in the development of threshold models since the development of a regression requires significant model variables. Mahabir, Hicks, Robichaud, and Fayek (2006) developed a multiple linear regression model to forecast breakup water levels in Fort McMurray, Alberta. Timing of breakup was not considered since an analysis of breakup at Fort McMurray indicated that 75% of breakup happens within a week of the historical mean breakup date. The regression was based on an extensive database which provide indications of winter severity, fall antecedent conditions, and spring severity, with multiple combinations of variables being able to model the maximum water level at spring breakup. Linear regressions are appropriate for modelling a continuous variable but can not be applied to a binary outcome. To be able to predict the formation of an ice jam (a binary outcome), logistic regressions can be used. White (1996) used a logistic regression to predict the formation of ice jams based on the date of maximum accumulated freezing degree days and stage. The model tended to overpredict the formation of ice jams and could not provide an estimate of the timing of ice jams. Additionally, basing the regression on a fixed date or assuming a known breakup date limits the transferability of a model and neglects the influence of climate change on river ice processes. Regression models can limit the arbitrary selection of input variables; however, they still are highly site dependent and require a long historical data record to be able to develop effective forecasting models.

Soft computing methods such as artificial neural networks, fuzzy systems, and neuro-fuzzy systems have also been applied to the forecasting of breakup severity and ice jams (Mahabir et al., 2002, 2007; Mahabir et al., 2006; Massie et al., 2002). These models have been applied as they help overcome the uncertainty around the unknown and complex non-linear relationship seen between input variables and the output (breakup or ice jam occurrence). Additionally, they allow for the incorporation of more qualitative concepts, e.g. a thick winter ice cover can

increase the risk of ice jams in the spring. A number of models have been applied to single sites with preliminary results showing reasonable results (Mahabir et al., 2002; Mahabir et al., 2006; Massie et al., 2002). An attempt to transfer a neuro-fuzzy model between two different locations was made by Mahabir et al. (2007) to show that models could be extended to regions where there is less data to support other forecasting models. However, the transferred model performance was worse than that of the original location, with false predictions occurring 50% of the time, indicating that the physical factors and calibration may still be too site specific to allow for general application to numerous sites.

Some models have focused only on predicting the timing of breakup through the use of water temperature models (Greene, 1983; Morales-Marin et al., 2019) or ice thickness models (Ma et al., 2001). These models assume that breakup occurs once the stream temperature reaches 0ºC or once an ice cover completely melts. Although these models can generally predict breakup within 10 days, they can not predict the severity of breakup or differentiate between mechanical and thermal breakup. The use of these models and their coupling with hydrological models is further discussed in Section 2.3.2.

2.2.2 Limitations of Current Tools

Although progress is being made on providing tools to help forecast breakup and ice jam severity there are some limitations to these models from a practical forecasting perspective. Given that there are no deterministic models of breakup and ice jam formation, these models rely heavily on empirical and statistical models. Current prediction tools tend to be site specific and have data requirements outside of what may be available in a practical setting. The variables utilized in the tools vary by site and can be arbitrarily since no deterministic model of breakup exists. Finally, current tools typically have high incidences of false positive predictions, where a prediction of an ice jam or severe breakup is made but does not actually occur.

Most empirical models which have been developed have only been applied to one specific site with the exception of the neuro-fuzzy model developed by Mahabir et al. (2007). By including variables like downstream lake levels (Wuebben & Gagnon, 1995) or the timing of breakup period (Galbraith, 1981), the models are inevitably site specific with no opportunity for transferability to other sites. Even if threshold and regression models use variables which are widely available across many sites, the site specific threshold values and linear constants must be

obtained. Additionally, the fact that variables are sometimes arbitrarily selected means than the same combination of variables may not provide significant results at other sites. A practical forecasting tool would be able to be transferrable to different sites even if only limited data exists.

The development of tools and models for forecasting have focused on a few key locations in Canada which have been the focus of many studies due to the severe and often frequent jams. These study locations include: the Saint John River in New Brunswick (Beltaos et al., 2012; Blackburn & Hicks, 2003; She & Hicks, 2006; Tang & Beltaos, 2008) the Athabasca River at Fort McMurray, Alberta (Beltaos & Krishnappan, 1982; Mahabir et al., 2002; Mahabir et al., 2006; She & Hicks, 2006) and the Hay River at Hay River, Northwest Territories (Brayall & Hicks, 2012; De Coste et al., 2017; Stanley & Gerard, 1992). The focus of literature in these locations has allowed for significant data collection and progress in the study of ice jams but as a consequence has led to the development of forecasting tools which rely on this level of available data. For example, the database used to construct the regression model by Mahabir et al. (2006) was based on a database of over 106 different variables starting in 1875. Much of Canada, especially in the northern regions which are prone to ice jams, have sparse hydrological and meteorological data networks to rely on. This data can be supplemented with ice observations in the winter but the level of detail of this information may vary, depending on the jurisdiction. In some cases, regions may not even have a record of which years ice jam floods have occurred let alone information on the timing or severity. In a practical forecasting situation, it is important that variables used in forecasting are those that are only easily measured, estimated or forecasted (White, 2003).

There is the general understanding that a measure of the winter severity and subsequent spring melt are good indicators of the severity of breakup. Identifying the appropriate indicators is often arbitrary as there are a large number of individual variables which can be used. For example spring severity can be indicated through degree days of thaw, solar radiation, linear heat flux, or surface water pre-breakup and breakup levels or combinations thereof (Mahabir et al., 2006). By selecting arbitrary variables to inform threshold and regression models, the transferability of the model between sites is limited and results will not be significantly different (White, 2003). The

use of stepwise selection of statistically significant variables has been suggested as an improvement over arbitrary selection (White & Daly, 2002).

Predictive ice breakup models tend to show results of high false positive predictions (White, 2003). In operation, some of the tools have been noted as being no better than an expert's educated guess.. Some models do not attempt to quantity the uncertainty or prediction error leading to low confidence in their application in a forecasting situation. In a practical forecasting situation, an understanding of the uncertainty in prediction is desirable to better inform decisions.

Ultimately, the forecasting of breakup timing and severity relies heavily on past experience and knowledge of breakup and ice jams within a watershed and real time observations of ice conditions and river gauges. It would be useful to have reliable, accurate, and practical forecasting tools that would aid decision making during this time. A practical tool would be transferrable between different locations, useful in regions with limited data, and provide an understanding of predictive capability, fueled by forecasted outputs from both climate models and hydrological models.

2.3 Hydrological Models

2.3.1 Overview of Hydrological Models

Hydrology helps describe the movement and distribution of fresh water around the earth's land surface including any exchanges with the atmosphere (Dingman, 2015). Hydrological models are built from numerical approximations of physical processes like snowmelt, evapotranspiration, and infiltration. They can be used to better understand a single process at the field scale, or simulation of an entire watershed. Models are employed for a wide variety of problems ranging from resource planning, reservoir management, to flood forecasting.

Given the range of applications which hydrological models can be used for, there is great variation in the type and structure of models. One key variation is in the spatial resolution of the model. The lowest level of resolution, lumped models, ignores any spatial variability within the basin and considers the entire basin as a single unit. Conversely, fully distributed models consider the spatial heterogeneity of inputs and parameters through dividing the basin into small elements, typically grid cells. Hydrological processes are simulated at the grid cell level with water routed between grid cells. Semi-distributed models can provide greater resolution than

simple lumped models but do not require the detailed complexity of distributed models. Semi-distributed models are based on dividing a basin into smaller subbasins in which water is routed between. The subbasins are then represented by a number of lumped regions, called HRUs, which have unique hydrological responses to forcing data (Kouwen et al., 1993; Wood et al., 1988).

Another means by which hydrological models differ is through the physical representation of hydrological processes. Model structure can range from empirical to physical representation of processes. Empirical models are defined by regressed relationships between inputs and outputs. These models tend to be black box models, in that they provide limited knowledge to the internal processes that control the outputs. Physical based models rely on representing hydrological processes through the conservation of mass, energy and momentum. Although these models can provide detailed spatial and temporal outputs, they can require a large number of parameters to run and can be computationally expensive. In between the simple empirical models and complex physical models are conceptual models. Conceptual models often provide simplified approximations of the physical processes. They are based on conservation of mass (water balance) and provide more insight into the hydrological processes than empirical models.

Calibration of hydrological models is the process in which model parameters are estimated to best represent the basin of interest, by matching observation data. Although some parameters may be able to be determined through measurement, many parameters represent unmeasurable characteristics of the basin. These parameters can be determined through manual calibration, where the modeler adjusts the parameters to best match observed data, and automatic calibration, in which algorithms are used to find parameters that provide optimized results. Validation is the testing of the calibrated model performance to independent data that was not used in calibration. Validation provides insight to ensure that the model can perform adequately for its intended purpose (Klemes, 1986).

One critique of hydrological models is that, from an operational perspective, streamflow is often the only outcome of interest. This can sometimes lead to the development of models which can match streamflow peaks well but does not provide a good representation of the entire hydrological system of a basin. These models can perform poorly under changing conditions and can be conflicting to the fundamental hydrological processes controlling a basin. The

development of more scientifically and operationally valid models is a major challenge in hydrological modelling (Fenicia et al., 2011; Kirchner, 2006). Through careful consideration of all components of a hydrological model from selection of robust and flexible model structures (Fenicia et al., 2011) to the calibration of a model to multiple data sources (Parajka & Blöschl, 2008) hydrological models can provide better insight and operational reliability in their application.

2.3.2 Coupled River Ice and Hydrological Models

Hydrological models can simulate the climatic and hydrological factors which influence river ice processes. However, to date, the coupling or integration of hydrological models with river ice models has been extremely limited. Typically the level of integration involves using the hydrograph outputs from hydrological models as inputs to river ice models. Beltaos et al. (2012) used flows forecasted by a hydrological model as input to a HEC-RAS model to predict ice jam flooding given that an ice jam had already formed. Daily flow values generated from the rainfall-runoff model HBV (Bergstrom & Forsman, 1973) have been used with 1D river ice model Mike-Ice (Theriault et al., 2010) to look at the impact of climate change on river ice on a regulated river (Timalsina et al., 2015). The hydrological model MESH (Pietroniro et al., 2007) and hydraulic river ice model RIVICE (Lindenschmidt, 2017) have been used concurrently to look at how reservoir operation can influence ice jam floods (Das et al., 2017; Rokaya et al., 2017, 2019). More recently, Morales-Marin et al. (2019) coupled MESH with a water temperature model for river systems to predict freeze up and breakup timing. The prediction of freeze up and breakup timing was solely based on a water temperature of 0ºC and did not consider other influences like ice thickness, or river flow.

The only integration of a river ice model with a hydrological model found in the literature was completed by Ma and Fukushima (2002). A 1D thermal river ice model was combined with a soil-vegetation-atmosphere-transfer (SVAT) model to model ice thickness over the winter. The model is based on calculating water temperature to determine the start of freeze up, defined by water temperature dropping below 0°C. Ice growth is determined through a simple accumulated degree day method whereas ice decay requires estimation of the heat flux between the water and ice. The timing of breakup was based on the complete decay of ice and does not consider any upstream hydrologic or hydraulic conditions. Although the estimated hydrographs and breakup

timing were reasonable, model results were only reported for a simulation period of one year, which does not allow for adequate model assessment.

By coupling a river ice model with a hydrological model, how the climatic and hydrological response of the watershed influence river ice can directly be considered. Hydrological models can also predict quantities of interest in areas where detailed historical data may be unavailable.

One of the limitations of hydrological models is that they are unable to model the hydraulic processes which can be an important variable in river ice processes. Therefore, certain processes like determining the exact location of an ice jam or the backwater effect from an ice jam could not be simulated in a hydrological model. However, the addition of hydraulics requires a significant increase in data requirements which would limit the usefulness of an integrated model in data spare regions.

2.3.3 Forecasting River Ice Breakup with Hydrological Models

Current prediction tools for breakup generally rely on correlating breakup timing and severity to discrete observations of variables which give an indication of the winter and spring severity. As a result, they require significant observation data to construct which is typically unavailable in many northern communities in Canada. They also tend to have arbitrary variable selection and be very site specific.

Hydrological models can address some of these limitations as they are able to simulate the complex relationships between climatic and hydrological factors which influence the winter and spring conditions that control breakup timing and severity. For example, a hydrological model with a river ice component would be able to simulate the continuous relationship between snow, ice, and temperature through winter and spring. Additionally, a hydrological model may be more practical in a setting where limited observation data is collected since the variables of interest are all simulated. To date, coupling of river ice models with hydrological models for this purpose has been extremely limited. The development and calibration of a hydrological model for ice forecasting may require objectives beyond matching streamflow as the realistic representation of different processes, like the accumulation and melting of snow, would be important to the forecast procedure.

This thesis demonstrates how a river ice model coupled with a hydrological model could be used to predict breakup timing and severity for a region with limited data. The development of the hydrological model focuses on a robust methodology to ensure that the model is fit for its purpose. The Liard basin, described in the following section, is used as a case study, for this objective.

2.4 Liard Basin

This research was initiated in part by the need for a flood forecasting model of the Liard basin for the Government of the Northwest Territories. The Liard basin has several communities which are at risk of ice affected and open water flooding. Breakup of the Liard River is an important event, since it triggers breakup on the Mackenzie River, the largest river in Canada. The following section provides an overview of the Liard River basin, its ice regime and flood risk. The model developed here of the Liard is intended to act as a test bed for this thesis but also for testing future models of wetland systems, permafrost thaw, and land use changes.

2.4.1 Overview

The Liard River, located in northern Canada, has a total drainage area of approximately 275,000 km^2. The Liard basin spans parts of the Yukon, Northwest Territories, British Columbia and Alberta as shown in Figure 2.1. It is the largest tributary to the Mackenzie River.

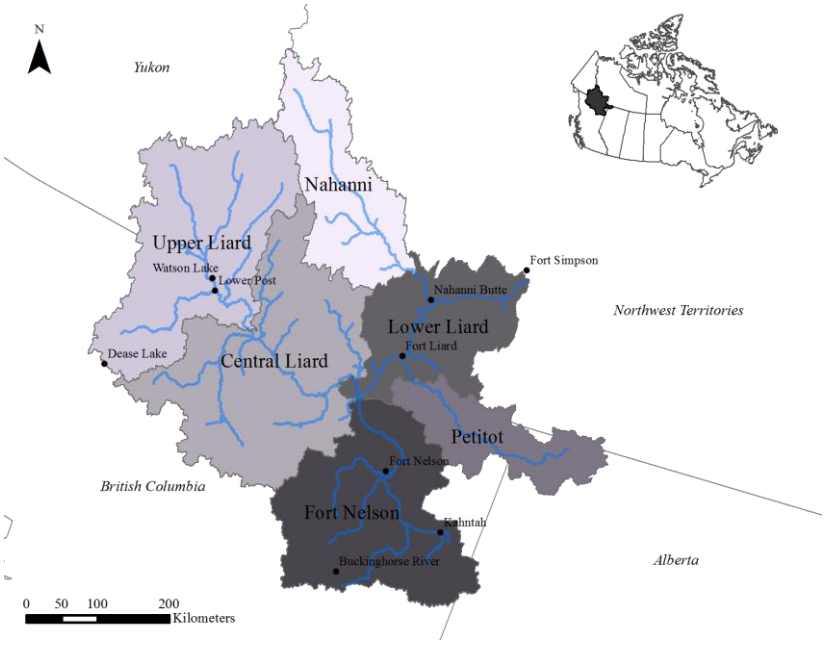

Figure 2.1:Overview of the Liard basin

The land cover within the basin is highly varied. The Nahanni region and upper and central Liard are characterized by the mountain ranges of the Northern Rocky Mountains, Columbia Mountains, and Mackenzie Mountains. The dominant vegetation in these regions is coniferous forest with high alpine tundra vegetation found at higher elevations. The Fort Nelson, Petitot and Lower Liard are more wetland dominated, with little topographic relief. This southern region is within the discontinuous permafrost belt. The combination of bogs, channel fens and permafrost plateaus within the region results in a unique hydrological response characterized by the hydraulic connectivity of the different landforms (Quinton et al., 2009). Elevation within the Liard basin ranges from 120 m at the outlet to almost 3000 m in the mountainous regions. Figure 2.2 shows the land cover and relief within the basin.

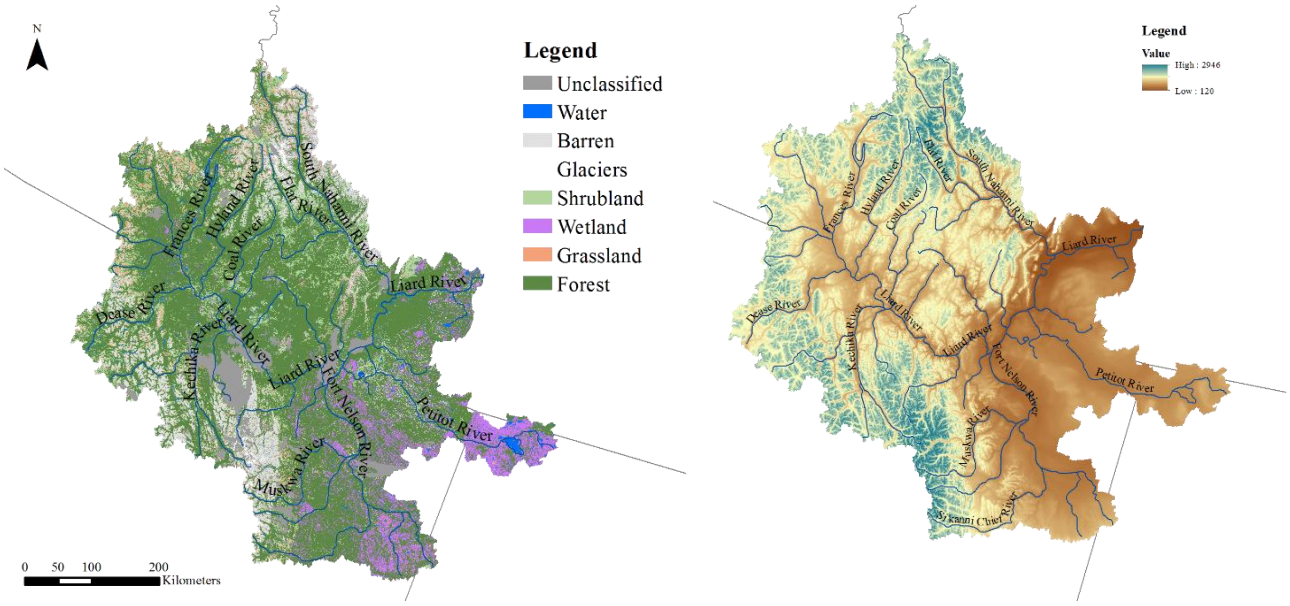

Figure 2.2: Land cover and topographic relief over the Liard basin

The Liard has a number of major tributaries including the Fort Nelson River, Dease River and South Nahanni River. There are no managed reservoirs within the basin and no large lakes.

For the entire basin, the average annual temperature is approximately -2°C varying from -0.6°C in the south to -4.3°C in the north. The annual precipitation from meteorological stations within the basin is approximately 490 mm, with approximately 60% of precipitation in the form of rainfall. Annual evapotranspiration for the basin is approximately 230 mm. Given the scale and physiographic differences of the basin, there can be significant variation in climate within the basin. For example, evapotranspiration ranges from close to 300 mm near Fort Simpson

(Quinton et al., 2004), where wetlands and surface water is abundant, to 150 mm in the south Nahanni range (Brook & Ford, 1980).

At the outlet of the Liard, the hydrograph is dominated by flows from the mountainous regions of the basin. The hydrograph typically begins to rise in April or May with the freshet from the mountains, and peaks in June. Flows then gradually decrease over the summer and fall months. The average annual flow at the outlet is approximately 2,500 cms. The annual peak is typically around 8,000 to 10,000 cms. Although most tributaries also have freshet dominated peaks, intense rainfall can result in late summer peaks larger than the freshet. A regime curve, describing the average monthly flow at the mouth of the Liard is shown in Figure 2.3.

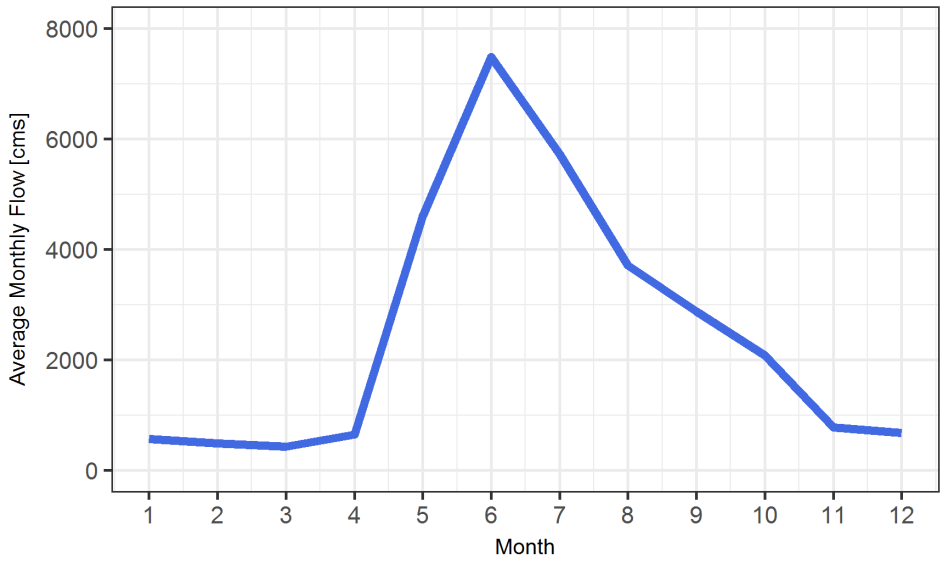

Figure 2.3: Average monthly flow of the Liard River near the mouth (10ED002)

Within the basin, there is significant variation in hydrological response due to the wide range of physiographic and climatic factors. Generally, the hydrology of the mountainous region is more well understood due to the dominance of the freshet. The hydrology of the wetland dominated portions of the basin is not as well understood, with many complicating factors such as thawing permafrost and hydraulic connectivity. Regions in the basin are also part of the Nahanni karst, a complex karst system where water moves through integrated conduits and multiple aquifers instead of a highly integrated groundwater system (Brook & Ford, 1980). Karst systems are known to have a unique hydrological response to rainfall and melt events.

2.4.2 Ice Regime

Within the Liard basin, breakup is typically initiated by the Fort Nelson river which flows north from British Columbia. The headwaters of the Fort Nelson are some of the more southern regions of the basin, in which snowmelt and the spring freshet occur first. After the confluence with the Fort Nelson river, breakup of the Liard progressively moves downstream towards the Mackenzie River. In the upper Liard, upstream of the Fort Nelson river, breakup can be sometimes be delayed by one week due to the higher latitudes and thus later freshet of these headwaters (Prowse, 1988).

Within the Liard basin, there is less available data related to river breakup and ice jams than in other northern rivers, for example the Athabasca River at Fort McMurray. This is likely a result of the basin size and remoteness. At the confluence of the Liard River and Mackenzie River, breakup has been known to occur both mechanically and thermally. However, over a period from 1978 to 1984, only two years exhibited larger thermal influences (Prowse, 1988). In all seven years, ice jams formed near the mouth with significant increases in stage due to ice jamming.

Breakup of the Liard River is a significant event, not only for communities within the basin, but for downstream communities on the Mackenzie River. Given that the Liard is the largest tributary to the Mackenzie River and its confluence is downstream from the stabilizing effects of Great Slave Lake, breakup on the Liard often initiates breakup of the Mackenzie River (Prowse, 1986).

2.4.3 Flood Risk within the Liard Basin

There are a number of small communities on the Liard River in British Columbia, the Yukon, and the Northwest Territories. In the Northwest Territories, Fort Liard, Nahanni Butte and Fort Simpson are all communities which have a history of open water and ice induced flooding. Figure 2.1 shows the location of these communities within the basin.

A comprehensive database recording flooding at these communities is unavailable. Table 2.1 summarizes historical flooding within the Liard basin based on available information from the Government of the Northwest Territories. This information was collected based on a variety of sources including books, historical archives, government reports, and news articles.

Table 2.1: Summary of Historical Flooding in the Liard basin

Location	Year	Description
Fort Liard	1896	Unknown
Fort Simpson	1918	Unknown
Fort Simpson	1963	Breakup related flooding caused by ice jams.
Fort Simpson	1972	Breakup related flooding. Unclear on formation and location of ice jams.
Fort Liard	1989	Breakup related flooding caused by ice jams.
Fort Simpson	1989	Breakup related flooding. Unclear on formation and location of ice jams.
Fort Liard	2010	Breakup related flooding. Unclear on formation and location of ice jams.
Nahanni Butte	2012	Flooding result of intense precipitation.

Given the history of breakup related flooding in the Liard it would be useful to be able to predict breakup related flooding. However, current prediction tools rely on data beyond what is available within the basin. A hydrological model of the Liard basin would be able to simulate variables of interest within the basin instead of relying on large historical data sets. Additionally, a hydrological model can address some of the limitations of current tools, as it could simulate the complex relationship between climate and hydrology.

This thesis demonstrates how a river ice model coupled with a hydrological model could be used to predict breakup timing and severity within the Liard basin. The development of the hydrological model focuses on a robust methodology to ensure that the model is fit for its purpose.

Chapter 3
Methods

The coupling of a river ice model with a hydrological model and subsequent prediction of breakup requires three components: predicting the timing of stable ice cover formation, simulating the thermal growth and decay of the ice after an ice cover has formed, and then using this information to inform a prediction on the timing and severity of breakup. The development of the different components requires river ice data or observations to validate and inform the model. This section starts by describing the limited sources of river ice data available in the Liard basin. This is followed by a description of the methodology behind the three model components and a discussion on the subsequent considerations for the hydrological model development.

3.1 River Ice Data Sources

The development of predictive models described in the following sections requires observation data to inform and validate the models. In particular, the timing of freeze up and breakup and a measure of the severity of breakup, such as stage, is required. In some communities or jurisdictions, detailed ice related data may be available due to a long history of research or interest in that area. However, within the Liard basin no detailed long-term record exists. To fill this gap in data sources in the Liard basin, a mix of information from historical databases with in situ observational data and information extracted from Water Survey of Canada stream gauges was used.

3.1.1 Canadian Ice Database

A Canadian wide observation database for river and lake ice has been compiled from information that was collected by various Canadian government agencies (Lenormand et al., 2002). The Canadian Ice Database (CID) contains in situ observations for both lakes and rivers which includes information like dates of freeze-over, maximum ice thickness, and dates when rivers or lakes are ice free. The single database is based on information from multiple agencies including the Meteorological Service of Canada, the Canadian Ice Service, and the Water Survey of Canada. The database contains information from 1822 to 2001, with a significant decline in the availability of information in the late 1980s and 1990s. Within the Liard basin, the database contains information for six different river locations. Information available at these six locations

is summarized in Table 3.1. Information was only considered from 1985 onwards to correspond with the hydrological model simulation period.

Table 3.1: Summary of Canadian Ice Database Information within the Liard basin

Location	Start Year	End Year	Total Years	Data Coverage (in years)					
				Maximum Thickness	First Ice Date	Permanent Ice Date	Completely Frozen Date	Melt Date	Ice Free Date
Fort Nelson River	1986	1993	7	5	4	0	4	7	7
Liard River near Fort Liard	1985	1996	11	7	10	1	11	8	8
Liard River near Fort Simpson	1985	1996	11	7	7	1	8	7	7
Liard River near Watson Lake	1985	1990	5	0	4	1	5	4	4
Muskwa River	1985	1986	1	0	0	0	0	1	1

Detailed information describing how the data was collected is not available therefore there is some uncertainty associated with the data. Notably, a corresponding measurement date is not associated with the maximum ice thickness, therefore it was assumed that this thickness could occur at any point through the season. Whether this measurement also included white ice, snow layers or the accumulation of frazil slush is also unknown.

3.1.2 Hamlet of Fort Liard Emergency Services

The hamlet of Fort Liard is one of the communities that is at risk of flooding during spring breakup on the Liard. A historic record of observed spring breakup is available through the community's emergency services (Hamlet of Fort Liard, 2017) . The date of spring breakup is available from 1997 to 2016, with photographs included of select years. In some years, a single date of when breakup occurred is provided whereas in other years a range of dates over which breakup occurred is given.

3.1.3 Hydrometric Records

Hydrometric records are readily available across Canada through the Water Survey of Canada. Information regarding ice processes can be extracted from the data flags and raw stage data.

Data Flags

As part of the data processing procedure, the Water Survey of Canada indicates flow data which was estimated due to the presence of ice in the stream with a B flag. The presence of ice in the stream will alter the relationship established between water level and flow under open water

conditions, requiring the ice effected streamflow to be estimated. This is illustrated in Figure 3.1 which shows stage-discharge data, with data tagged with a B flag clearly not following the open water relationship.

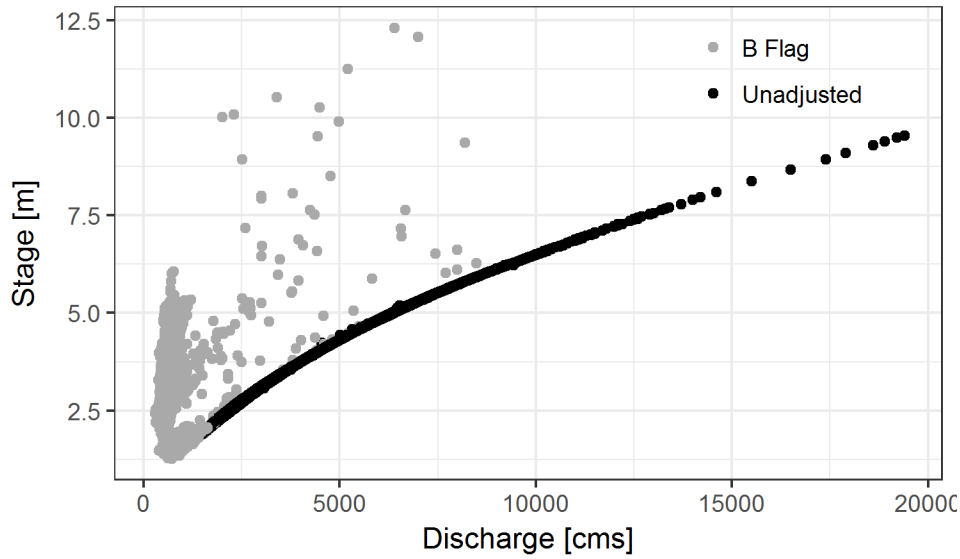

Figure 3.1: Stage discharge curve showing B Flags at 10ED002 (Liard River near the mouth)

The first and last appearance of the B flag over winter have been used as proxies for the timing of freeze up and breakup in some studies (Bonsal et al., 2006; Morales-Marin et al., 2019; Zhang et al., 2001). However, the Water Survey of Canada does not provide consistent guidelines for the application of B flags or field observations to verify them, which can result in information that is highly uncertain. For example, some gauges have the B flag consistently applied on the same date every single year. Additionally, the first B flag may just indicate that there is increased frazil production, but not when an ice cover has formed. The last B flag may indicate when the river is free of all ice, but not the actual breakup timing. A comparison of the B flag data to the observation data in the Canadian Ice Database at the mouth of the Liard indicated that the B flags on average occurred 18 days prior to the field observation of an ice cover forming as indicated by the completely frozen date in the CID database. Given the high uncertainty in this information, data flags were not used as a source of information to inform and validate the ice related analysis.

Stage Data

More detailed and better informed data can be derived from the raw stage data collected by the Water Survey of Canada (Beltaos, 1990b). This methodology proposed by Beltaos (1990b) has also been used to determine freeze up and breakup timing in a number of studies (Beltaos, 1997; de Rham, Prowse, & Bonsal, 2008; de Rham, 2006).

As illustrated in Figure 3.2, during freeze up, the stage of the hydrograph will rise sharply. This rise in stage is caused by increased accumulation of ice flocs and ice floes within the river. The stage will reach a peak and then decrease and stabilize. The peak of the stage indicates an ice cover has formed at the gauge and the subsequent stabilization is a result of smoothing of the underside roughness of the ice cover.

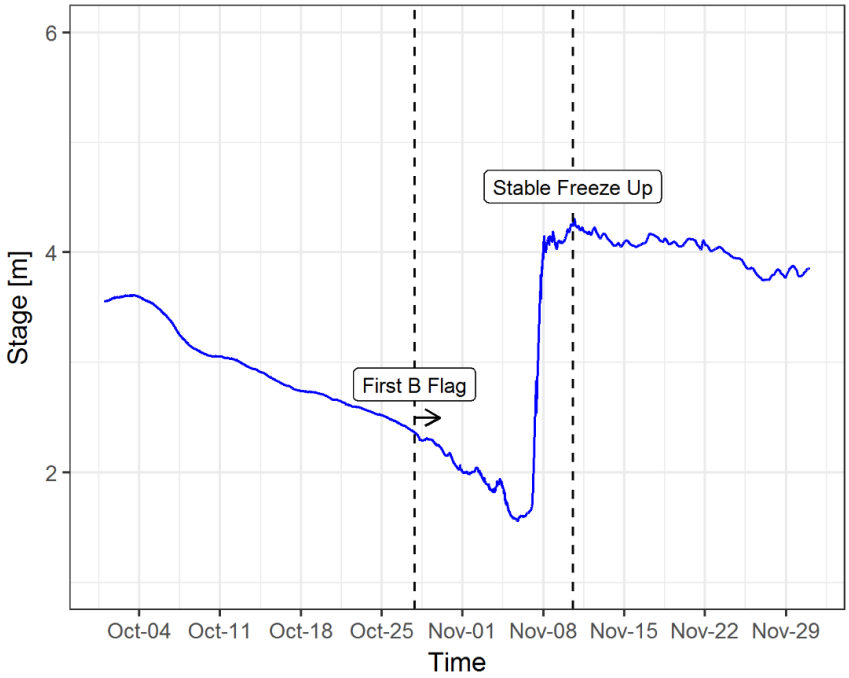

Figure 3.2:Example of freeze up timing from raw stage data (10ED002 - Liard River near the Mouth)

There are some conditions in which using the stage data may not be applicable, including conditions where a stable ice cover does not form or where there are upstream flow and stage controls which end up suppressing the peak during freeze up. Ideally, the stage readings would be supported by additional observation data. There is only one point of overlap between the CID observations and available stage data within the Liard basin to validate the stage readings. In

1996, at the mouth of the Liard the observation of complete freeze over and estimate of stable freeze up from stage data were within one day of each other.

During breakup, sharp changes in the stage will also occur due to hydraulic effects from changing ice conditions (Figure 3.3). The initiation of breakup (H_b) can be determined by the first significant peak during this period of time. This peak generally indicates that the ice cover has began to break and move. The maximum stage at breakup (H_m) gives a general indication of the severity of breakup. It can be the result of a number of different mechanisms such as backwater from a downstream ice jam, flood peak from an upstream jam releasing, or an evolving ice jam at that specific location.

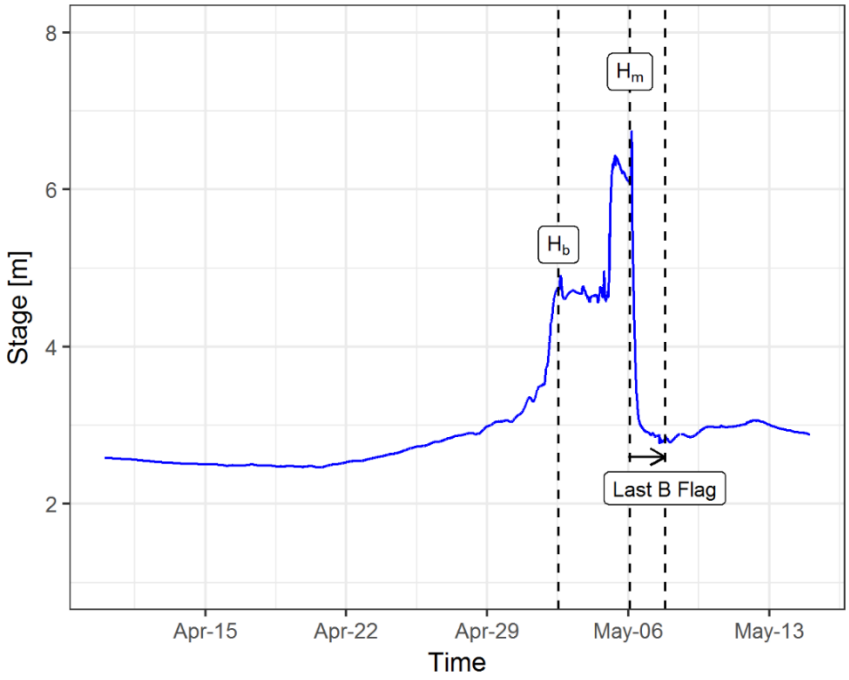

Figure 3.3: Breakup Timing at 10ED002 (Liard River near the Mouth)

Like freeze up, there are situations which arise which makes the identification of breakup timing and severity difficult. Particularly, there can be an absence of multiple peaks due to rapid increases in stage caused by the release of ice jams upstream or as a result of thermal breakup events where breakup occurs during conditions when the stage is falling

There are other limitations to using raw hydrometric data to determine freeze up and breakup timing. The dynamic nature of river ice sometimes means that gauges are damaged and the required freeze up or breakup data is missing. Additionally, not all hydrometric stage data has

been digitized by the Water Survey of Canada. In the Northwest Territories, data is only available in a digital format from 1996 onwards.

To supplement the observational data, and provide indications of breakup severity, freeze up and breakup timing was estimated from hydrometric data at three gauges within the Liard basin. Two of the locations along the Liard River are located adjacent to communities of interest for flood forecasting. The Flat River gauge was included to provide a smaller drainage area and different hydrologic conditions than the Liard River to test the estimation methods. Data from the gauge at Fort Liard was verified using the observation data from the Hamlet of Fort Liard. Table 3.2 summarizes the data availability from the three gauges.

Table 3.2: Summary of extracted breakup and freeze up data availability

Station	Gauge Name	Start Year	End Year	Total Years	Available Years		
					H_b	H_m	H_f
10EA003	Flat River near the Mouth	1996	2016	20	9	9	12
10ED001	Liard River at Fort Liard	1996	2016	20	19	17	19
10ED002	Liard River near the Mouth	1996	2016	20	16	13	18

3.2 Determining Freeze up Timing

Approaches to simulating the timing of river freeze up have largely been based on modeling water temperature (Assel, 1976; Bilello, 1964; Morales-Marin et al., 2019; Shen et al., 1984). These models typically require upstream water temperature measurements or the determination of the headwater temperatures through other techniques, like remote sensing. Within a remote region with sparse data and limited resources, the practicality of obtaining this information may not be realistic in an operational setting. Additionally, these models generally assume that an ice cover has formed once water temperature drops below the freezing point. However, freeze up is a dynamic process which often involves the supercooling of water below the freezing point, the generation and accumulation of frazil into an ice cover, and consolidation of the ice cover. As a result, the timing of the formation of a stable ice cover may not necessarily correspond to the timing of water temperature dropping below the freezing point. Numerical models which can simulate water temperature, the suspended and surface ice concentration, and the rate of ice-cover progression have also been used to simulate freeze up (Lai et al., 1991). However, these types of models are not practical in a situation with sparse data as they require significant data and parameterization.

Taking into consideration the limited data and resources within the Liard basin and the dynamic nature of ice formation, a statistical methodology was undertaken to predict the timing of stable freeze up. Although statistical methods do not provide the insight of physical models, their advantage is that they are simple to apply to complex non-linear relationships to which physical or conceptually based models are unavailable.

3.2.1 Logistic Regression

The simulation of freeze up is based on a logistic regression. As with linear regression, a combination of linear variables is used to predict an outcome; however, in logistic regressions the outcome is considered a binary variable instead of a continuous variable. In this application, the dependent variable is freeze up (i.e. if the river is frozen or unfrozen).

The logistic regression model is based on the function:

$$p = \frac{1}{1 + e^{-x'\beta}}$$

where $x'\beta$ is the linear predictor, which in the case of a single independent variable would be written $x'\beta = \beta_0 + \beta_1 x_1$. The coefficients in the linear predictor are solved using the method of maximum likelihood. Logistic regressions are confined between 0 and 1, as shown in Figure 3.4. A specified probability, typically 0.5, is used as a threshold for determining the dichotomous outcome.

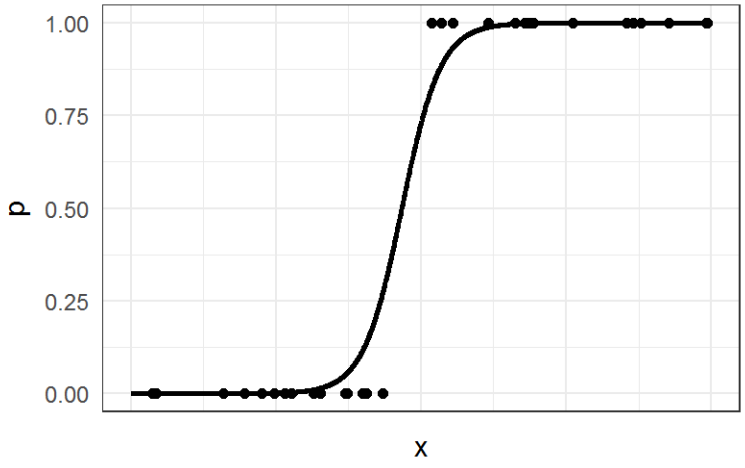

Figure 3.4: Distribution of a logistic regression

3.2.2 Development of Prediction Model – Variable selection

From a physical perspective, the formation of a stable ice cover is strongly controlled by river flow and water temperature. Not only does flow influence the rate of cooling of a river but also influences the rate of surface ice progression, the thickness of accumulation, and applied forces which cause ice covers to collapse and thicken (Shen, 2010). Flow is a variable which is readily available from historical gauges and which can be simulated within the hydrological model. Since water temperature is not being explicitly modelled, air temperature is considered instead as it is widely available and is included in the hydrological model simulation. Relationships between water and air temperature have been well documented between daily mean, maximums, and minimums (Morrill et al., 2004; Webb et al., 2003) . The use of cumulative freezing degree days (CFDD) is a common measure of the cumulative energy gain or loss in a system and has been used to determine ice thickness (Ashton, 1986) and snow melt (Rango & Martinec, 1995), where CFDD is defined by:

$$CFDD = \sum_{i=0} (T_f - T_a^i)$$

where $T_a{}^i$ is the air temperature on day i [°C] and T_f is the freezing point [°C]. CFDD measures can vary depending on when they are initiated (i.e., the time corresponding to i equal to 0) and the freezing point temperature.

A combination of all variables in Table 3.3 were considered in the formation of the logistic regression. Up to two variables were considered in each logistic regression (flow and air temperature). Air temperature was defined through CFDD measures. The air temperature value, initiation date of CFDD, and freezing temperature for the CFDD measures were varied, as indicated in Table 3.3. The result was a total of 96 different variable combinations.

Air temperature data was based on the Environment Canada climate station closest to the gauge of interest. Within the hydrological model, some minor variation between measured and modelled values are expected as the hydrological model will take into consideration orographic effects.

Table 3.3: Variables considered in the development of the logistic regression freeze up

Variable	Values
Flow	Flow
	No Flow
CFDD – Daily Air Temperature	Daily minimum temperature
	Daily maximum temperature
	Daily mean temperature
CFDD - Start Point	First day below 0°C
	First day below 2°C
	First day below 5°C
	First day below 7°C
CFDD - Freezing Temperature	0°C
	-1°C
	-2°C

3.2.3 Development of Prediction Model – Logistic Regression

Logistic regressions rely on an iterative approach to solve the method of maximum likelihood therefore it is important to have a sufficient sample size to inform the model. Since the occurrence of freeze up is only one event each year, the two weeks prior to and after freeze up were considered in the regression, with the two weeks following freeze up considered "frozen" and the two prior "unfrozen." In this manner, the logistic regression determines if the river is frozen with the first date that this occurs considered the timing of freeze up.

The logistic regression was based on three different gauges within the Liard basin (Liard River near the Mouth, Liard River at Fort Liard, and Flat River near the Mouth). Individual regressions were developed for each gauge, therefore the prediction of freeze up at other locations would require the development of site specific coefficients.

The different combination of independent variables outlined in Table 3.3 were tested to ensure that all variables were significant. Of the 96 combinations, 31 had significant variables at all three gauge locations. Combination of variables which were not significant at all three sites were not considered further. To compare the logistic regression model performance, the Akaike Information Criterion (AIC) was used. AIC is defined by:

$$AIC = -2(log\ likelihood) + 2k$$

where *k* is the number of model parameters and the log likelihood is a measure of model fit. Lower AIC values indicate models which reduce the number of parameters while providing the best model fit. AIC values are only applicable to the data set of interest and since the three gauges were based on separate data the values could not be directly compared across sites. Therefore, the AIC values were ranked and the model which provided the minimum mean rank across the three sites was selected as the optimal model. The results of the top five models are summarized in Table 3.4.

Table 3.4: Summary of top five performing logistic regression models

Model ID	Model Description				AIC			Rank			Average Rank
	Flow	Starting Point (First Day Below)	Temperature	Freezing Point	10EA003	10ED001	10ED002	10EA003	10ED001	10ED002	
2	No	0°C	Min Temp	0°C	342	229	439	9	1	12	7
1	No	0°C	Mean Temp	0°C	323	399	433	4	11	10	8
5	No	0°C	Mean Temp	-1°C	339	231	443	8	2	15	8
26	No	5°C	Min Temp	0°C	349	243	414	16	3	6	8
8	No	0°C	Mean Temp	-2°C	336	245	448	6	4	16	9

The model with the best performance is based on using CFDD starting the first day where the mean temperature is below 0°C, using the daily minimum temperature values and a freezing point of 0°C. A default probability threshold of 0.5 was used in the model. A manual sensitivity analysis to this threshold value was undertaken to ensure that the threshold minimized the difference between predicted and observed values. The analysis confirmed that the default probability of 0.5 was appropriate for the model (Figure 3.5). Results from the application of the model are discussed in Chapter 5.

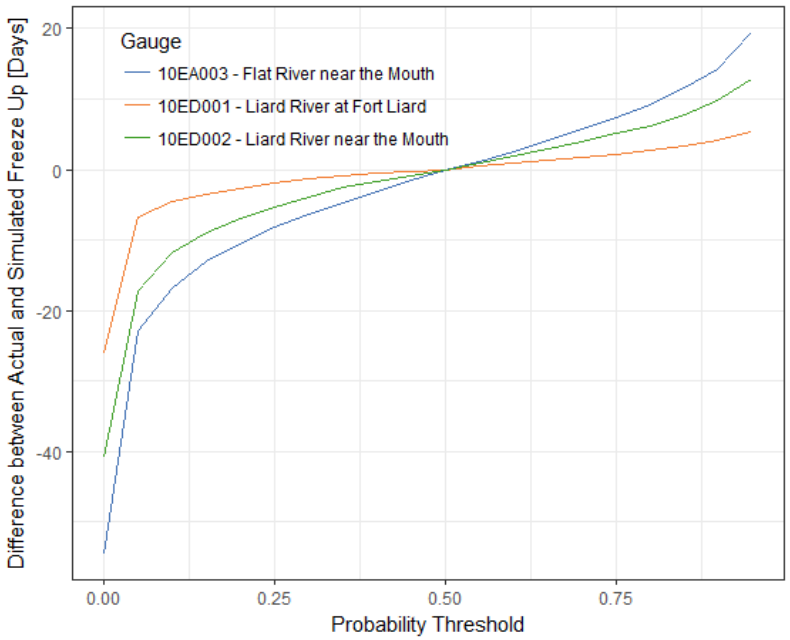

Figure 3.5: Sensitivity of results to probability threshold value

3.3 Thermal Ice Growth and Decay

Once a stable ice cover has formed, ice will grow and decay due to the balance of energy fluxes at the top and bottom of the ice. A number of numerical and analytical models exist which simulate this growth and decay process. These models range from simple degree day approaches (Ashton, 1986; Shen & Yapa, 1985) to more complex finite difference models (Greene & Outcalt, 1985; Shen & Chiang, 1984a). One of the limitations of these more complex models are data requirements. Notably, these models tend to require water temperature, velocity, and depth to be able to calculate the turbulent heat flux. Water temperature data is not widely available, making this component difficult to estimate. Furthermore, some models require relative humidity and wind speed to calculate the surface energy flux. Although this data is more widely available than water temperature, the data is typically recorded hourly and can be intermittent at older stations.

Ashton (2011) proposed a simple methodology for simulating ice growth, decay, and the formation of white ice which emphasizes the use of readily available data. Simulation only requires air temperature and precipitation records as inputs. The model performed well at numerous sites across Canada and the U.S for rivers and lakes.

Ice growth within the model is based on quasi steady state heat conduction:

$$q_i = k_i \frac{dT_i}{dz}$$

where q_i is the flux of heat through the ice [W/m^2], k_i is the thermal conductivity of the ice [W/m/°C] and T_i is the temperature of the ice [°C]. At the bottom of the ice, the rate of ice production is set equal to the surface flux of heat into the ice:

$$\frac{dh_i}{dt} = \frac{1}{\rho_i \lambda}(q_i - q_{wi}) = \frac{1}{\rho_i \lambda}\left(k_i \frac{T_m - T_s}{h_i} - q_{wi}\right)$$

where h_i is the thickness of ice [m], ρ_i is the density of ice [kg/m^3], λ is the latent heat of fusion [kJ/kg], q_{wi} is the flux of heat from water to the undersurface of the ice [W/m^2], T_m is the melting temperature [°C] and T_s is the surface temperature of the ice [°C].

In the formulation of ice growth, heat flux from the water to ice is neglected. Instead of solving for the surface temperature or assuming surface temperature is equal to air temperature, the surface heat flux is described using a simple heat transfer coefficient H_{sa} [W/m^2/°C] where:

$$q_i = H_{sa}(T_s - T_a)$$

Daily ice growth, Δh [m], can then be calculated from:

$$\Delta h = \frac{1}{\rho_i \lambda} \frac{T_m - T_a}{h_i/k_i + h_s/k_s + 1/H_{sa}} \Delta t$$

where T_a is the daily average air temperature [°C], h_i and h_s are the ice and snow thickness [m], and k_i and k_s are the thermal conductivity of ice and snow [W/m/°C]. H_{sa}, the surface heat transfer coefficient, is expected to be in the range from 10 W/m/°C to 20 W/m/°C. The density of ice, ρ_i, is assumed to be 913 kg/m^3 and λ, the latent heat of fusion, is 334 kJ/kg.

In certain conditions, the weight of snow overtop of the ice can cause the ice layer and portion of the snow layer to depress below the water surface. This causes the submerged snow to turn to slush, which then freezes to form white ice. As a result of this occurring, the ice thickness tends to be thicker than if white ice did not form. The layer of white ice and the decreased thickness of snow both will lead to a larger ice thickness. In the formulation of white ice within the model, Ashton (2011) uses the concept of isostasy to determine when white ice will form. In an analysis of 26 years of river ice data at multiple sites across northern Canada and the U.S, positive isostasy was often found to not result in the formation of white ice on rivers, with no obvious

conditions resulting in white ice formation on rivers. Given that the formation of white ice conditions could not easily be predicted for rivers, the formation of white ice was ignored within this analysis of river ice thickening and decay.

Ice decay is based on the ice melting from the surface when the net energy flux is positive. The net energy flux q_{NET} [W/m^2] in a simplified form is:

$$q_{NET} = q_{SW} + q_{LW} + q_H$$

where q_{SW} is the net shortwave radiation [W/m^2] and q_{LW} [W/m^2] is the net longwave radiation. is a function of the surface and air temperature. Within Ashton's (2011) analysis , net longwave radiation was assumed to be a constant value and shortwave radiation was based on tabulated shortwave radiation data from (List, 1951). With the integration of the model into a hydrological model, both longwave and shortwave radiation will be simulated using alternative methods. The sensible and latent heat flux, q_H [W/m^2], is based on a simple degree day formulation:

$$q_H = H_{ia}(T_s - T_a)$$

where H_{ia} is a heat transfer coefficient which varies between 10 to 20 W/m/°C. The daily thinning of ice, Δh [m], is then calculated by:

$$\Delta h = \frac{q_{net}}{\rho_i \lambda} \Delta t$$

Shortwave radiation is not reduced by the fraction which penetrates the ice cover nor is turbulent heat transfer from water considered. Ashton (2011) justified this by assuming that any shortwave radiation that does penetrate the ice cover is immediately returned to the ice cover through the turbulent heat transfer and causes melt at the bottom of the ice cover

The model is initialized based on knowing when freeze up of the river has occurred. Therefore, the methodology outlined in Section 3.2 is used to obtain when freeze up has occurred. Once freeze-up has occurred an ice thickness of 0.01 m is used as the initial point in the model. Realistically, the initial ice thickness may be larger due to consolidation processes during freeze-up, so the initial ice thickness will be used as a calibration parameter. When the ice thickness is less than 0.01 m, it is assumed that no ice cover exists on the river.

3.4 Determining Breakup Timing and Severity

3.4.1 Breakup Timing

As described in Section 2.2, no deterministic models exist to simulate breakup timing or severity. Tools which do exist are largely based on correlating discrete hydrometeorological observations which give an indication of the winter and spring severity. Variables which are typically used like antecedent soil moisture, winter snowpack, and forecasted rain, theoretically would all have an influence on the shape of the resulting hydrograph, notably on the rising limb. The rising limb of a hydrograph during the freshet provides an integrated response of both the winter and spring conditions. The rising limb for a basin will show different responses depending on factors like snowpack, soil moisture, spring temperature etc.

The timing of river ice breakup has been shown to be correlated to the nature and the rise of the hydrograph. Goulding, Prowse, and Bonsal, (2009) showed a significant relationship between the timing of the spring pulse and the timing of breakup on the Mackenzie Delta where the spring pulse is defined when the cumulative difference from the year's mean flow is the largest (Cayan, Kammerdiener, Dettinger, Caprio, & Peterson, 2001). The rise in hydrograph is also an important indicator in practical forecasting situations (J. Nafziger, personal communication, December 12, 2018). Visually, breakup on the Liard occurs on the steep rising limb, shortly after the hydrograph begins to rise, as shown in Figure 3.6.

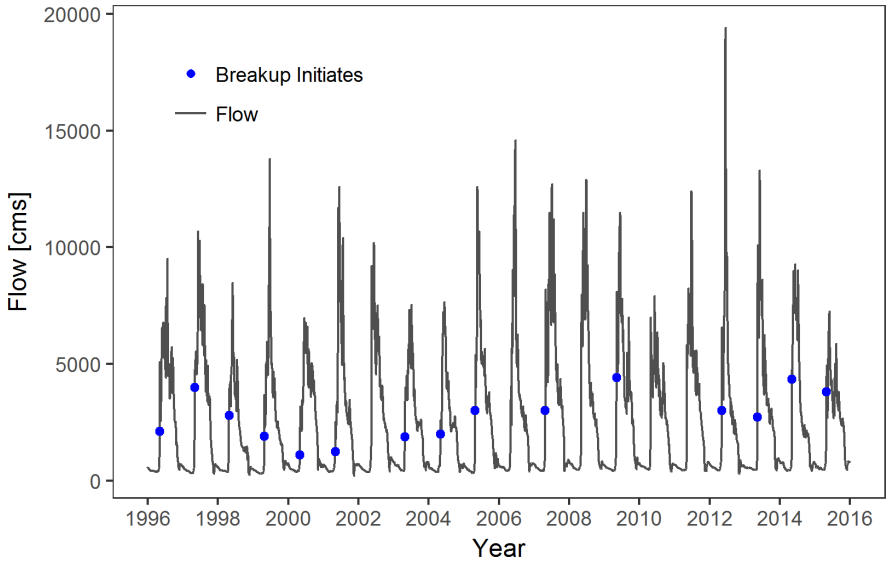

Figure 3.6: Relationship between breakup initiation and hydrograph rise at the Liard River near the Mouth (10ED002)

This rise in the hydrograph which occurs as a result of the hydrometeorological conditions of the basin is a point in time which could be forecasted readily by a hydrological model. Historically, the development of hydrological models for forecasting has primarily focused on the magnitude and timing of flood peaks (Krause et al., 2005). However, a robust hydrological model which is developed for criteria beyond matching flood peaks, could be improved to intentionally forecast the rise in the hydrograph and subsequent breakup.

The timing of the initial rise of the hydrograph has been defined in a number of ways in literature. Cayan et al. (2001) defined the spring streamflow pulse as the julian day when the cumulative departure from the year's average flow is the most negative. Burn (1994) defined the start of freshet as the time when flow exceed 1.5 times the mean flow of the previous 16 days, with manual adjustments being made as necessary. For the purposes of this analysis, it was found that using the minimum cumulative mean flow from the start of the water year, minimized spread in the time to breakup and required fewer manual adjustments than the two previous methodologies outlined. The cumulative mean at day *n* is calculated by:

$$CM_n = \frac{Q_1 + \cdots + Q_n}{n}$$

where Q_1 is the average daily flow at the start of the water year and Q_n is the average daily flow at day *n*. As shown in Figure 3.7, the point of minimum cumulative mean flow occurs just prior to the sharp rise in the hydrograph.

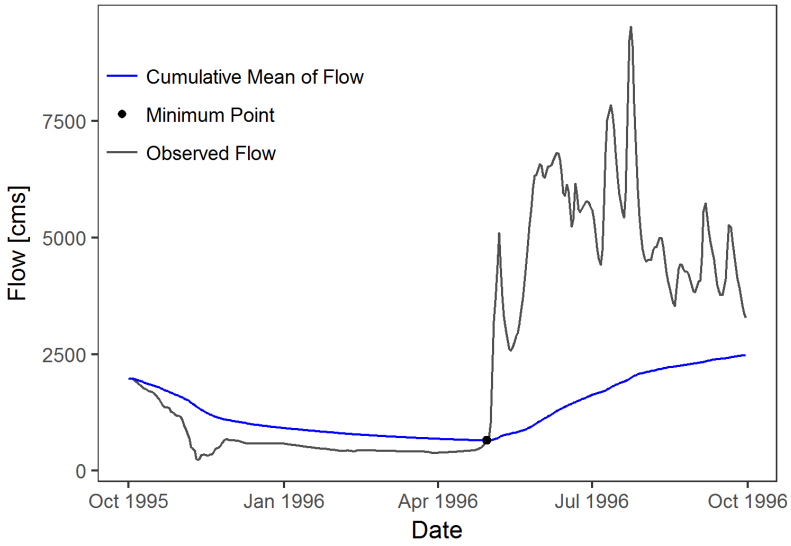

Figure 3.7: Timing of the rise of the hydrograph through the use of cumulative mean flow

There is strong correlation between this point on the hydrograph and breakup timing within the Liard as shown in Figure 3.8 and summarized in Table 3.5.

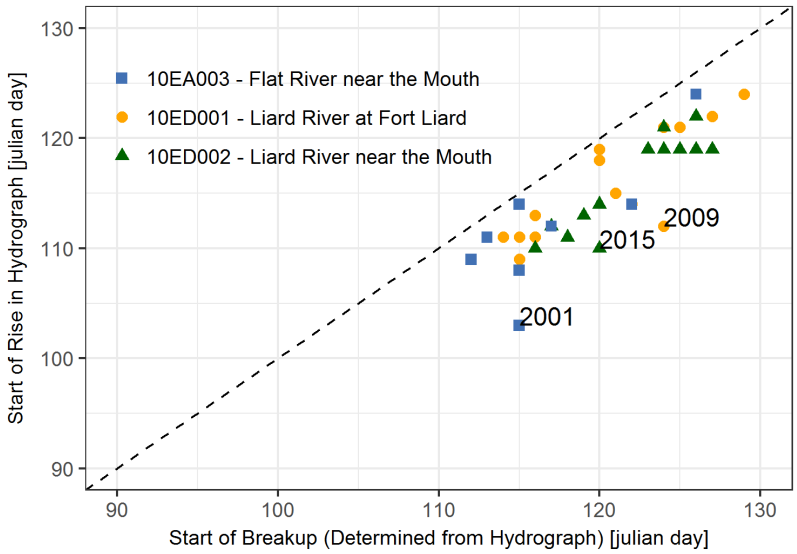

Figure 3.8: Correlation between the rise in hydrograph and start of breakup

Table 3.5:Summary of correlation coefficients between breakup and rise of hydrograph on the Liard

Gauge	R^2
10ED001 – Liard River at Fort Liard	0.86
10ED002 – Liard River near the Mouth	0.94
10EA003 – Flat River near the Mouth	0.77
All	0.87

On average, once initiation in the rise of the hydrograph occurs, breakup will occur within a week of that point (Figure 3.9). In general, the years where there is a larger lag between the initial rise in the hydrograph and breakup is a result of a slower increase in the initial rise in the hydrograph.

Forecasting this rise in the hydrograph, does not necessarily give the exact timing of breakup but only the knowledge that breakup is imminent. Trying to find an exact empirical relationship or threshold to distinguish the exact day of breakup after the rise in the hydrograph is not realistic with the limited knowledge and data of historical breakup dates on the Liard.

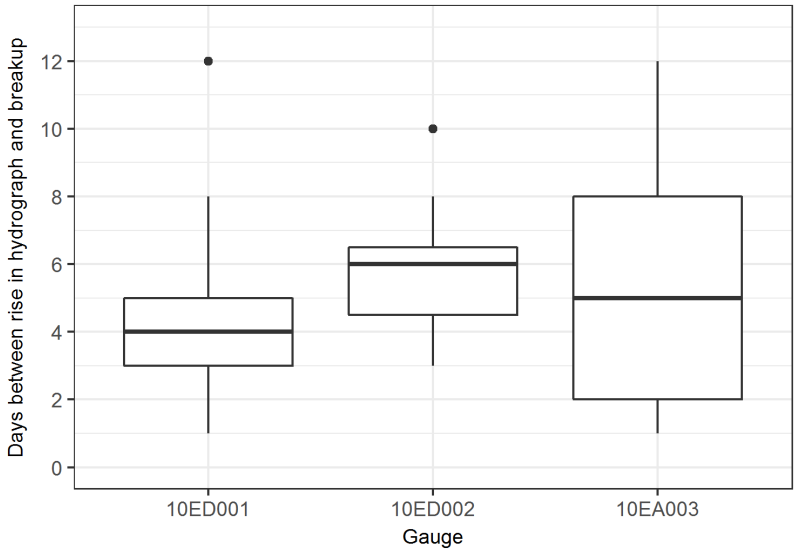

Figure 3.9: Spread between initial rise in hydrograph and breakup initiation

3.4.2 Breakup Severity

Once the approximate timing of breakup is known, it is also beneficial to be able to forecast the severity of breakup. A useful forecasting tool for breakup severity would minimize the number of false predictions. False predictions can be classified as false negatives, where a severe event occurs which was not predicted, or as false positives, where a severe event is predicted but does not occur. False negative predictions have higher consequences in forecasting as they lead to inadequate warning and preparation for high severity flood events. Therefore, an emphasis should be placed on minimizing false negatives. However, at the same time, minimizing false negative predictions can lead to a higher number of false positive predictions, as more events are considered positive to reduce the number of false negative predictions. This issue is common among many current breakup forecasting tools (White, 2003), resulting in low confidence in the performance of the tool. A careful balance must be made between minimizing the false negative and false positive predictions, with a larger emphasis on minimizing false negatives.

To define true and false predictions, a measure of the severity of historical events within the Liard basin is required. A limited database of flood events is available from the Government of the Northwest Territories, which identifies two significant breakup events at Fort Liard in 1989 and 2010 and one significant event at Fort Simpson in 1989. It is possible that minor flooding occurred in other years but has not been documented within this database. For example, in 2008 a newspaper article (Thompson, 2008) notes that minor flooding of two crawl spaces occurred in

Fort Liard. To supplement the information on breakup severity, the maximum stage recorded during breakup at nearby Water Survey of Canada gauges was used. The maximum stage during breakup has been used by other studies as a proxy for breakup severity (Goulding et al., 2009) and within the Liard has been directly attributed to conditions created by ice jams (Prowse, 1986). Maximum stage measurements during breakup may not be available for all years due to malfunctions with the gauges.

A classification scheme which assigns a high, medium, or low breakup intensity to each year was developed for Fort Liard and Fort Simpson based on the known historical events and stage data. The classification of the different years on record at the two locations are shown in Figure 3.10 and Figure 3.11. Years in which significant flood damage was known to occur during breakup are considered high intensity. Years with high stage data but with no documented flood damage are considered medium intensity. For example, at Fort Liard, 2006 and 2010 have similar maximum stage records; however, flooding is only known to have occurred in 2010. This results in 2006 classified as medium intensity and 2010 classified as high intensity. The gauge malfunctioned in 2008 at Fort Liard but given that minor flooding was known to have occurred it was classified as a medium intensity year. Years with low stage data with no known flood damage are considered low intensity.

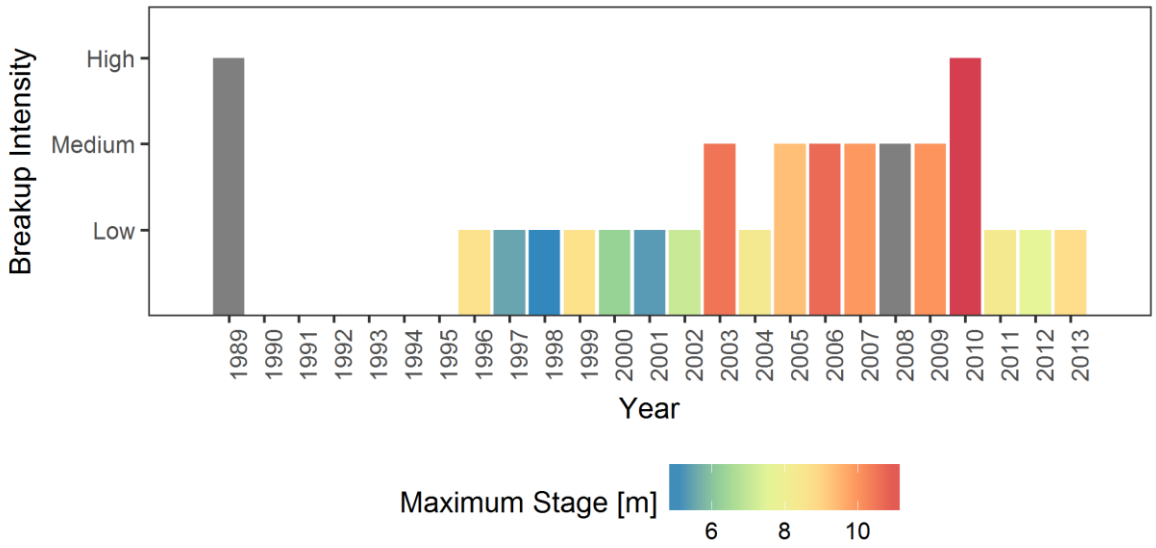

Figure 3.10:Assumed breakup intensity at Fort Liard (10ED001) based on known floods and maximum stage

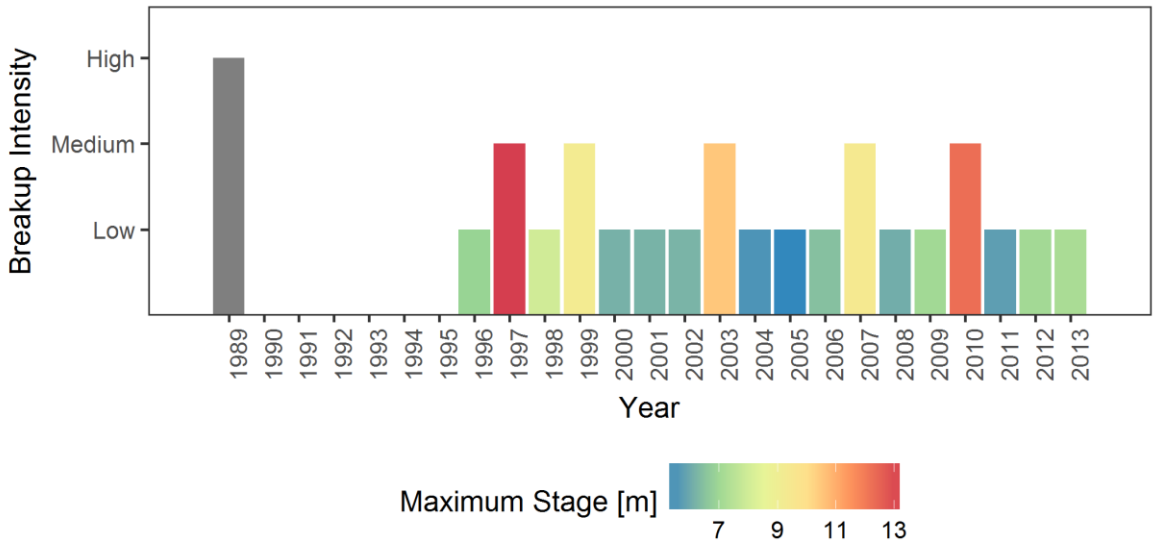

Figure 3.11:Assumed breakup intensity at Fort Simpson (10ED002) based on known floods and maximum stage

The definition of false negative and false positive predictions are based off of the three classifications of high, medium, and low intensity as shown in Figure 3.12.

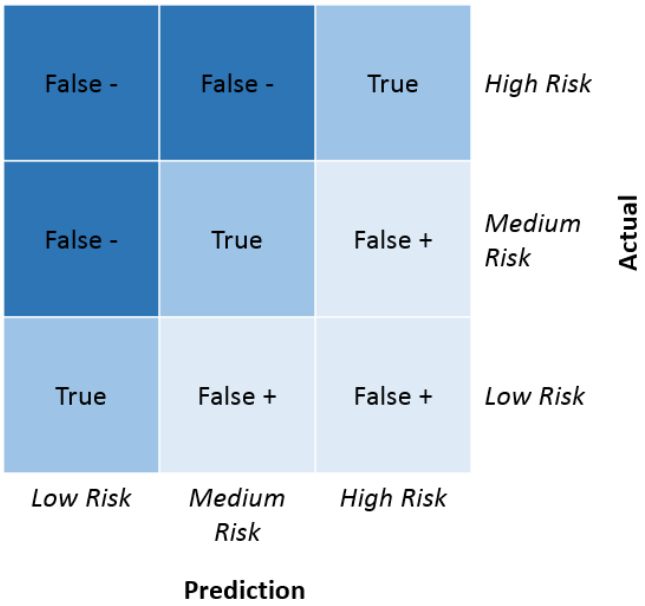

Figure 3.12: Definition of prediction classifications

In addition to minimizing false predictions, a forecast of breakup severity should only rely on values that can be easily modelled or measured. The severity of breakup can be thought of as a trade off between resisting and driving factors. As described by Turcotte & Morse (2015), these driving and resisting factors can be defined by a range of direct to indirect indicators. Ideally,

prediction tools would be based on direct indicators such as shear forces for the driving factor and ice strength for resisting factor. However, these direct indicators are typically difficult to both measure and model, making them impractical for use in a forecasting tool. For this reason, the forecast of breakup severity should rely on direct indicators which can still be readily modelled or measured.

Discharge was selected as a key indicator of severity as this data is widely available through the Water Survey of Canada and can be readily forecasted using a hydrological model. Typically when it comes to the development of hydrological models for forecasting flooding, an emphasis is put on simulating historical peaks correctly. The development of a hydrological model for forecasting river ice breakup severity must also focus on the flow simulation during the breakup period, often the rising limb of the hydrograph.

Ice thickness is another direct indicator which can be simulated within the hydrological model which takes into consideration both the growth of the ice during the winter season and the subsequent degradation in the spring. Figure 3.13 below shows the progression of modelled ice thickness versus observed flow for Fort Simpson and Fort Liard, using Ashton's (2011) ice thickness model . Detailed results on the performance of the river ice model are included in Chapter 5. However, for the purposes of explaining the methodlogy for forecasting breakup severity some results are included within this section. Data which only falls within the B flag period (indicating ice conditions) and after the maximum ice thickness has been reached are shown in the figures. Years where significant flooding occurred are highlighted.

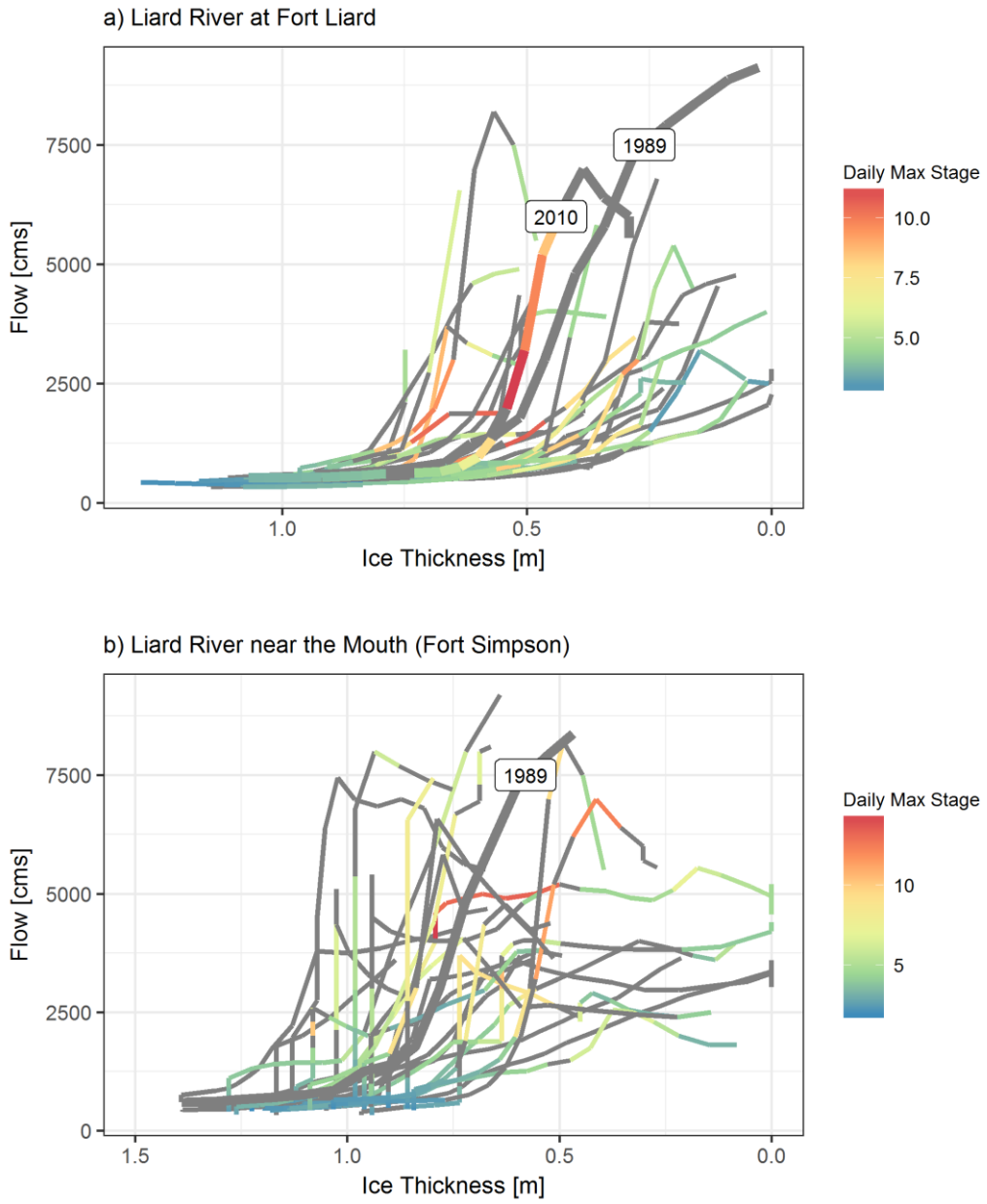

Figure 3.13: Progression of modelled ice thickness with flow at a) Fort Liard and b) Fort Simpson. Thick lines indicate years where significant flooding occurred.

At Fort Liard, there appears to be a fair relationship between years when flooding occurred and years where the flow has increased rapidly with a somewhat thick ice cover. However, this relationship is not notable at Fort Simpson, where the rapid increase in flow relative to ice thickness occurs for many of the years with insignificant stage data. As well, the relationship does not appear to exist for years where high stage data was recorded but no flooding occurred.

The breakup period is relatively short, therefore getting the decay of ice over that period would be very important for forecasting breakup severity. There are a number of uncertainties associated with the ice decay, notably the relationship with snowmelt and the influence of water temperature, later discussed in Chapter 5. Given the associated uncertainty with the rate of decay, using the decay of ice thickness with respect to flow may not be an appropriate method for forecasting breakup severity.

Cumulative shortwave radiation is an important factor in the degradation of both the ice thickness and strength during the spring thaw period. Incoming shortwave radiation can be readily simulated in a hydrological model using analytical methods. These methods have been shown to have excellent results compared to measured incoming shortwave radiation (Allen et al., 2006) and in general can be done so with a higher level of confidence than the thinning of ice. Figure 3.14 shows the relationship between flow and cumulative shortwave radiation at Fort Liard and Fort Simpson. The years in which high flows occur with low cumulative shortwave radiation correspond well to years where significant flooding occurred.

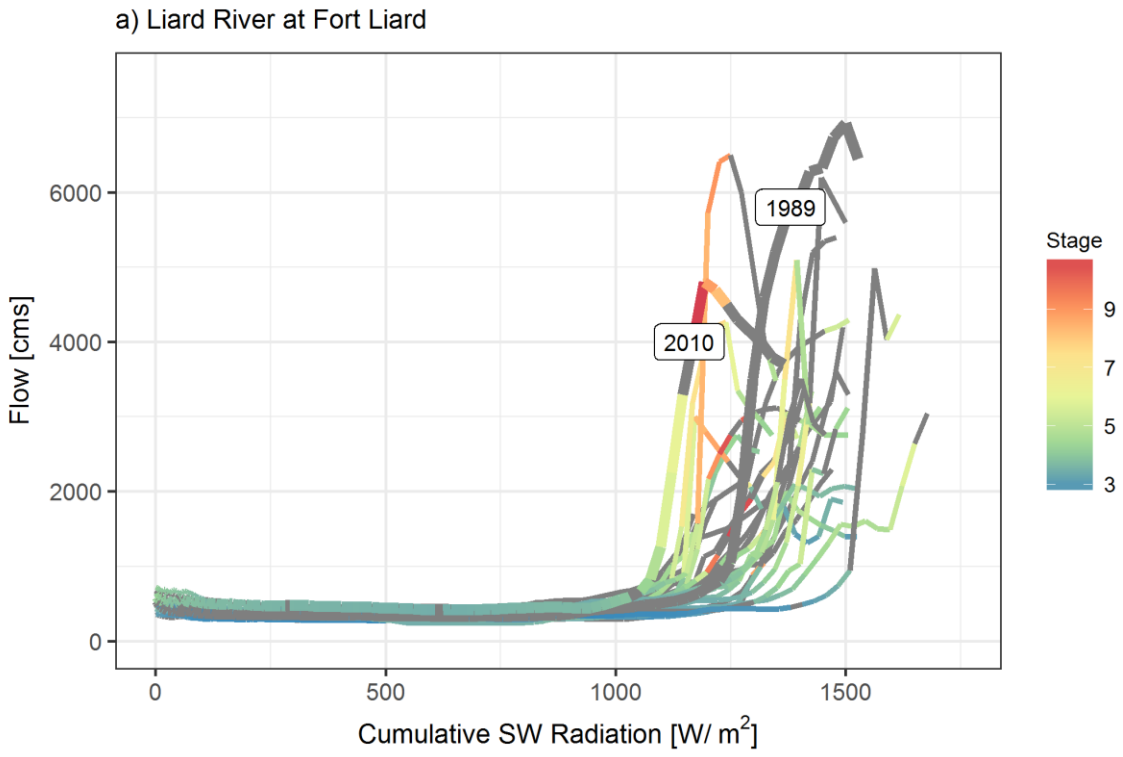

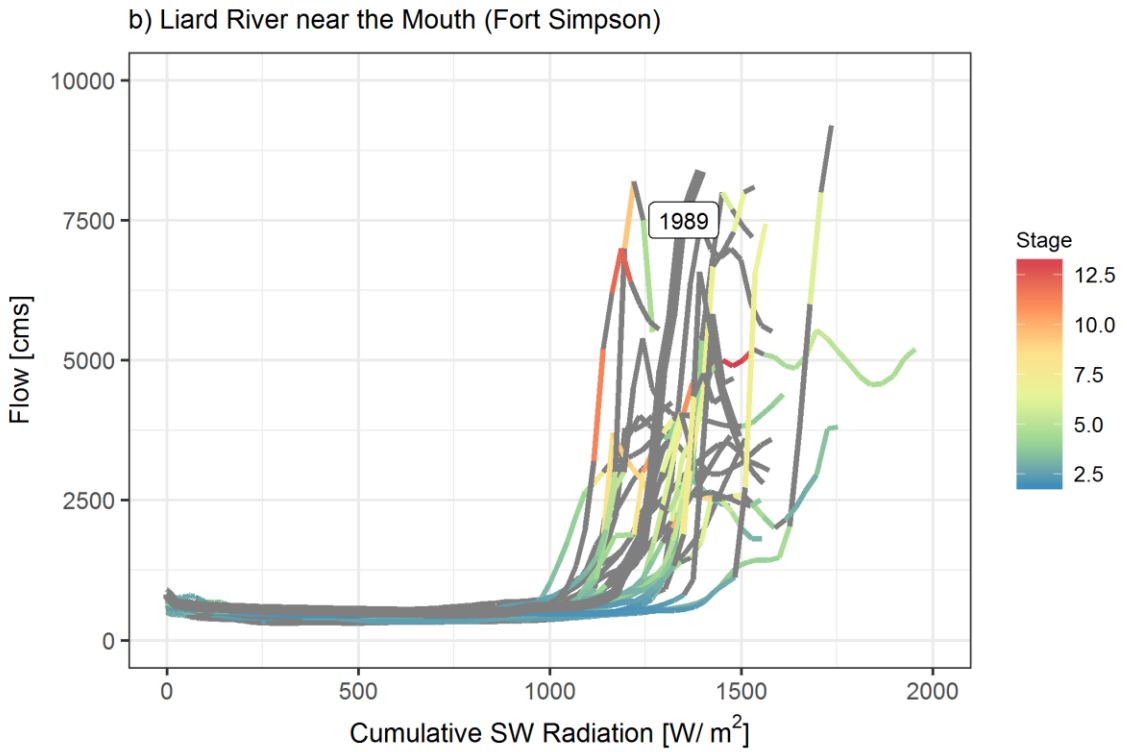

Figure 3.14: Cumulative shortwave radiation and flow near a) Fort Liard and b) Fort Simpson

When determining breakup severity, consideration also needs to be given to ice thickness, as the growth of ice thickness over winter also plays a role in the severity of breakup. A mild winter would result in a thinner ice thickness, which would likely contribute to a lower breakup severity. Therefore, the thickness of the ice prior to the start of breakup should also be incorporated into the forecast of severity.

A multiplicative risk index model was used to develop a forecast based on the ice thickness at the start of breakup and the relationship between flow and cumulative shortwave radiation. Ice thickness, flow, and cumulative shortwave radiation thresholds were developed to quantify the associated variables as low, medium or high severity. The overall breakup intensity was then defined by:

$$Breakup\ Risk = f_1(ice\ thickness) \cdot f_2(Q, SW\ Radiation)$$

The severity of ice thickness, flow and shortwave radiation was based on a scale from one to three, with three indicating high severity. The result is six breakup intensity values which are classified into high, medium, and low breakup intensity as summarized in Table 3.6.

Table 3.6: Definition of breakup risk intensity as it relates to the breakup risk value

Breakup Risk Intensity	Breakup Risk Value
High	9
Medium	6
Medium	4
Low	3
Low	2
Low	1

The thresholds to define the severity of ice thickness and severity of flow and shortwave radiation were based on minimizing the false positive and false negative predictions. An automated procedure for developing the thresholds was used based on the Pareto Archived DDS (PADDS) (Asadzadeh & Tolson, 2009) search algorithm. A weighting scheme was given to the different classifications of false positive and false negatives, as shown in Figure 3.15. This ensured that high intensity events which were predicted as low intensity were given a higher weighting than medium intensity events which were predicted as low intensity.

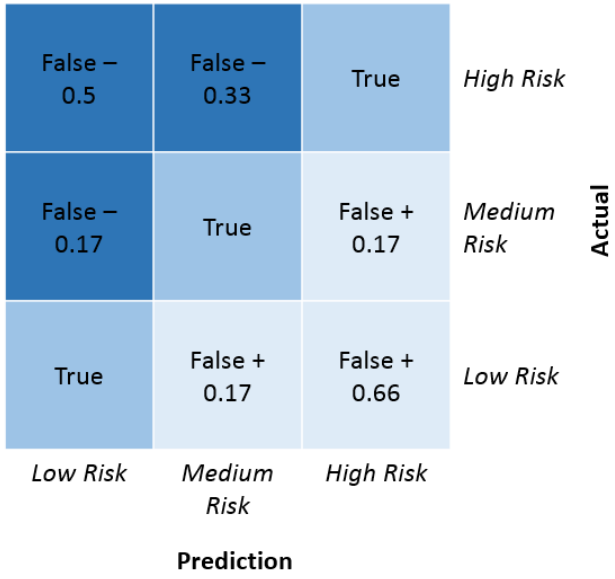

Figure 3.15: Weighting of false positive and false negative predictions for PADDS

The algorithm was used to minimize the number of false negatives and the number of false positives using 5000 runs. This allowed for the trade off between false negative and false positive predictions to be visually examined for the most appropriate thresholds. The trade off curves are shown below in Figure 3.16 for Fort Liard and Fort Simpson, with the selected trade off indicated for each location. The optimization problem was run a second time using only flow and shortwave radiation as an indication of breakup to ensure that the inclusion of ice thickness

improved the overall results and was not an arbitrary addition to the prediction model. The weighting of the false negative and false positives using only shortwave radiation and flow are also indicated in Figure 3.16 showing that the inclusion of ice thickness did improve the overall prediction.

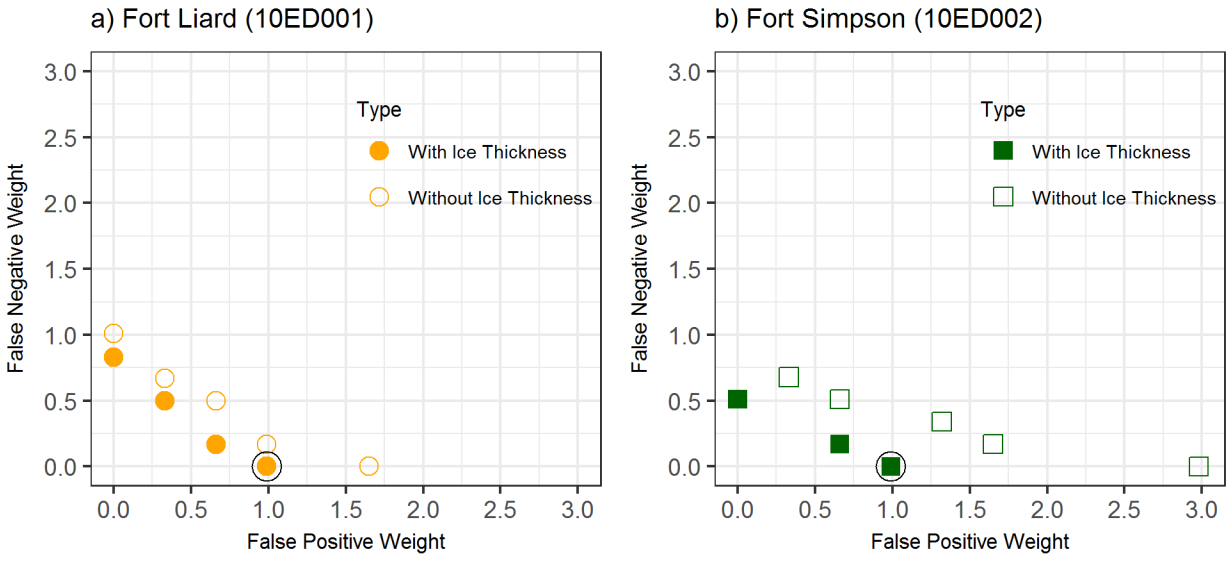

Figure 3.16: Pareto curve showing trade off between number of false negative and false positive predictions for a)Fort Liard and b) Fort Simpson

The thresholds associated with Fort Liard are shown in Figure 3.17 and Figure 3.18 with the resulting performance summarized in Figure 3.19.

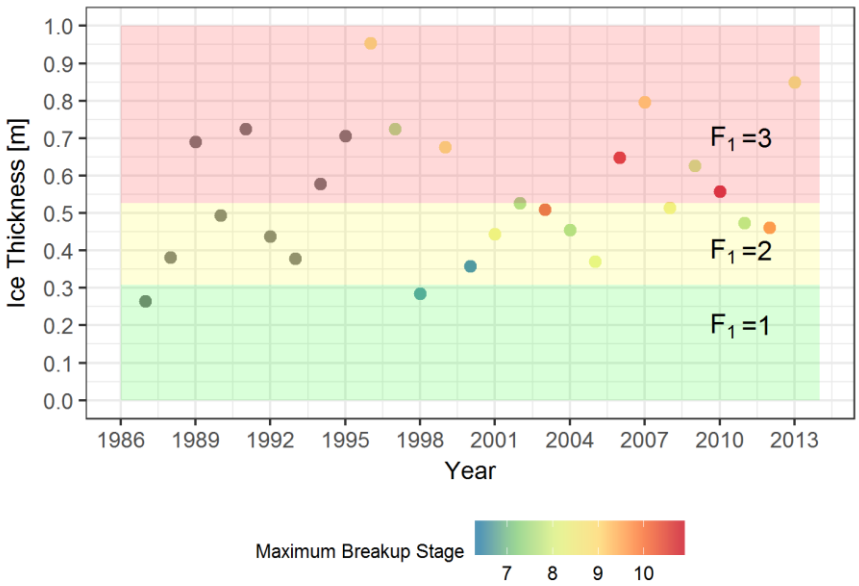

Figure 3.17: Ice thickness thresholds for Fort Liard (10ED001)

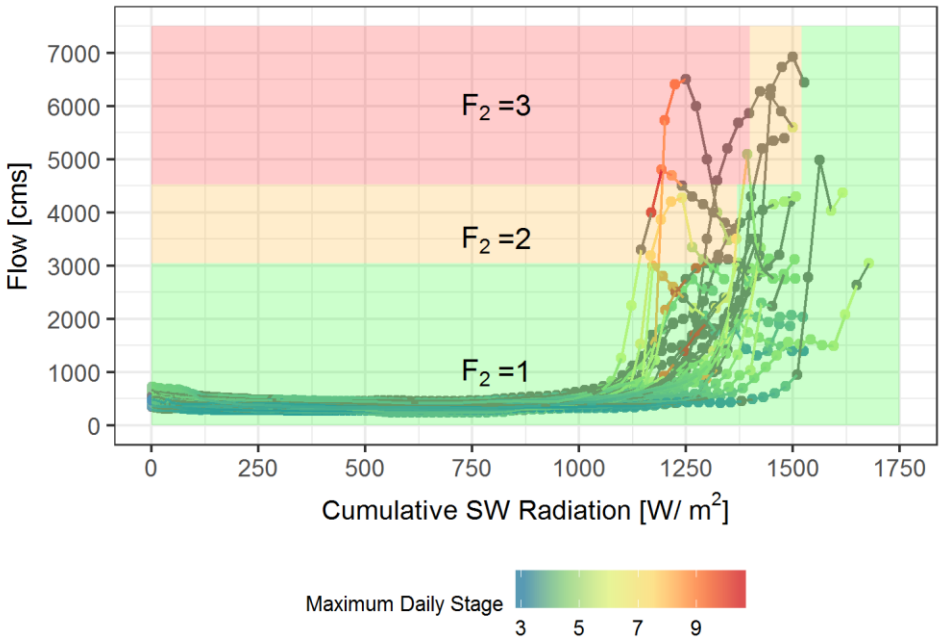

Figure 3.18: Flow and cumulative shortwave radiation thresholds for Fort Liard (10ED001)

Figure 3.19: Summary of prediction results for Fort Liard (10ED001)

The thresholds associated with Fort Simpson are shown in Figure 3.20 and Figure 3.21 with resulting performance summarized in Figure 3.22.

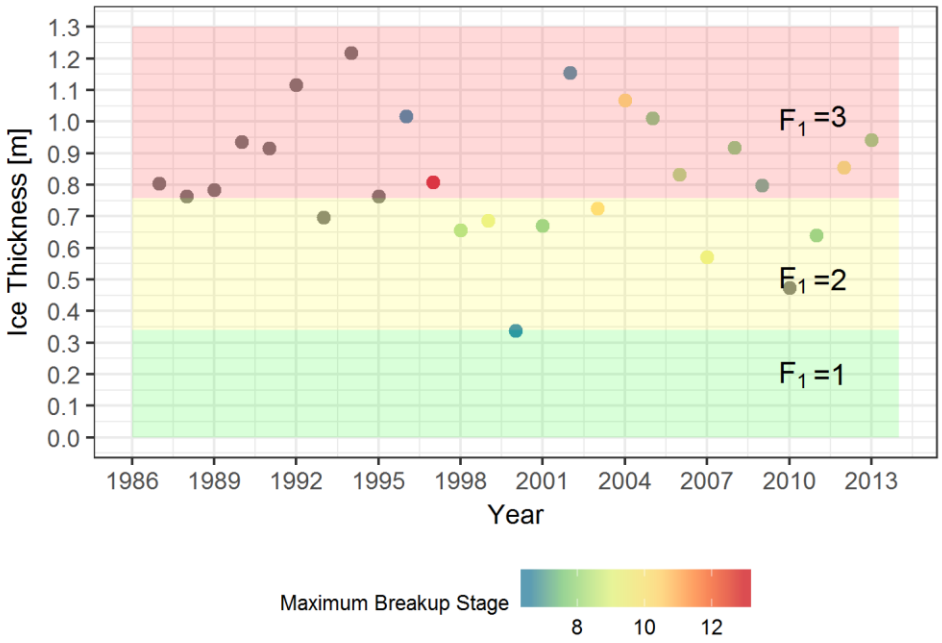

Figure 3.20: Ice thickness thresholds for Fort Simpson (10ED002)

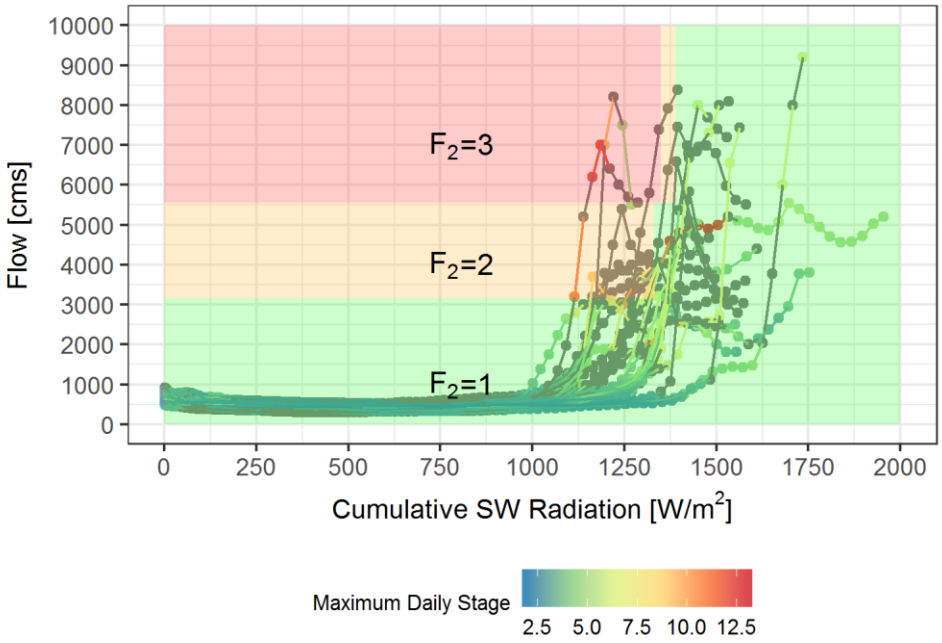

Figure 3.21: Flow and cumulative shortwave radiation thresholds for Fort Simpson (10ED002)

Figure 3.22: Summary of prediction results for Fort Simpson (10ED002)

Given the limited information and uncertainty within the basin related to break up severity, the rate of false negatives and false positive for both locations is considered acceptable. The prediction method resulted in no false negative events which is promising for forecasting. Overall, the rate of false negatives and false positives for both prediction methods is comparable to other locations and methodologies, as summarized in Table 3.7. Table 3.7 is based on other methodologies which used all available data for calibration.

Table 3.7: Summary of false negative and false positive prediction rates for different predictive models

Location	**Method**	**Source**	**# of Years**	**False Negatives**	**False Positives**
Fort Liard, NWT	Threshold	-	19	0%	15%
Fort Simpson, NWT	(Hydrological Model)	-	19	0%	15%
Platte River, NE	Logistic Regression	(White, 1996)	39	3%	21%
Oil City, PA	Discriminant Function	(White & Daly, 2002)	50	2%	12%
Oil City, PA	Neural network	(Massie et al., 2002)	50	1%	6%
Fort McMurray, AB	Fuzzy expert system	(Mahabir et al., 2002)	22	0%	9%

Results of applying the breakup forecasting methodology using simulated flow and estimated breakup timing from the hydrological model are discussed in Chapter 5.

3.5 Hydrological Model Considerations

The river ice processes described in the preceding sections were coupled with the hydrological model using MATLAB. Outputs from the hydrological model are used as inputs to the river ice model in MATLAB. In the future, the river ice model can be integrated into the Raven modelling framework's hydrological process library. Raven is an open source flexible hydrological modelling framework (Craig & Raven Development Team, 2018). Raven relies on a large library of hydrological process representations which can be used to construct hydrological models. Since it is flexible, the model structure can easily be varied with processes added or removed to better represent the physical system.

The river ice model and subsequent breakup forecasting is reliant on the results of complex climatic and hydrologic interactions. Since the model may also be used for forecasting open water flows operationally, the development of the Liard basin model must be robust and realistic, being able to adequately simulate everything from late summer rainfall related peaks to the rising limb of the freshet.

There are a number of challenges to developing valid and realistic hydrological models, especially in large, spatially heterogeneous watersheds. Among these are the issue of equifinality in which a number of different parameter sets provide acceptable results, the potential for inadequate representation of processes within the model, and a lack of data to properly characterize spatial heterogeneity (Beven, 2006; Fenicia et al., 2008; Freer & Beven, 2001; Kirchner, 2006). The model development, outlined in Chapter 4, focuses on approaches to developing a high performing model through methods like calibrating to multiple data sources and including the model structure in the calibration procedure.

Chapter 4
Hydrological Model Development

A semi-distributed hydrological model of the Liard basin was developed to support forecasting of river ice breakup. The model may also be used operationally by the Government of the Northwest Territories for flood forecasting and as a research platform for testing improvements to modelling wetlands and long-term land cover change. This section outlines the development of the hydrological model including the input data, discretization, model structure, and calibration process. This is followed by a summary and discussion of the model performance. Results related to river ice and breakup are discussed in detail in Chapter 5.

4.1 Input Data

The development of a hydrological model requires data to discretize the landscape, climate forcing data, and hydrological data to calibrate and validate the model. The data used in the development of the model of the Liard basin along with any pre-processing steps is summarized in the following section.

4.1.1 Discretization Data

Land cover and topographic data was used as a basis for the discretization of subbasins and HRUs for the hydrological model. Land cover data was based on the Canadian Land Cover Geobase Series (Natural Resources Canada, 2015). The raw data contains eight land cover types (unclassified, water, barren, bryoids, shrubland, wetland, herb, and forest). For the purposes of the model, the land cover was simplified by combining the bryoids and herb classes with the wetland class. Spatial information regarding glacier land cover within the Liard basin was obtained from the CanVec topographic data series (Natural Resources Canada, 2019). The proportion of land cover in the Liard is summarized in Table 4.1.

Table 4.1: Land Cover Proportion within the Liard Basin

Land Cover	Percent of Basin Area
Forest	59.9%
Shrubland	10.8%
Barren	9.6%
Wetland	8.3%
Unclassified	7.1%
Grassland	2.4%
Water	1.6%
Glacier	0.3%

There is some uncertainty associated with the land cover information used in the model discretization. Notably, in the Central Liard there are several localized areas which are unclassified. Within the model, any land cover which was unclassified was assigned the dominant land cover within its subbasin. This resulted in the majority of unclassified land cover being considered forested. There is also uncertainty associated with the differentiation between forest and wetland land cover in the Petitot, Fort Nelson and Lower Liard. This is especially evident along the Alberta-British Columbia border where a visible change in the wetland land classification occurs across the border.

Topographic information for the model was based on the Canadian Digital Elevation model (CDEM) (Natural Resources Canada, 2013). A digital elevation model with a resolution of 150 m was used to discretize the model.

4.1.2 Climate Forcing Data

The model requires daily temperature (maximum, minimum, and average values), and precipitation as climate inputs to the model. A total of 52 Environment Canada weather stations exist within or near the Liard basin with an additional number of provincial or territorial stations. However, many of the stations operate seasonally in the spring and summer or have significant gaps in their data record. Given that the winter months and spring freshet are significant to the basin hydrology and river ice processes, seasonal stations were not considered as suitable for the model. Stations which had less than ten years of data were also excluded. From the remaining 25 stations, ten were selected which maximize the amount of observation data (hydrometric and snow data) available to calibrate and validate the model. Climate datasets which had been adjusted for precipitation and temperature corrections by Mekis and Vincent (2011) were used over uncorrected data The location of the ten climate gauges is shown in Figure 4.1.

Missing data at each station was infilled based on data from the closest station with available data on that day. Given the large spatial heterogeneity of the Liard, it is understood that any model interpolation of the climate data is highly uncertain. The presence of multiple mountain ranges compounds this uncertainty due to orographic effects.

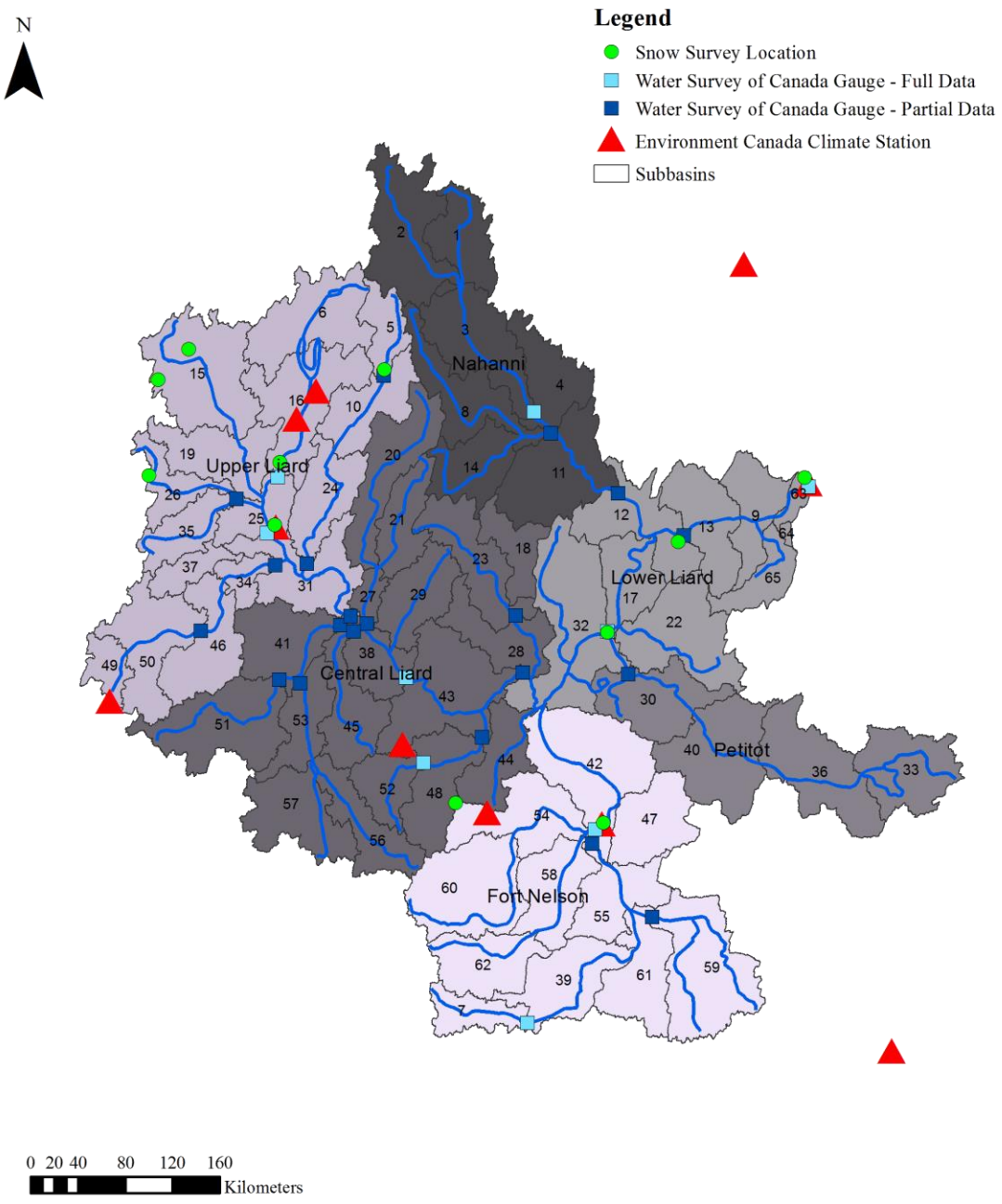

Figure 4.1: Overview of climate data and hydrometric data used in development of the hydrological model

4.1.3 Hydrological Data

Three sources of hydrological data were used to calibrate and validate the model: hydrometric data, snowpack data, and evapotranspiration data.

A total of 29 Water Survey of Canada hydrometric gauges were used in the calibration and validation of the model. Of the 29 gauges, only nine gauges have data that covers the entire 20 year calibration and validation period. The 20 gauges with only partial data coverage were still included in the calibration and validation process to exploit the amount of information available to inform the model. The gauge locations are shown in Figure 4.1.

Streamflow data from the Water Survey of Canada can be flagged as estimated or under ice conditions. The estimated data flag indicates that there was no measured data available, or there was a missing period of data within the day and streamflow had to be estimated using an indirect method. Under ice conditions, streamflow values are also estimated to consider the presence of ice which alters the fundamental stage-discharge relationships used to measure streamflow. Given the high uncertainty associated with these streamflow values, they were not included in the model calibration or validation.

Snow survey data and annual evapotranspiration data were also used to inform the model calibration procedure. Historical snow data was obtained from the provincial and territorial governments. Eleven sites with manual snow measurements were used, as shown in Figure 4.1. Annual evapotranspiration rates were based on previous field work and modelling exercises within the basin. Table 4.2 summarizes the annual evapotranspiration benchmarks used in the calibration process.

Table 4.2: Summary of Evapotranspiration Rates used in Model Calibration

Location	Approximate Rate (mm/year)	Source
Lower Liard	300	(Quinton et al., 2004)
Nahanni Range	160 – 250	(Brook & Ford, 1980)
Basin Wide	190 – 250 (modelled values)	(van der Linden & Woo, 2003b)

4.2 Model Discretization

The Liard basin model is based on a semi-distributed discretization scheme which breaks the entire basin into smaller subbasins. Within these subbasins the landscape is further discretized into hydrological response units.

4.2.1 Subbasins

Subbasins were delineated from the DEM based on hydrometric gauge locations, major river intersections, and major changes in topography. A total of 65 subbasins are included in the model with an average size of 4,100 km^2. The smallest subbasin, with an area of 140 km^2, was included in the model due to related research that is of interest at this location (Quinton et al., 2019). The subbasins are shown in Figure 4.1.

In the model, flow is routed between subbasins using Raven's diffusive wave routing algorithm. Channel geometry for the subbasins was estimated based on the mean annual peak flow and subbasin area, as outlined in the methodology by Andreadis, Schumann, & Pavelsky (2013).

4.2.2 Hydrological Response Units

HRUs were discretized based on the following scheme:

- Seven land classes (Forest, Shrubland, Grassland, Wetland, Glacier, Barren, Water)
- 12 250 m elevation bands (Ranging from 250 m to 3000 m)
- Three aspect classes (North, East/West, South) applied where the landscape slope was greater than 20°

To reduce the overall number of HRUs, aspect was defined between 0° and 180° instead of 0° and 360°. An east and west facing slope will receive the same amount of energy over a day therefore differentiating between the two slopes is not necessary.

The HRUs were discretized by overlaying the subbasins, land class, elevation, slope, and aspect data using ArcMap. The initial discretization led to a large number of small, fragmented HRUs. To simplify the discretization, any HRUs which were less than 0.5 km^2 were merged with adjacent larger HRUs. The HRUs were further simplified by consolidating HRUs which were less than 1% of the subbasin area with similar HRUs using the RavenR package (Chlumsky & Craig, 2019). Similar HRUs were defined based on land cover, and slope, aspect, and elevation

thresholds. The final number of HRUs included in the model was 1107. HRUs were assigned the average slope, aspect, latitude and longitude of their non-contiguous area.

4.3 Model Structure

The semi-distributed model was built with Raven, a flexible hydrologic framework (Craig & Raven Development Team, 2018). Raven allows for the model structure to emulate other hydrological models or for a custom model structure to be created for the basin of interest. The HBV-EC model structure was used as an initial model structure (Hamilton et al., 2001). The HBV-EC model structure is based on the HBV model (Bergstrom & Forsman, 1973) which has been successfully applied in northern and mountainous basins making it applicable to the basin of interest. A strict HBV-EC model structure was not kept through calibration, as the model structure was modified to better represent the specific hydrological functions within the basin. The final input file with the process descriptions is included in Appendix A. HBV-EC is a conceptual rainfall-runoff model and includes routines for soil moisture, snow accumulation and melt, glacial release, and groundwater response, as shown in Figure 4.2.

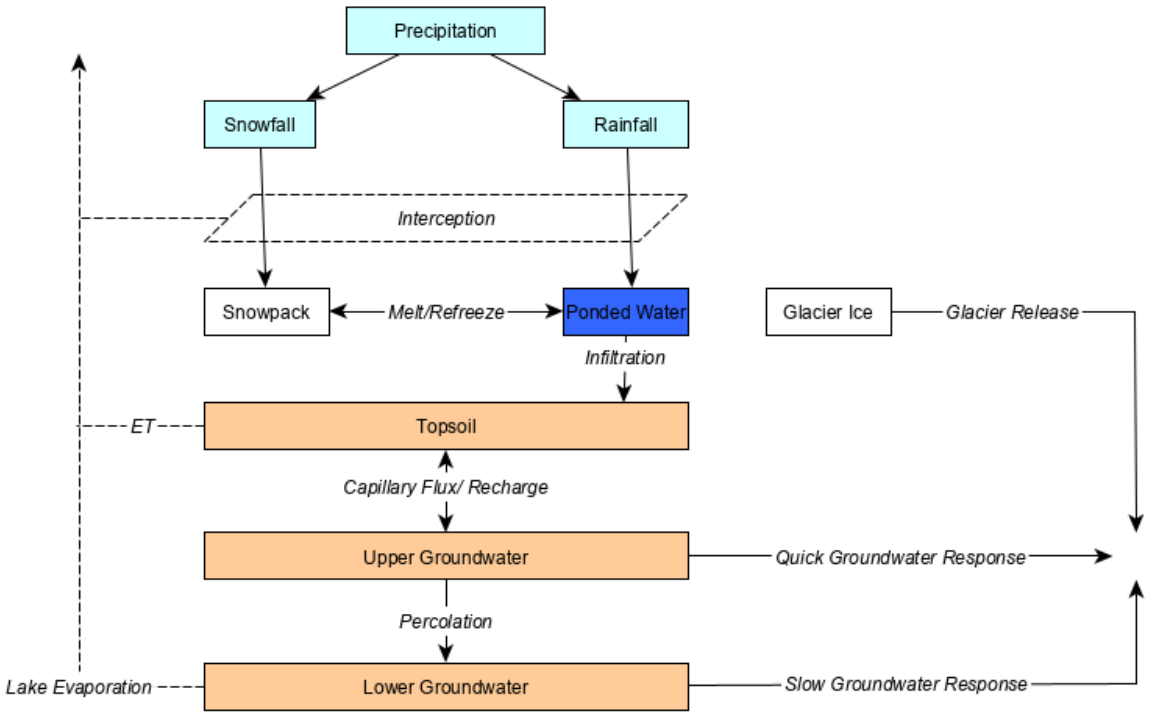

Figure 4.2: Conceptual diagram of HBV-EC model structure

4.4 Calibration Procedure

The calibration approach followed for the model is based on strategies which have been suggested and applied in literature to improve the calibration and overall function of hydrological models by constraining model parameters and exploiting available data. This includes the calibration of internal processes within the model and the calibration of the model structure.

The calibration of internal processes, such as evapotranspiration and snow accumulation, to observation data has been used to reduce parameter uncertainty in calibration (Anderton et al., 2002; Bergstrom et al., 2002; Cao et al., 2006). Basing the calibration of a model only on matching the simulated hydrograph to the observed hydrograph can lead to unrealistic representation of hydrologic processes within the model and a wider range of appropriate parameter values. By ensuring that internal processes are also representative of observation data, parameters within the model are constrained and process representation is more realistic.

The calibration of model structure is reliant upon the availability of a flexible modelling framework. Many hydrological models exist, each with their own model structure and set of associated assumptions and parameters (Abbott et al., 1986; Bergstrom & Forsman, 1973; Pietroniro et al., 2007; Wood et al., 1992). These models are typically based on the idea that a general model structure is appropriate for a wide variety of basins each with their own climate and physiography. As a result, the model structure can ignore or misrepresent hydrologic processes that are occurring within the basin. A flexible modelling framework allows for the modeler to have complete control over the model structure representation, easily altering, adding, or removing processes. This control can be used to better understand and improve representation of hydrological processes and catchment behavior (Clark et al., 2011; Fenicia et al., 2011, 2008). With fixed model structures, calibration primarily focuses on the modification of parameters, however a flexible model framework allows the model structure to be explicitly considered in the calibration process. This direct consideration of model structure can help in better understanding the basin's response, especially in basin's with limited prior knowledge of the hydrological properties and processes.

The calibration process for the Liard basin model used a combination of manual and automatic calibration, with a large emphasis on the manual calibration. The manual calibration was

completed first to gain a better understanding of the basin and make changes to the model structure where required. Automatic calibration was used to further refine model results from automatic calibration.

The manual calibration procedure used an iterative, stepwise, and multicriteria approach to manually modify parameters and model structure. Subbasins were analyzed from upstream to downstream focusing on two different analysis metrics: percent bias and Nash Sutcliffe Efficiency (NSE) (Nash & Sutcliffe, 1970). Percent bias gives an indication if the model is over or underestimating streamflow throughout the simulation. Nash Sutcliffe Efficiency describes how closely the model matches the observed streamflow, with a range from -∞ to 1. Both metrics were used to analyze a single gauge's response to the calibration process, but also to compare how different gauges within the basin performed.

By comparing metrics across different gauges, how the calibration of a single upstream gauge influenced other upstream gauges was considered. This approach helped identify regions where there were discrepancies in performance which could be further examined for differences in hydrological responses and potential changes to model structure.

Throughout the calibration procedure, the manual modification of parameters and model structure followed a methodical and iterative process, as shown in Figure 4.3. This iterative approach helped to focus and justify the manual changes made to the model.

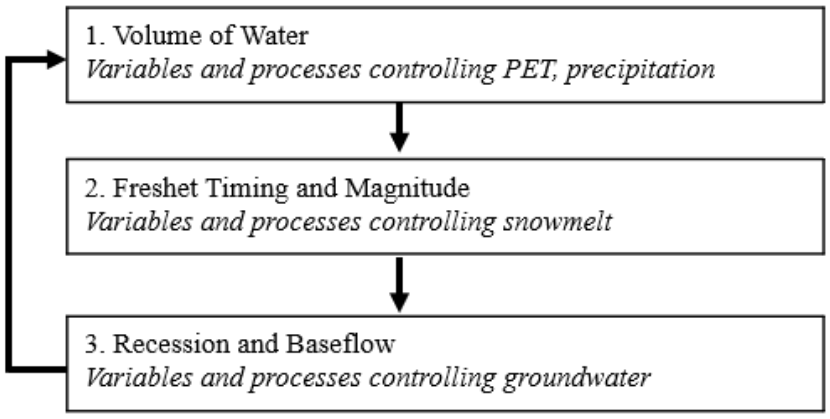

Figure 4.3: Iterative and methodical calibration focus for manual calibration of parameters and structure

Concurrent to the examination of diagnostic metrics and hydrographs, internal processes within the model were analyzed to ensure that they were being realistically represented. This included the examination of snow accumulation and melt at snow survey sites within the basin, the comparison of regional and basin wide annual evapotranspiration rates, and the decomposition of hydrographs into various flow components. The simulated snow data was visually compared to the observed snow data looking for consistent biases within the model. No numeric metric was used to quantify the performance since snow measurement data typically has large spatial variability and uncertainty associated with it. Using synthetic tracers in Raven, the hydrographs were decomposed into different flow sources including snowmelt, quick flow, baseflow, glacier release, and wetland overflow. Through decomposing the hydrographs into various components, the calibration was guided to the processes most in need of modification to improve different components of hydrograph fit.

The automatic calibration procedure , used as a finishing step, utilized the Dynamically Dimensionally Search (DDS) algorithm (Tolson & Shoemaker, 2007) to refine the parameter values from the manual calibration. The automatic calibration was only based on the nine gauges which cover the full calibration and validation period. The objective function of the automatic calibration was based on an area weighted Kling Gupta Efficiency (KGE) (Gupta et al., 2009) of the nine gauges. The objective function is penalized by 0.01 when the percent bias values are outside of a given range. A total of 26 parameters were calibrated during automatic calibration. These parameters were selected based on the knowledge gained during manual calibration and were generally deemed very sensitive or influential upon the model results. Appendix B contains the parameters targeted during automatic calibration and their associated range. The automatic calibration was based on 10,000 model runs.

The model calibration and validation period ran from 1985 to 2005 with 1985 to 1986 being used as a spin up year, 1986-1996 used for calibration and 1996-2005 used for validation. An extended simulation period from 1985 to 2014 was used in the analysis for breakup prediction to accommodate the limited availability of river ice data within the basin.

4.5 Model Results and Discussion

4.5.1 Basin Wide Results

The calibrated model performs well at all scales of the model, from smaller upstream subbasins to the outlet. Performance metrics for the nine gauges which cover the entire calibration and validation period are summarized in Table 4.3. KGE values during calibration are shown in Figure 4.4 for all gauges used in the calibration procedure. Note all values disregard winter measurements.

Table 4.3: Basin wide calibration and validation metrics

Station	Station Name	Area, km^2	Calibration			Validation		
			NSE	% Bias	KGE	NSE	% Bias	KGE
10AA001	Liard River at Upper Crossing	32,600	0.84	5.2	0.89	0.85	1.0	0.92
10AB001	Frances River near Watson Lake	12,800	0.71	-12.6	0.80	0.76	-10.0	0.83
10BE001	Liard River at Lower Crossing	104,000	0.86	5.6	0.91	0.88	6.1	0.92
10BE004	Toad River above Nonda Creek	2,540	0.87	-8.8	0.89	0.88	-3.5	0.86
10CB001	Sikanni Chief River near Fort Nelson	2,180	0.40	9.5	0.69	0.42	18.6	0.68
10CD001	Muskwa River near Fort Nelson	20,300	0.67	9.2	0.74	0.58	25.6	0.70
10EB001	South Nahanni River above Virginia Falls	14,500	0.67	-3.4	0.83	0.70	3.13	0.85
10ED001	Liard River at Fort Liard	222,000	0.80	10.1	0.83	0.81	10.1	0.87
10ED002	Liard River near the Mouth	275,000	0.70	10.1	0.83	0.70	14.1	0.81

The model also performs well in the extended simulation period. No consistent decrease in model performance is observed with time. Figure 4.5 shows the KGE values during the extended simulation at gauges with available data. The length of data at each gauge in the figures is not necessarily the same.

In general, the model has excellent performance in the Upper, Central, and Lower Liard. The hydrograph within these regions is dominated by the freshet, making it relatively simple to simulate adequately. The communities which are of interest for forecasting (Fort Liard, Fort Simpson, and Nahanni Butte) are all within this region. Of the three communities only Fort Liard and Fort Simpson have nearby gauges to assess model performance. Hydrographs at these two locations for select years of calibration, validation, and extended simulation are shown in Figure 4.6 and Figure 4.7.

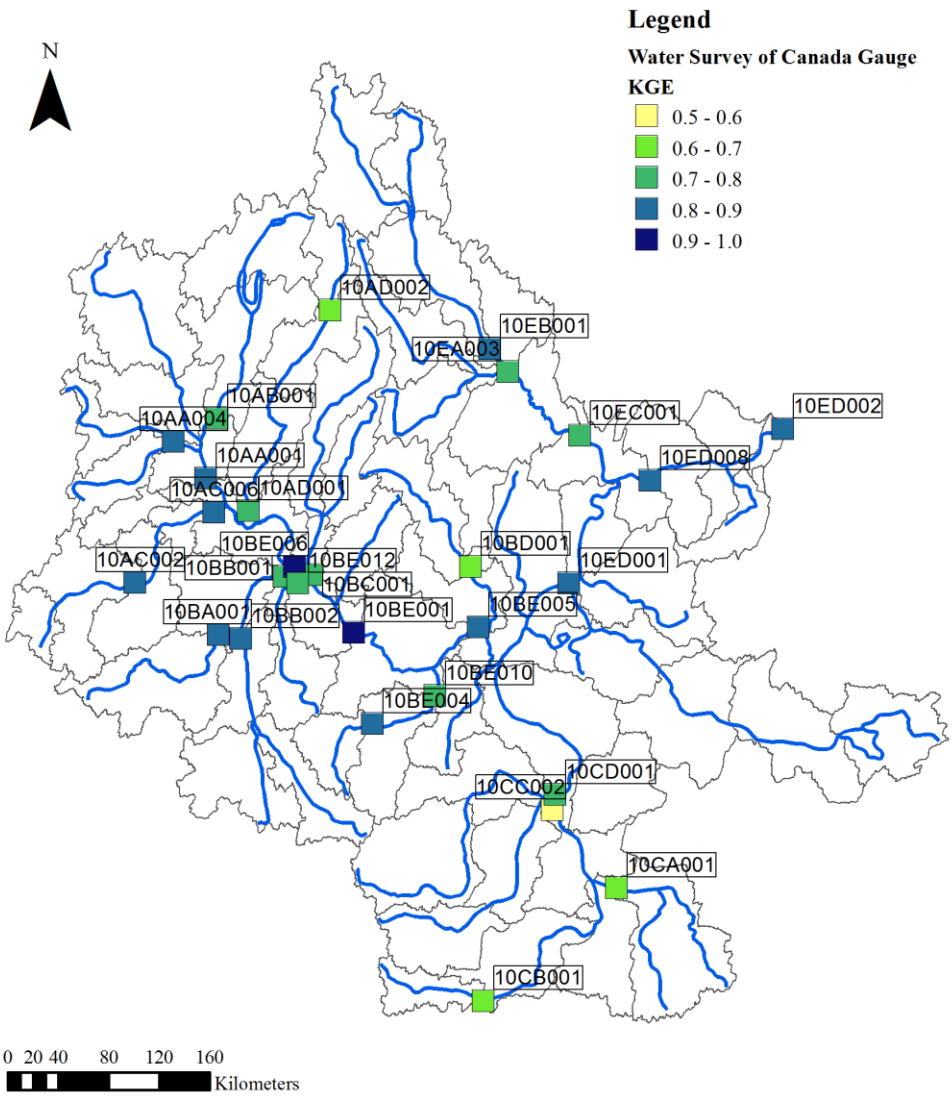

Figure 4.4: KGE values during the calibration period for all gauges

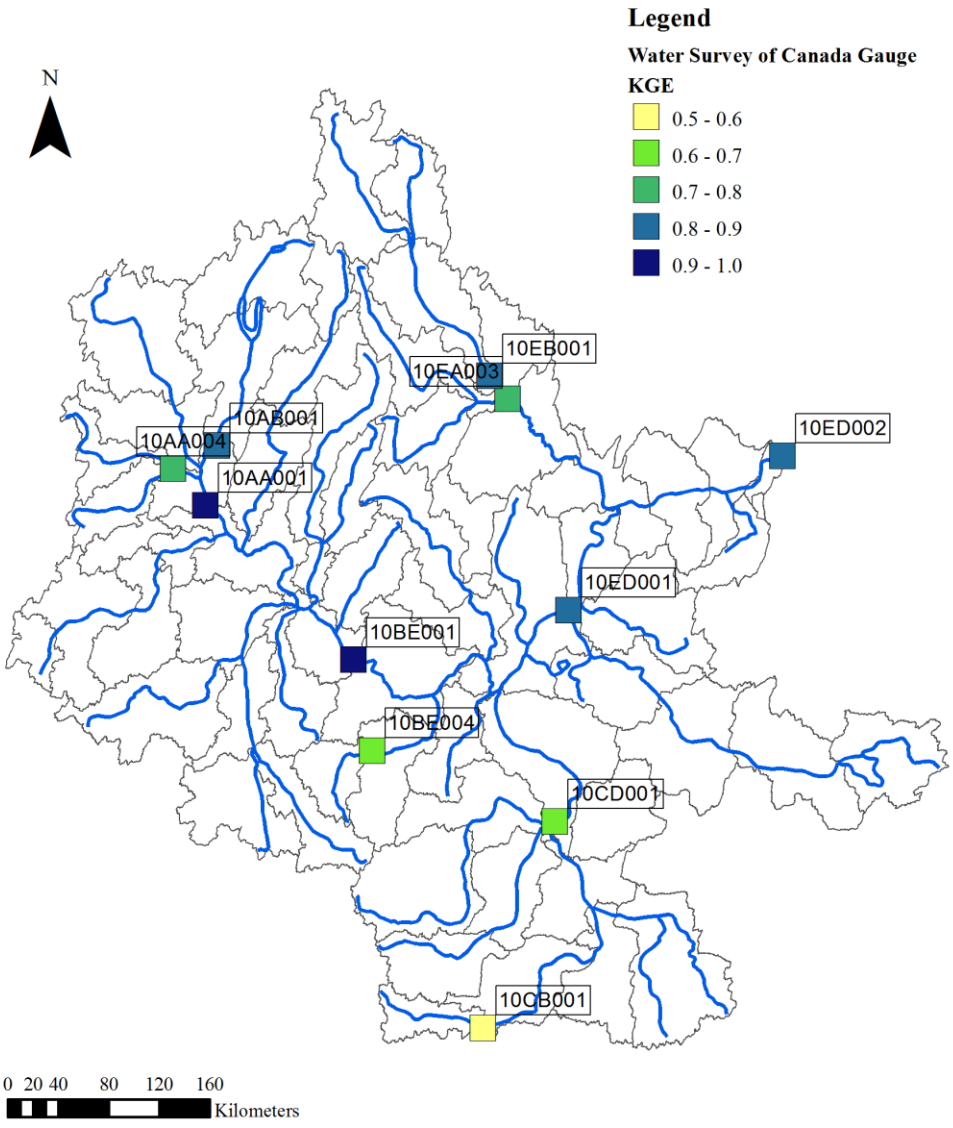

Figure 4.5: KGE values during the extended simulation period

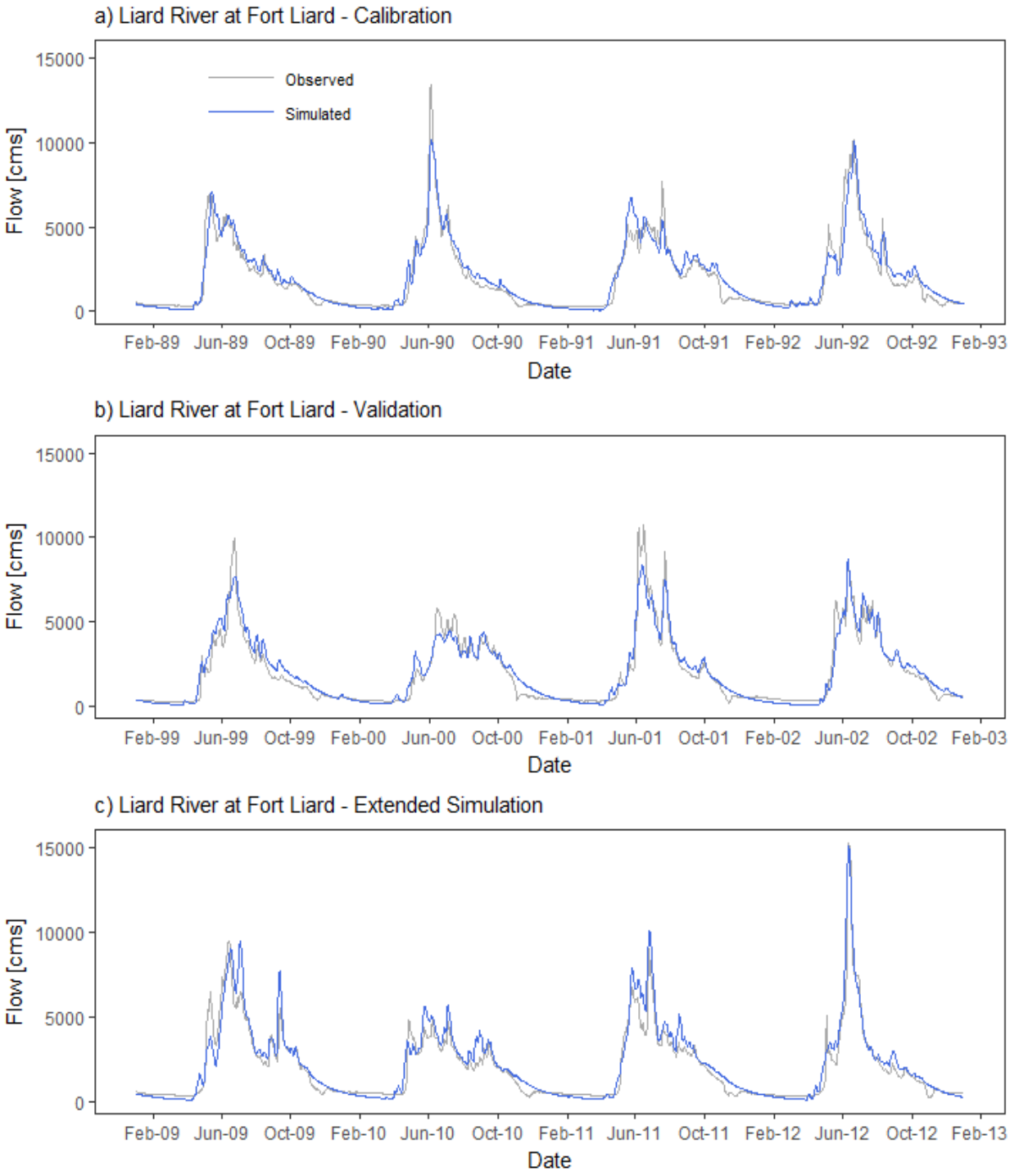

Figure 4.6: Hydrographs of select years during the calibration, validation, and extended simulation period for the Liard River at Fort Liard (10ED001)

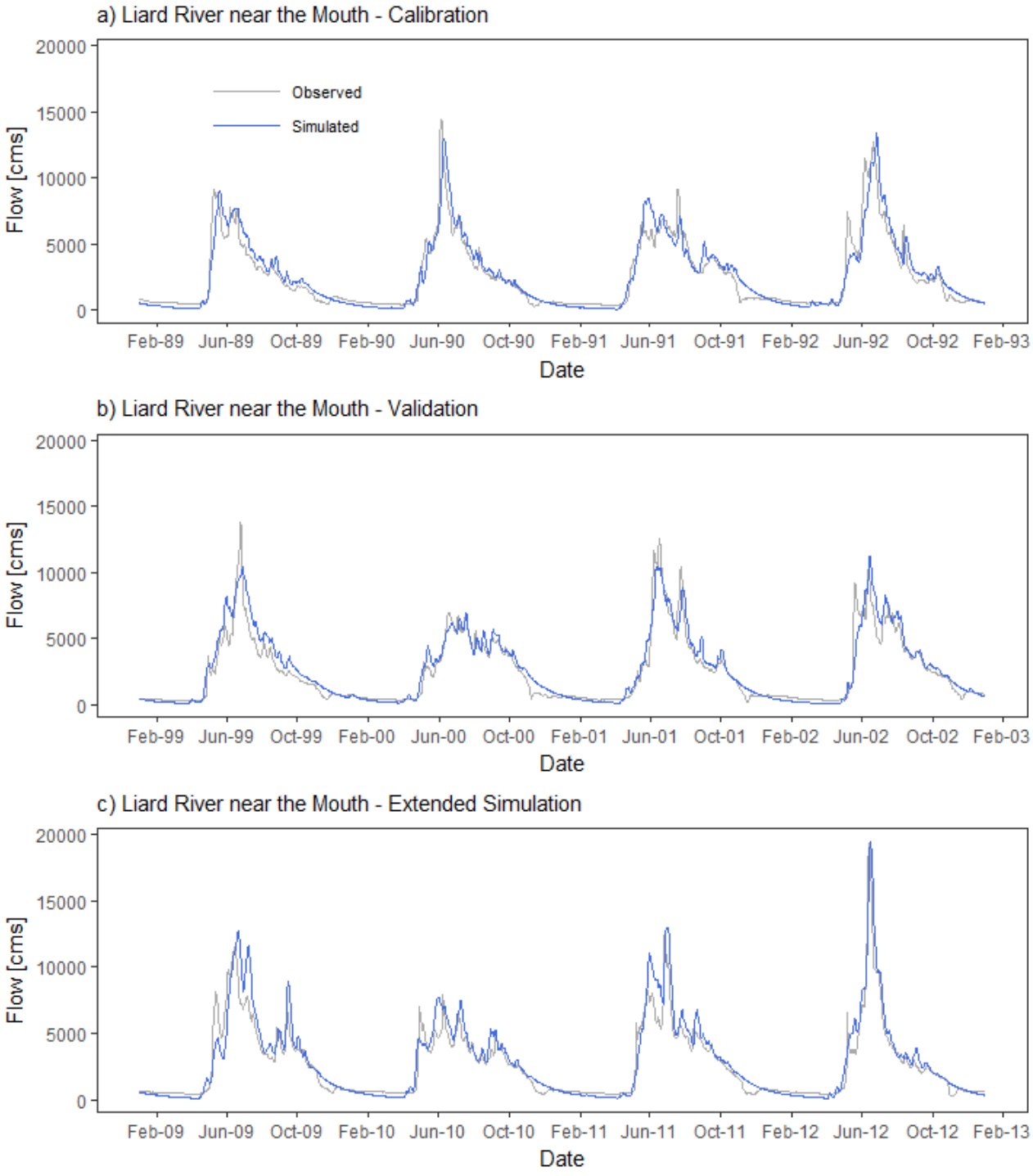

Figure 4.7: Hydrographs of select years during the calibration, validation, and extended simulation period for the Liard River near the Mouth (10ED002)

The model is able to capture the timing and magnitude of peak flow at these two gauges reasonably well as shown in Figure 4.8 and Figure 4.9. Years which resulted in observed and

simulated peaks from different events are not included in the figures. 1991 in Figure 4.6 and Figure 4.7 is an example of when observed and simulated peaks occurred from different events.

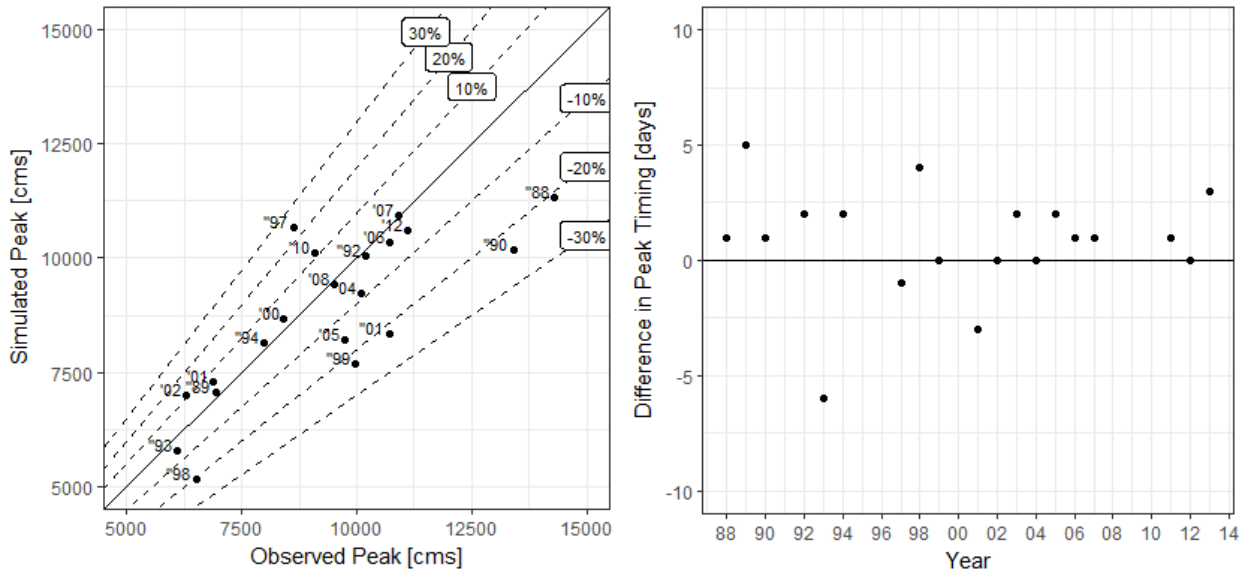

Figure 4.8: Peak error and timing error at Liard River at Fort Liard (10ED001)

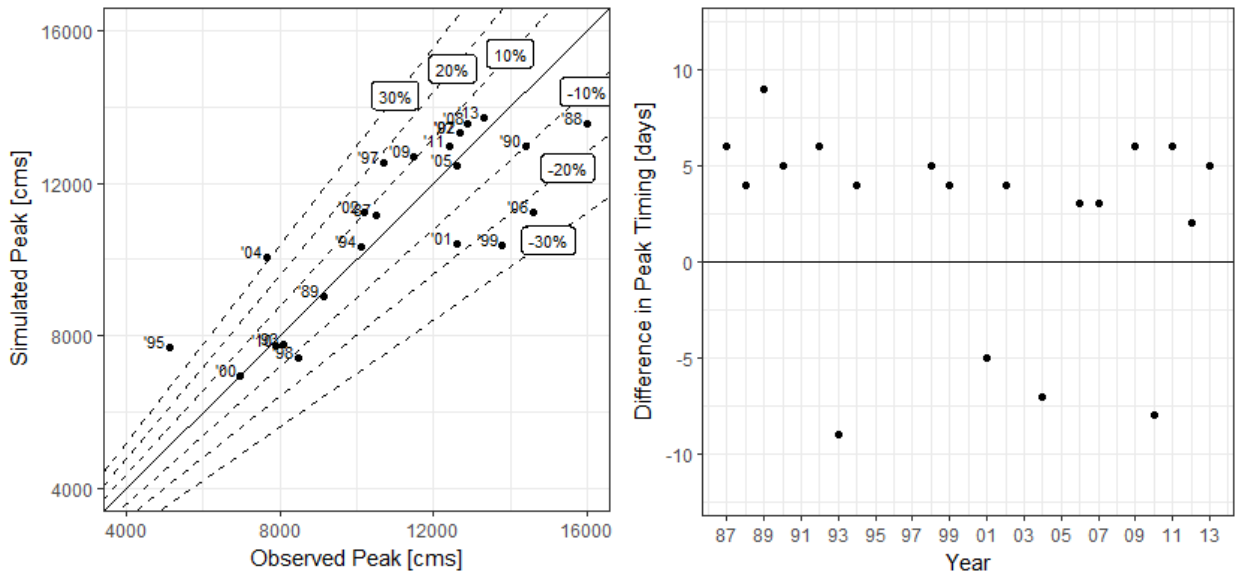

Figure 4.9: Peak error and timing error at Liard River near the Mouth (10ED002)

The timing of peaks at the Liard River at Fort Liard is on average two days after when the actual peak occurred. Further downstream at the Liard River near the mouth the error increases to an average of four days after when the actual peak occurred.

The timing of the start of the rise of the hydrograph is also an important point on the modelled hydrograph, as this point indicates that breakup is imminent. The timing of the rise of the hydrograph was calculated as described in Section 3, using the minimum cumulative mean flow from the start of the water year. The timing of the observed and simulated hydrograph rise at the three gauges of interest is shown Figure 4.10.

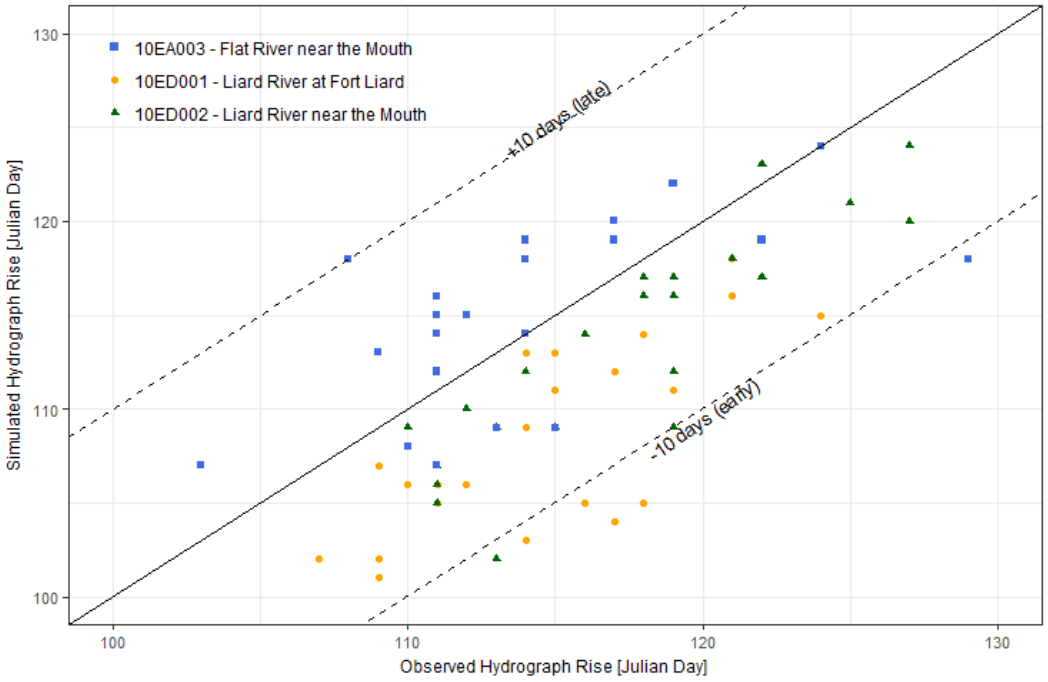

Figure 4.10: Comparison between the observed and simulated rise in hydrograph

The two gauges on the Liard (10ED001 and 10ED002) tend to simulate the rise in the hydrograph earlier than the observed hydrograph. At the upstream gauge, Liard River at Fort Liard (10ED001), the rise in the hydrograph occurs on average five days early. At the downstream gauge, Liard River near the Mouth, the rise occurs on average 7 days early. At Flat River (10EA003) there is no consistent bias in the model simulating the rise early or late. The early rise in the hydrograph which is occurring at 10ED001 and 10ED002 appears to occur as a result of snowmelt from the forested regions of the Fort Nelson, Petitot and Lower Liard regions of the basin. Despite the discrepancy between the timing of the start of the rise in the hydrograph, in general the model can simulate the slope of the main rising limb of the hydrograph well. Figure 4.11 shows an example of the early rise in the hydrograph timing and the overall rising limb performance.

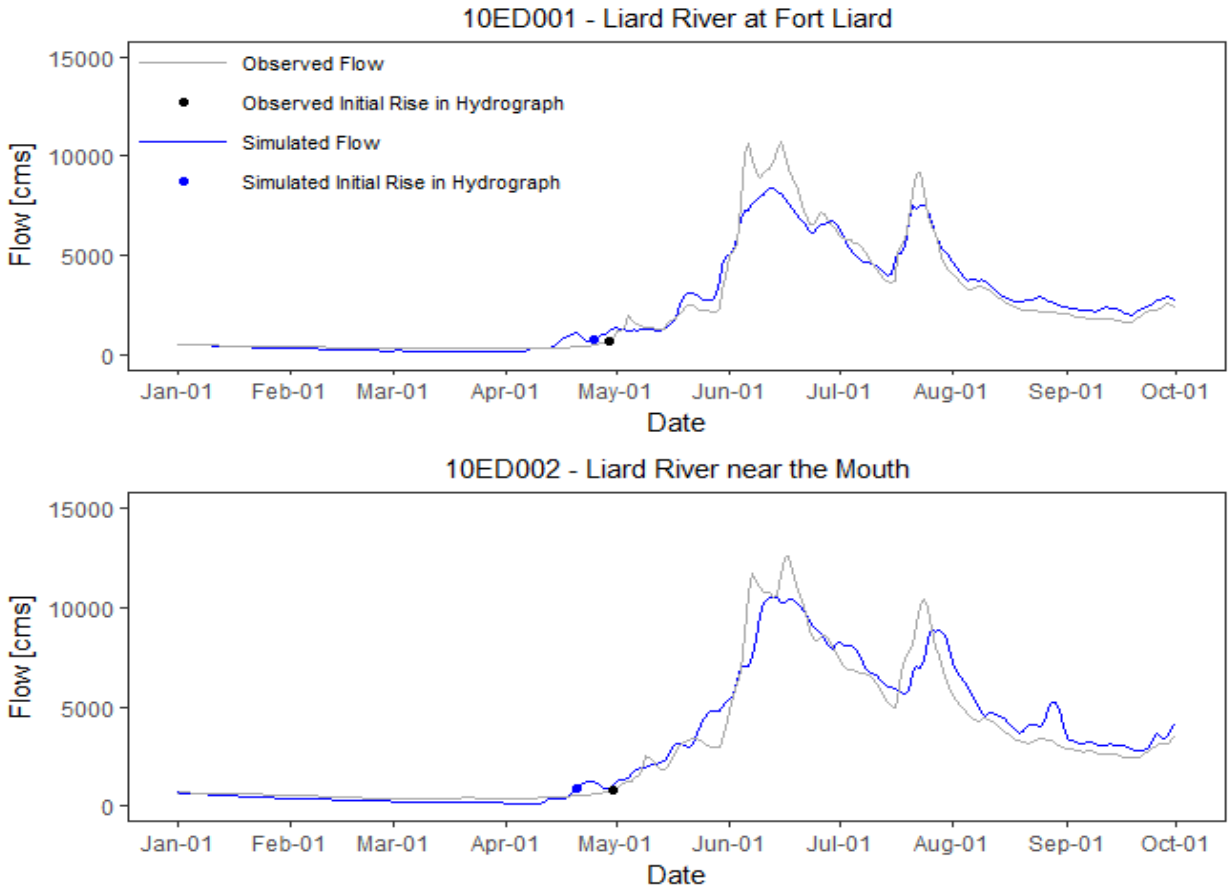

Figure 4.11: Hydrograph for 2001 along the Liard River showing the early bias in the rise of the hydrograph and the slope of the rise in the hydrograph

The bias in the rise in the hydrograph will need to be accounted for when forecasting the timing of breakup at these two locations. Since observations which were flagged as ice conditions were not considered in the calibration and validation metrics, this point was only visually calibrated during manual calibration as it would always occur when ice is present. In the future, potential improvements could be made by including this point more explicitly in the calibration process.

In addition to representing the hydrograph well, the model also can simulate snow accumulation and melt, and annual ET values similar to field observations across the basin. Snow accumulation at select snow survey sites are shown in Figure 4.12 and annual ET rates summarized in Table 4.4. The snow survey data is representative of point measurements within the basin, therefore variability between the point measurement and the modelled values are expected. Consistent biases between the model simulation and measurements were not observed.

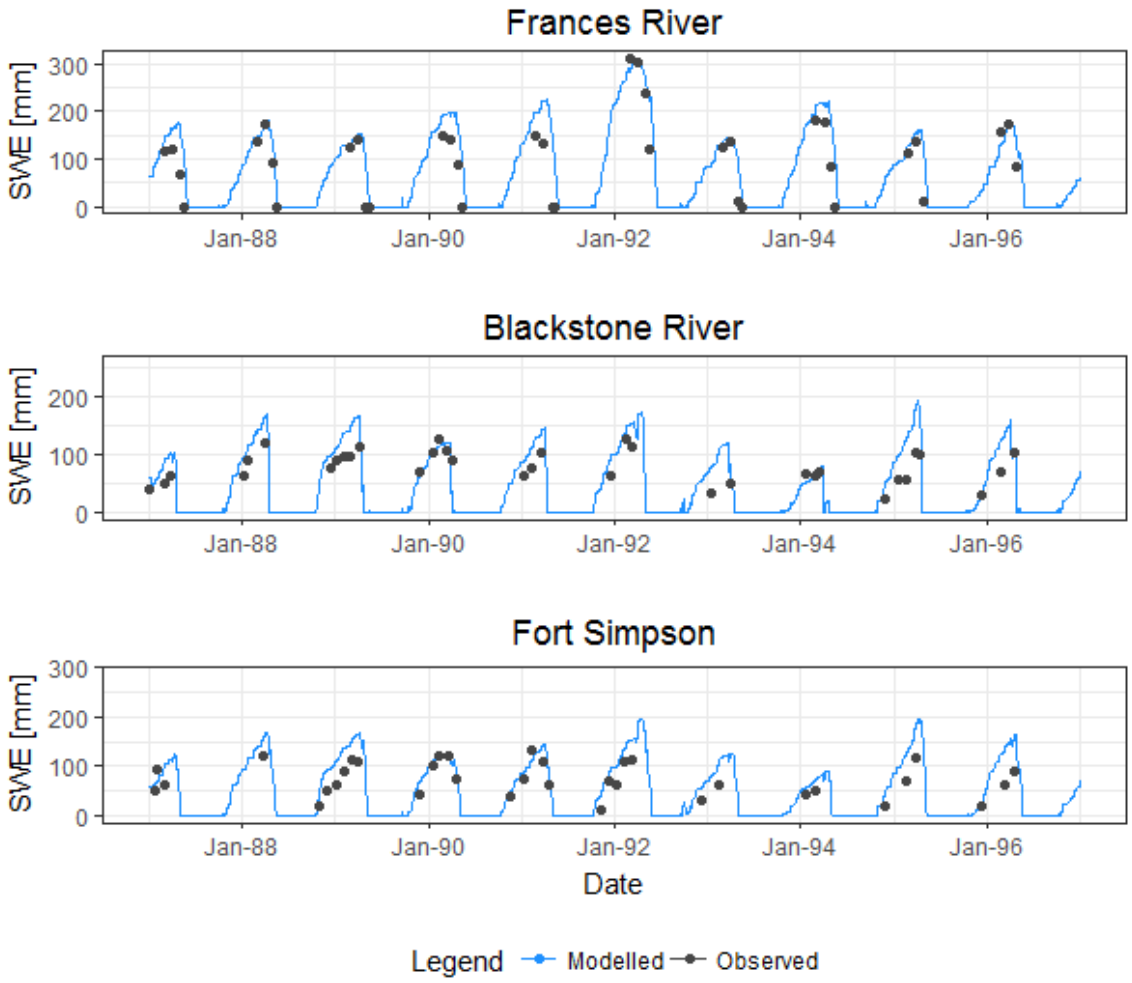

Figure 4.12: Simulated snow water equivalent (SWE) and measured SWE at select snow survey locations

Table 4.4: Summary of modelled evapotranspiration rates across the basin

Annual ET Location	Approximate Rate (mm/year)	Modelled Rate (mm/year)
Lower Liard	300	285
Nahanni Range	160 – 250	188
Basin Wide	190 – 250	230

4.5.2 Model Structure Modifications

Through the calibration procedure, some modifications were made to the initial HBV-EC model to better represent the hydrological processes throughout the basin. Across the entire basin, the lake evaporation routine was eliminated from the model and open water evaporation added instead. The lake evaporation function in the original HBV model is simulated by a moisture dependent evaporation rate from the lower soil structure and is not physically based. Using the

original lake evaporation function resulted in annual evapotranspiration rates across the basin double that of the approximate values expected. Using open water evaporation within the model reduced the amount of evapotranspiration occurring to reasonable rates and allowed for regions with more open water (i.e. lakes and wetlands) to have higher levels of evapotranspiration than other regions within the basin.

The manual calibration procedure also highlighted specific regions which required more consideration to the variation of hydrological processes and responses within the basin. The wetland dominated landscape of the Fort Nelson, Petitot and Lower Liard was one region known to have fundamentally different responses from the mountainous basins. Figure 4.13 shows the impact of model structure on the model performance within this region. The initial model structure which worked well in the mountainous regions of the model, did a poor job simulating the falling limb of the hydrograph. Additionally, individual events tended to be underestimated. Modification were made to the model structure to better represent the wetland dominated landscape. This included modifying the groundwater structure to not include a slow reservoir response. Additionally, a simple wetland structure was added which required depression storage to reach a certain threshold before being released to the channel.

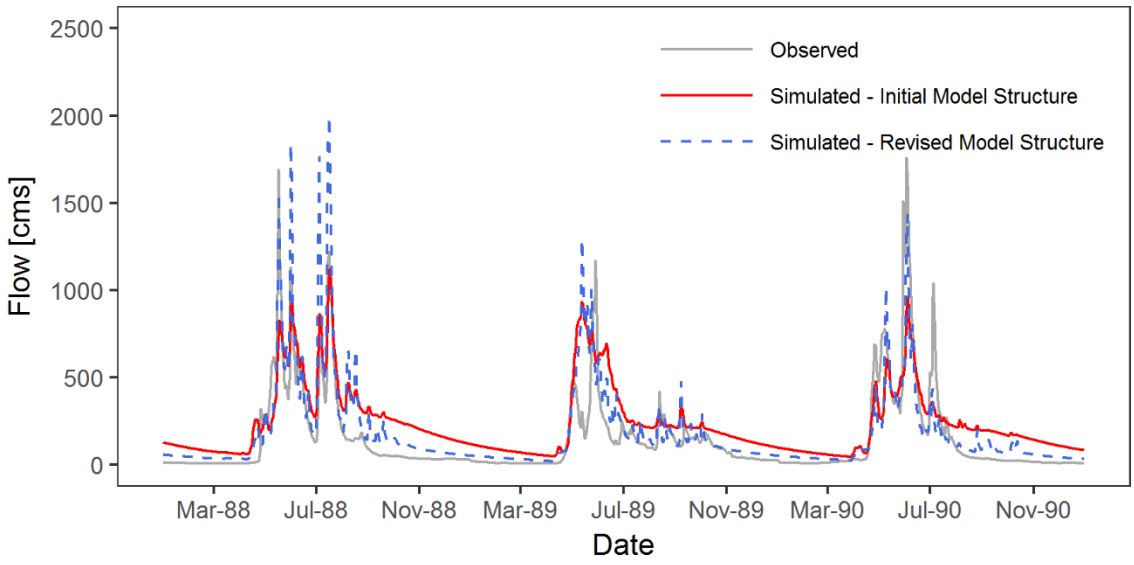

Figure 4.13: Hydrographs at Fort Nelson River above Muskwa River (10CC002) showing impact of model structure on results

There are some uncertainties and limitations related to the wetland dominated region within the model which require consideration. Notably, the classification of wetlands in the land cover data is highly uncertain with visible differences in provincial classification schemes seen in the data. Additionally, this region receives intense localized summer storms which can cause large peaks in the summer. The two meteorological stations used in the model for this region do not necessarily capture these localized storms resulting in the simulation missing these peaks. In addition, fill and spill hydrology is known to occur within this region (Connon et al., 2015), and is not explicitly treated in the model. The model only considers a single effective threshold across the entire wetland landscape when in reality different thresholds will be occurring for each individual wetland.

The other region where the manual calibration procedure led to identification of an anomalous hydrological response was in the Nahanni region. The Nahanni region is mountainous with a freshet dominated hydrograph; therefore, it was expected that the parameters and model structure from the other mountainous regions would also work well in this basin. However, examination of the hydrograph showed that although the general timing and magnitude was appropriate in the simulated hydrograph when using the initial model structure, the simulated hydrograph was much smoother than the observed hydrograph, as shown in Figure 4.14. Upon further research, it was discovered that the Nahanni range is part of a large complex karst system with surface springs, conduit systems, and multiple aquifers which explain the rapid responses seen in the observed hydrograph (Brook & Ford, 1980). As a result, the groundwater structure within this basin were modified to better represent the karst system based on a conceptual model structure developed by Hartmann et al. (2013) specifically for karst systems.

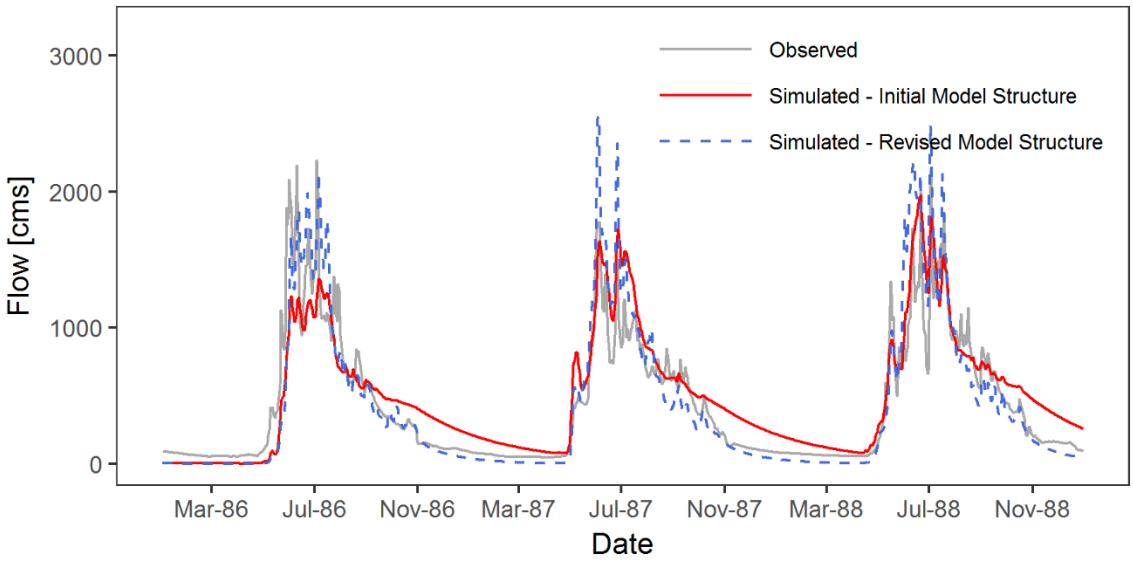

Figure 4.14: Hydrographs at South Nahanni River above Clausen Creek (10EC001) showing impact of model structure on results

4.5.3 Comparison to Existing Models

There are other documented models of the Liard basin which have been developed for research purposes. The models used to simulate the Liard include CLEVER (Luo et al., 2015), SLURP (Thorne, 2011; Thorne & Woo, 2006; van der Linden & Woo, 2003b, 2003a) and LIARDFLOW (van der Linden & Woo, 2003a). The model performance of the Raven model has been compared to these models where applicable and is summarized below.

CLEVER Model

The CLEVER model of the Liard was developed as part of a study of provincial wide flood forecasting for the province of British Columbia (Luo et al., 2015). In the study, the model simulation is based on a one year period, where the model is run for 30 days, with the first 20 days of each model run used for calibration. As a result, the CLEVER model can achieve a high NSE value and low percent bias, as indicated in Table 4.5. A simulation period of one year does not allow for adequate assessment or comparison of the model to the Raven based model, which utilizes a 20 year simulation period and only one parameter set.

Table 4.5: Comparison of Raven and CLEVER model performance for the Liard basin

Station ID	Station Name	Raven		CLEVER	
		NSE	% Bias	NSE	% Bias
10BE001	Liard River at Lower Crossing	0.85	5.6	0.96	0.7

SLURP Model

A number of models of the Liard basin using the SLURP semi-distributed model have been developed. Thorne (2011) developed a model which was calibrated using only the outlet gauge, for the period from 1973 to 1990. No validation period was used. Thorne and Woo (2006) also developed a model of the Liard which was calibrated using the outlet gauge which compared three different climate sets. The calibration was based on a one year period (1998-1999 water year) and the validation was based on a two year period (1999-2001 water years). Van der Linden and Woo (2003a, 2003b) used three subbasins within the Liard to compare model complexity and transferability of hydrological model parameters. In both instances the model was calibrated using a three year period from 1985 to 1988. A validation period from 1981 to 1984 was used, however no model diagnostics are reported during validation. Table 4.6 compares the various SLURP models to the Raven model performance. Since van der Linden & Woo presented model performance results graphically, a range of NSE values is given instead of an exact value. Performance from Thorne and Woo's (2006) model which used in situ climate data (Environment Canada climate stations) is indicated in the table.

Table 4.6: Comparison of Raven and SLURP model performance for the Liard basin

SLURP Model	Station ID	Station Name	Raven NSE	SLURP NSE
Thorne (2011)	10ED002	Liard River near the Mouth	0.70	0.75
Thorne & Woo (2006)	10ED002	Liard River near the Mouth	0.7	0.87
	10ED001	Liard River at Fort Liard	0.8	0.78
	10BE001	Liard River at Lower Crossing	0.86	0.76
	10AA001	Liard River at Upper Crossing	0.84	-1.1
	10AB001	Frances River	0.71	-2.1
	10CC002	Fort Nelson River above Muskwa River	0.34	-0.2
	10EB001	South Nahanni River above Virginia Falls	0.67	-7.1
Van der Linden & Woo (2003a)	10ED002	Liard River near the Mouth	0.70	0.8-0.9
	10CD001	Muskwa River near Fort Nelson	0.67	0.4-0.6
	10BB001	Kechika River near the Mouth	0.72	0.6-0.8
Van der Linden & Woo (2003b)	10CD001	Muskwa River near Fort Nelson	0.67	0.6-0.8

During validation, Thorne & Woo (2006) reported an NSE value of 0.80 whereas the Raven model has an NSE value of 0.70.

In general, the Raven model has comparable or better performance in terms of NSE values to the SLURP model, even though there is significant differences in the calibration period and number of gauges used in the development of the model. The model developed by Thorne & Woo (2006) only used a one year calibration period, therefore it is difficult to obtain an adequate understanding of model performance. However, this model demonstrates that when a model is only calibrated to the outlet gauge, the model can compensate for hydrological processes at the subbasin level causing significantly poorer performance within these subbasin. In contrast, the Raven model has strong performance at different scales within the model.

LIARDFLOW

LIARDFLOW was used by van der Linden and Woo (2003a) in their comparison of model complexity on performance within the Liard basin. A modified version of LIARDFLOW was also used within the study which increased the model complexity through utilizing modules from SLURP for precipitation, snowmelt, infiltration, evapotranspiration and groundwater storage. The LIARDFLOW models were based on a three year calibration period from 1985 to 1988 and a three year validation period from 1981 to 1984. Table 4.7 summarizes the performance of the LIARDFLOW model against the Raven model. Since results are presented graphically a range of values is given for the original LIARDFLOW model and various modified versions. No validation metrics were reported in the study.

Table 4.7: Comparison of Raven and LIARDFLOW model performance for the Liard basin

Station ID	Station Name	Raven	LIARDFLOW	
		NSE	NSE (Monthly)	NSE (10 Day)
10ED002	Liard River near the Mouth	0.70	0.6-0.9	0 – 0.8
10CD001	Muskwa River near Fort Nelson	0.67	0.5-0.7	0.2 -0.8
10BB001	Kechika River near the Mouth	0.72	0.1-0.6	0 – 0.8

4.5.4 Discussion

Predicting river ice breakup with a hydrological model requires that the hydrological model be able to provide realistic results at multiple scales and for variables beyond just streamflow. The model of the Liard basin developed in Raven followed a number of unique strategies and features when compared to other hydrological models of the Liard basin, and hydrological models in general, which resulted in a high performing model. Notably, the model structure was explicitly considered during calibration and the calibration process made use of multiple

objectives and multiple gauges. The model calibration also focused heavily on manual calibration with automatic calibration only used to fine tune the model performance.

By using a flexible modelling framework, the model structure could be explicitly included in the calibration process. This resulted in a number of modifications to the original HBV-EC model structure to better represent the hydrologic processes and conditions occurring within the Liard basin. The lake evaporation structure was replaced with a more physically based open water evaporation process within the model. A simple wetland structure was included to improve model performance in the wetland dominated portion of the basin and a karst groundwater structure was added to the model to better represent the influence of a karst system in the Nahanni region of the basin. The modifications to the model structure allowed for consideration of the "uniqueness of place" (Beven 2000) and for a better understanding of the basin's hydrology. Given that this basin is large, spatially heterogeneous, and relatively data sparse an improved understanding in the basin's hydrology is important for developing a realistic and robust model. Notably, the inclusion of model structure in the calibration process allowed for the discovery that the Nahanni range was part of a complex karst system. Discrepancies in the model structure performance within this basin and the subsequent testing and modifying of the groundwater structure helped identify this feature within the Liard basin that would likely have been overlooked otherwise.

The development of the model was based on a calibration strategy that relied on multiple hydrometric gauges and multiple objectives. Many hydrological models like the SLURP based Liard model (Thorne & Woo, 2006) are based on calibrating to a few a gauges, or a single gauge. As a result, the model will perform well at the few gauges to which the model is calibrated to but can lead to large discrepancies in performance elsewhere within the basin. The SLURP model (Thorne & Woo, 2006) highlights this, with the calibration at the outlet gauge achieving a NSE value of 0.87 but with internal subbasins having negative NSE values. The calibration of the Raven model made use of 29 different hydrometric gauges during manual calibration and 9 gauges during automatic calibration. This helped constrain parameters to ensure that the model performs well and provides realistic results at different scales within the model. During manual calibration, no explicit multi-objective criteria was defined, however the performance across multiple gauges was compared alongside snow and evaporation data. This further constrained

parameters and ensured that internal processes within the model were being appropriately represented. During automatic calibration, an explicit multi-objective criteria was defined based on an area weighted KGE of the nine gauges, penalized by percent bias. This multi-objective criteria helped maintain the excellent performance of the model at different scales.

The calibration process relied heavily on manual calibration. This allowed for components like the model structure to be easily modified and a through understanding of the basin and model function. Table 4.8 summarizes the difference in model performance after manual and automatic calibration at the nine gauges which cover the full calibration and validation period within the model within the Liard.

Table 4.8: Model performance after manual and automatic calibration

Station	Station Name	Manual Calibration			Automatic Calibration		
		NSE	% Bias	KGE	NSE	% Bias	KGE
10AA001	Liard River at Upper Crossing	0.85	0.0	0.89	0.84	5.19	0.89
10AB001	Frances River near Watson Lake	0.65	-4.8	0.78	0.71	-12.58	0.80
10BE001	Liard River at Lower Crossing	0.86	1.1	0.88	0.86	5.62	0.91
10BE004	Toad River above Nonda Creek	0.69	-12.4	0.76	0.87	-8.81	0.89
10CB001	Sikanni Chief River near Fort Nelson	0.41	6.5	0.68	0.40	9.53	0.69
10CD001	Muskwa River near Fort Nelson	0.64	10.4	0.71	0.67	9.18	0.74
10EB001	South Nahanni River above Virginia Falls	0.57	-4.3	0.76	0.67	-3.48	0.83
10ED001	Liard River at Fort Liard	0.79	7.9	0.83	0.80	10.15	0.83
10ED002	Liard River near the Mouth	0.69	8.1	0.82	0.70	10.13	0.83

The development of the model based on manual calibration alone resulted in performance very comparable to the results after automatic calibration. The automatic calibration maintained or improved results incrementally at most gauges, with larger improvements in performance at Frances River near Watson Lake (10AB001), Toad River above Nonda Creek (10BE004), and South Nahanni River above Virgina Falls (10EB001). Although manual calibration is a more time consuming process, it allowed for a good understanding of the basin and model function and for the model structure to be explicitly considered in the calibration approach.

The primary purpose of the model is to be used as a basis for predicting the timing and severity of breakup. However, the model may also be used for forecasting open water flooding and as a platform for improving wetland and long term land use simulations. Overall, the model performance will be adequate for these objectives. The model can simulate open water

conditions well but also provide realistic representations of processes which strongly influence river ice like the snow accumulation and melt, and the rising limb of the hydrograph.

Chapter 5
Results and Discussion

This chapter focuses on the results of the coupled hydrological model and river ice model. This includes analysis of the simulated freeze up timing, ice growth, breakup timing, and breakup severity. Throughout the chapter the final calibrated model of the Liard basin, as described in Chapter 4, is used.

5.1 Freeze up Timing

As described in Section 3.2, a logistic regression was developed to predict the timing of freeze up based on cumulative freezing degree days accumulated from the first day where the mean temperature is below 0°C. The resultant logistic regression model coefficients from the three gauges are summarized in Table 5.1.

Table 5.1: Logistic Regression Coefficients

Gauge Name	Gauge	Intercept	B_1	Data Period
Flat River near the mouth	10EA003	-4.49	0.006	2002-2013
Liard River near Fort Liard	10ED001	-5.00	0.045	1996-2013
Liard River near the mouth	10ED002	-4.26	0.012	1996-2013

The simulated timing of freeze up from the logistic regression was compared against freeze up timing extracted from the raw stage data (Section 3.1.3) and using observations from the Canadian Ice Database (CID) (Section 3.1.1). Raw stage data within the Liard is only available after 1996 whereas the CID covers data up to 1996 in some locations. For 1996, the average difference between the CID observation and freeze up timing from the raw stage data is only one day. Due to the small difference in timing, the CID observation of complete freeze over was deemed to be an appropriate date to make a direct comparison to even though the logistic regression is based on the timing of stable freeze up, as extracted from the raw stage data. The CID data also provides a validation data source as all available raw stage data was used to develop the logistic regression. Additionally, freeze up timing was simulated at a fourth independent location, Liard River at Upper Crossing (10AA001), as another form of validation The location of all stations used in simulating and validating freeze up are shown in Figure 5.1

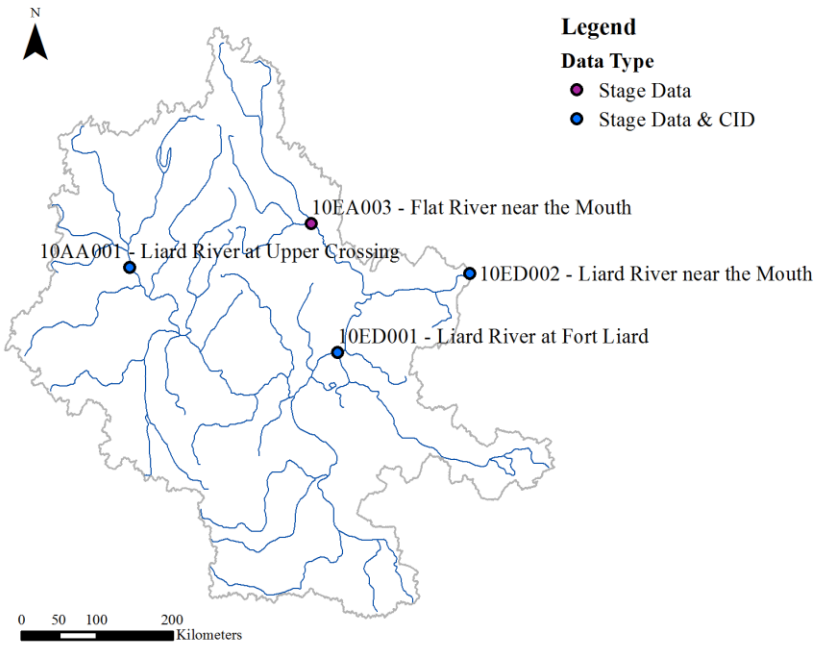

Figure 5.1: Location of observation points used for verifying freeze up timing simulations

The modelled and observed freeze up dates are shown in Figure 5.2 for the two different data sources. The dashed lines on Figure 5.2 indicate 10 days prior to and after observed freeze up. The spread between modelled and observed data is shown in Figure 5.3 and related metrics summarized in Table 5.2.

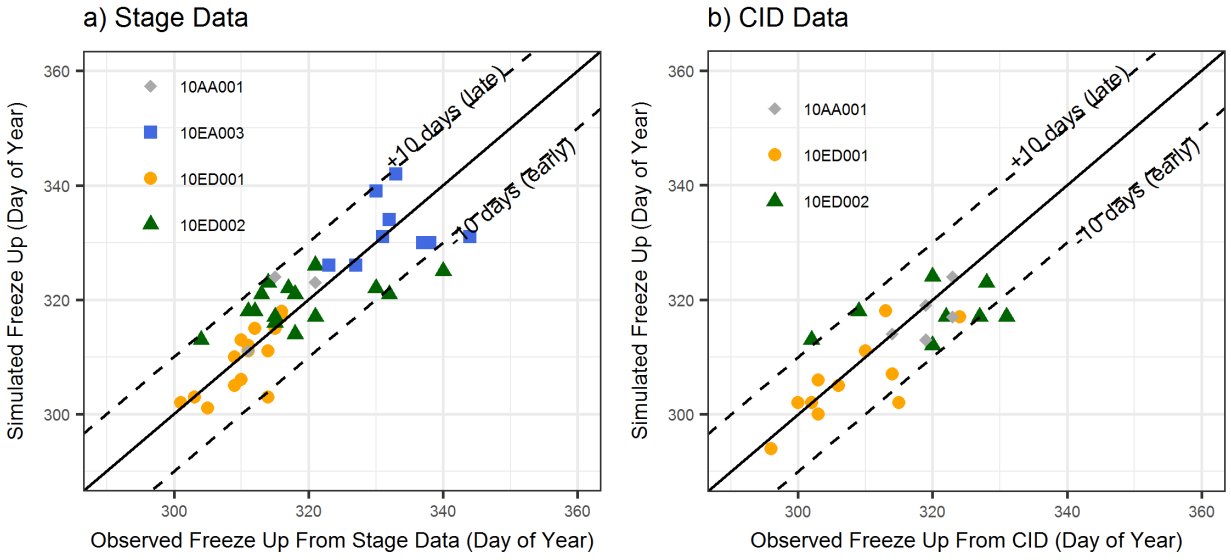

Figure 5.2: Comparison of modeled freeze up timing to observed freeze up timing from stage data and CID database observations

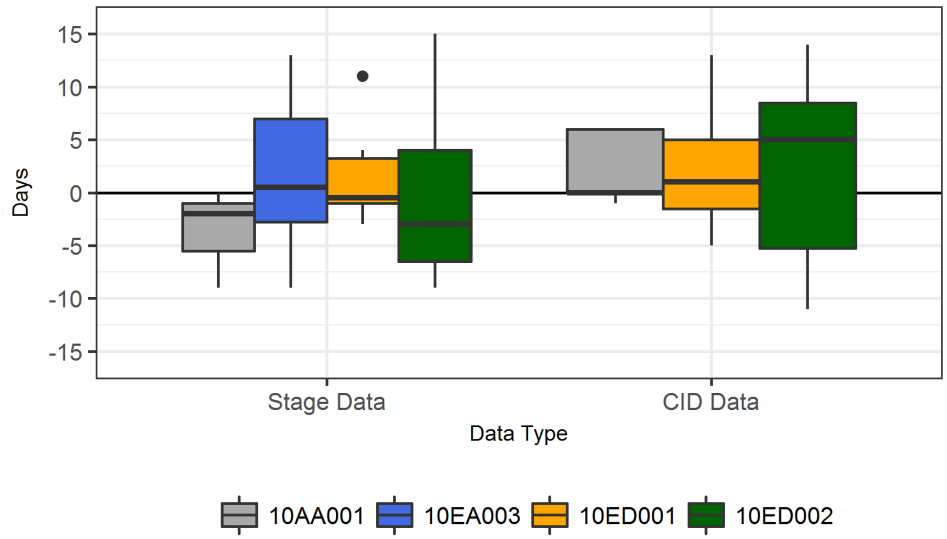

Figure 5.3: Difference between observed and modelled freeze up timing by gauge and observation data type

Table 5.2: Freeze up timing performance metrics by gauge and validation data type

Observation	Gauge	Bias [d]	Mean Absolute Error [d]	R^2
Manual	10AA001	-3.7	3.7	0.58
	10EA003	1.3	5.9	0.02
	10ED001	0.8	2.4	0.67
	10ED002	-0.8	6.4	0.34
	Overall	0.04	4.6	0.68
CID	10AA001	2.2	2.6	0.41
	10ED001	2	4	0.64
	10ED002	2.3	8.3	0.14
	Overall	2.1	5.1	0.61
All	Overall	0.7	4.8	0.67

In general, the regression predicts the timing of freeze up within one week of the observed freeze up date. The model adequately represents the stable freeze up timing from the raw stage data and the observation of complete freeze over from the CID. There is a slight decrease in performance when comparing the simulated freeze up to the CID observations. This is likely due to the logistic regression being based on the timing of stable freeze up from the raw stage data instead of the complete freeze over observation from the CID database.

Within the hydrological model, the timing of freeze up is used as an initiation point for simulating ice growth. Given the relatively small error between predicted and observed freeze up timing, and the overall duration of winter, the model is deemed appropriate for this purpose.

5.2 Ice Growth and Decay

The 1D river ice model, described in Section 3.3, was coupled with Raven to simulate ice growth and decay through the winter. The river ice model was implemented in MATLAB with HRU specific outputs (temperature, snow, shortwave radiation) from the hydrological model used as inputs to the model.

Within the Liard basin there is limited information available on ice thickness to validate the ice thickness simulations. The Canadian Ice Database contains three observation locations which provide annual maximum ice thickness measurements. The three locations, Liard River near Fort Liard, Liard River near Fort Simpson, and Fort Nelson River are shown in Figure 5.4. Information on when the maximum ice thickness measurement was collected is not contained within the database therefore the simulated maximum over a season was compared to the measured value. As a result, there is some uncertainty to whether the measured value is a true seasonal maximum.

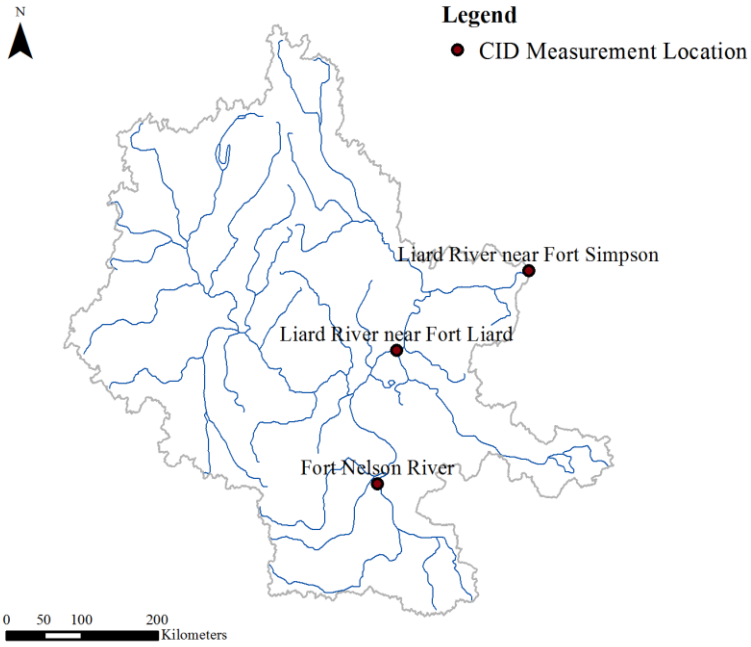

Figure 5.4: Location of observations with maximum ice thickness data in the Canadian Ice Database

The ice model was calibrated to the measured maximum ice thickness values by modifying parameters which influenced the growth phase. The over winter depth of snow cover is the most critical component to simulating ice thickness, as noted by Ashton (2011). Snow cover data on

the rivers was not available at these locations to help validate the model. Instead snow density and thermal conductivity were calibrated in conjunction with the modelled snow water equivalent from the hydrological model. Snow density values between 150 kg/m^3 and 250 kg/m^3 were used to maintain consistency with measured values from snow survey data in the Yukon and Northwest Territories. Thermal conductivity was varied between 0.15 W/m/°C and 0.3 W/m/°C as per the simulations completed by Ashton (2011). The surface heat transfer coefficient, H_{sa} was also varied between 10 and 20 W/m^2. However, this has a small influence comparative to the snow thickness on the overall growth of ice. Finally, the initial ice thickness was also used as a calibration parameter since a larger river like the Liard River would have a thicker, more consolidated ice cover during freeze up when compared to a smaller river like the Fort Nelson. Table 5.3 summarizes the calibrated parameters at each location.

Table 5.3: Calibrated Parameters for River Ice Simulations

Location	ρ_s [kg/m^3]	k_s [W/m/°C]	H_{sa} [W/m^2]	Initial Ice Thickness [m]
Fort Nelson River	150	0.15	10	0.01
Liard River near Fort Simpson	200	0.3	20	0.3
Liard River near Fort Liard	200	0.2	20	0.3

The measured ice thickness at Fort Nelson is consistently thinner than the measured values on the Liard River, resulting in a discrepancy between the calibrated parameters. A comparison between the cumulative freezing degree days at the different locations and the maximum ice thickness values, shown in Figure 5.5, showed that the temperature at Fort Nelson is comparable to that at Fort Liard, and not significantly warmer, which would explain the discrepancy in thicknesses.

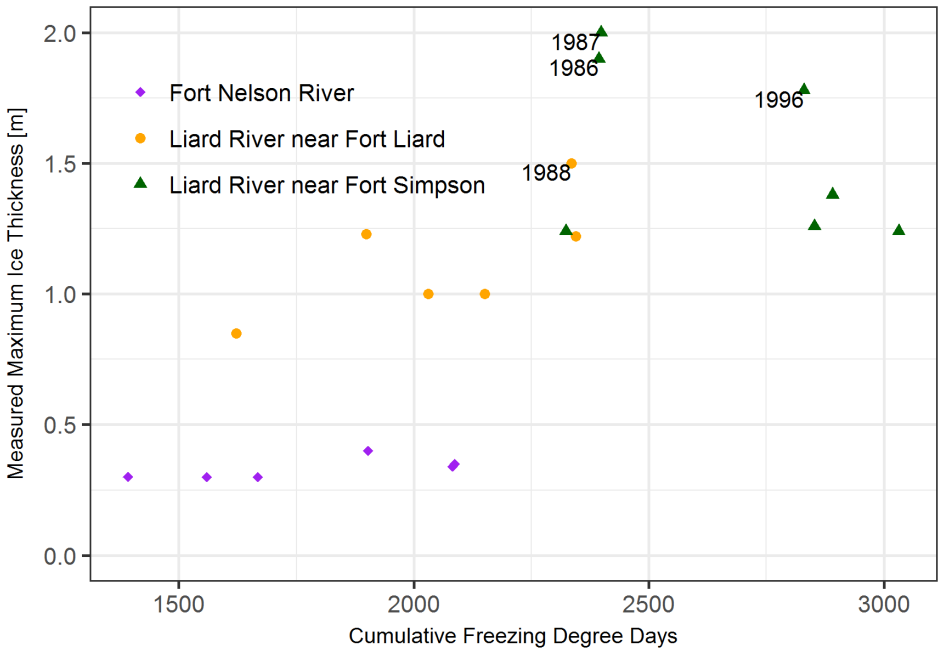

Figure 5.5: Comparison of measured maximum ice thickness to cumulative freezing degree days

There is some uncertainty associated with the measured values as no measurement date is associated with them. It is possible that the maximum values were based on measurements completed earlier in the winter season and did not reflect the true maximum. Some other possibilities for the discrepancy between locations include an increased level of snow ice formation on the Liard River, differences in stream temperature due to groundwater sources, as well as differences in snow accumulation due to local conditions, like blowing wind. However, it should be noted that the calibrated parameters at Fort Nelson are still within a reasonable range of reported values

No measurement data was available to calibrate the thinning of the ice against. Some consideration was given to the rate of decay, ensuring that the ice did not always melt well before the last B flag date. A surface albedo of 0.5 was used as per Ashton (2011), and the latent and sensible heat was corrected for diurnal fluctuations using:

$$q_H = 10(T_a + 2)\ when\ T_a < 5°C$$

and:

$$q_H = 15(T_a)\ when\ T_a \geq 5°C$$

in which q_h is the sensible and latent heat fluxes and T_a is the average air temperature.

The thinning of ice was initiated when the net energy flux was greater than 0 and all snow had melted from the surface of the ice. The overall timing of the thinning of ice is therefore sensitive to the timing of snow melt. In reality, ice would likely begin to decay prior to the complete melt of snow due to some conductive heat transfer through the snow as well as due to the heat flux from the water. In some years of the model simulations, snow did not fully melt until a substantial rise in the hydrograph had occurred resulting in fairly thick ice covers with high flows for years where low breakup severity was recorded. The increase in flow would be correlated with increased stream temperatures, indicating that some level of melt of the ice would occur, prior to the snow fully melting, as heat flux from water has been shown to be a significant during the melting process (Prowse & Marsh, 1989).

In general, the model tends to underestimate thicker ice covers, as indicated in Figure 5.6. As a consequence, the model does not have good R^2 values between the modelled and measured maximum thicknesses for individual locations (Table 5.4), although correlation is higher for thicknesses less than 1.5 m.

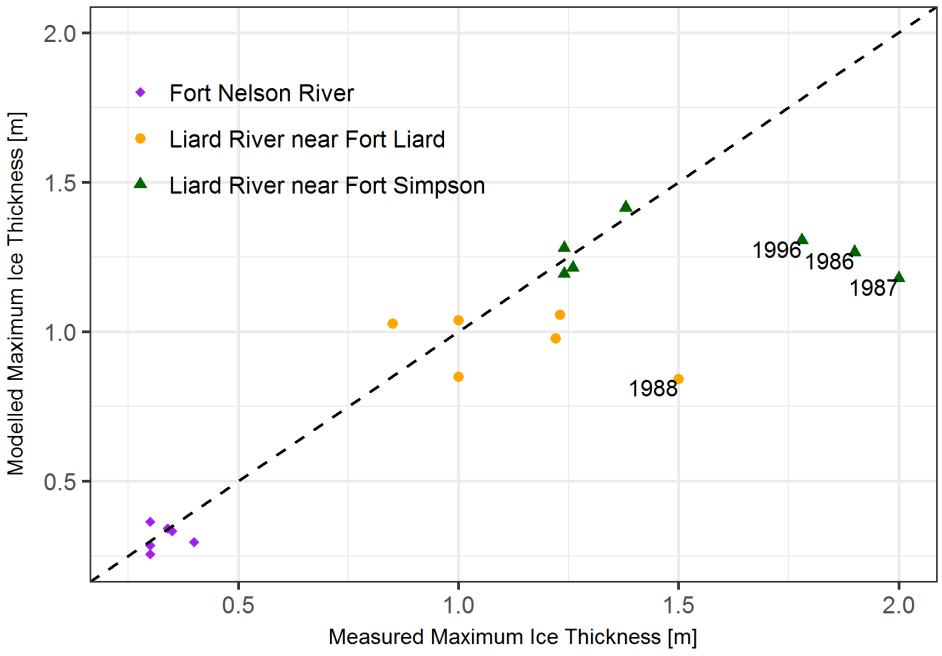

Figure 5.6: Comparison of simulated maximum ice thickness and measured maximum ice thickness

Table 5.4: Summary of model metrics for simulated maximum ice thickness

Location	Root Mean Square Error (m)	Coefficient of Correlation (R^2)
Fort Nelson River	0.05	0.01
Liard River near Fort Simpson	0.45	0.01
Liard River near Fort Liard	0.28	0.09
Overall	0.31	0.77

The comparison of cumulative freezing degree days in Figure 5.5 also showed that the thicker ice covers (larger than 1.5 m) which the model underestimated did not necessarily correspond to colder years. These thicker ice covers may be a result of white ice formation. The formation of white ice occurs when the weight of snow overtop of the ice depresses the ice and snow below the water level. In general, this causes an overall thicker ice cover due to the added white ice and the thinner insulating snow cover overtop the ice. Ashton (2011) used isostasy as an indication to whether white ice could or could not form on rivers or lakes, defined by:

$$Isostasy = \frac{\rho_s}{\rho_w} h_s - \frac{\rho_w - \rho_i}{\rho_w} h_i$$

Positive isostasy values indicate that the weight of snow is enough to cause the formation of white ice. The isostasy values were simulated throughout the years when thicker ice covers occurred, however they never reached positive values. Ashton (2011) did indicate that for river ice, no consistent isostasy conditions led to the formation of white ice therefore, it is still possible that white ice may have formed these years.

Overall, the simulation of ice thickness was imperfect but deemed adequate for the purposes of understanding for severe breakup. The calibration parameters can vary based on the location and size of the river and therefore should be carefully considered if no measurement data is available. The Ashton (2011) model implemented here was selected given that it emphasizes using only readily available data (air temperature). There are a number of more complex ice models which exist that explicitly consider things like the increase in snow density over the winter (Ménard et al., 2002), or the heat flux from the water (Shen & Chiang, 1984b), which may be more appropriate for detailed ice modelling. In the future, additional snow thickness and river ice thickness during both thickening and thinning would be useful to further train and validate the river ice model.

5.3 Breakup Timing and Severity

5.3.1 Breakup Timing

As discussed in Section 4.5, the hydrological model does an adequate job simulating the timing in the rise of the hydrograph, as defined by the minimum cumulative mean flow from the start of the water year. The model does have an early bias at the Liard River at Fort Liard (10ED001) and Liard River near the Mouth (10ED002) which will need to be considered during forecasting breakup timing until this artefact in the model simulation can be corrected. On average the model predicts the rise in the hydrograph five days early at Fort Liard and seven days early near the mouth.

Once the rise in the observed hydrograph occurs, breakup typically occurs within four days at Fort Liard, six days near the mouth, and five days on the Flat River (10EA003). Taking into consideration the bias and time lag between the rise in the hydrograph and breakup, the approximate timing of breakup can be estimated based on the following formula:

$$d_{breakup} = d_{rise} + \Delta d_{bias} + \Delta d_{lag}$$

where $d_{breakup}$ is the estimated timing of breakup, d_{rise} is the modelled rise in the hydrograph, Δd_{bias} is the average bias in the hydrological model and Δd_{lag} is the average lag between the rise in the hydrograph and breakup. Figure 5.7 and Figure 5.8a show the difference and spread between the known timing of breakup and the estimated timing of breakup based on this methodology. In general, using this method for simulating breakup timing results in the simulated breakup date being within one week of the observed breakup date with a mean absolute error of 3 days and a bias of -0.3 days. Individual performance metrics are summarized in Table 5.5.

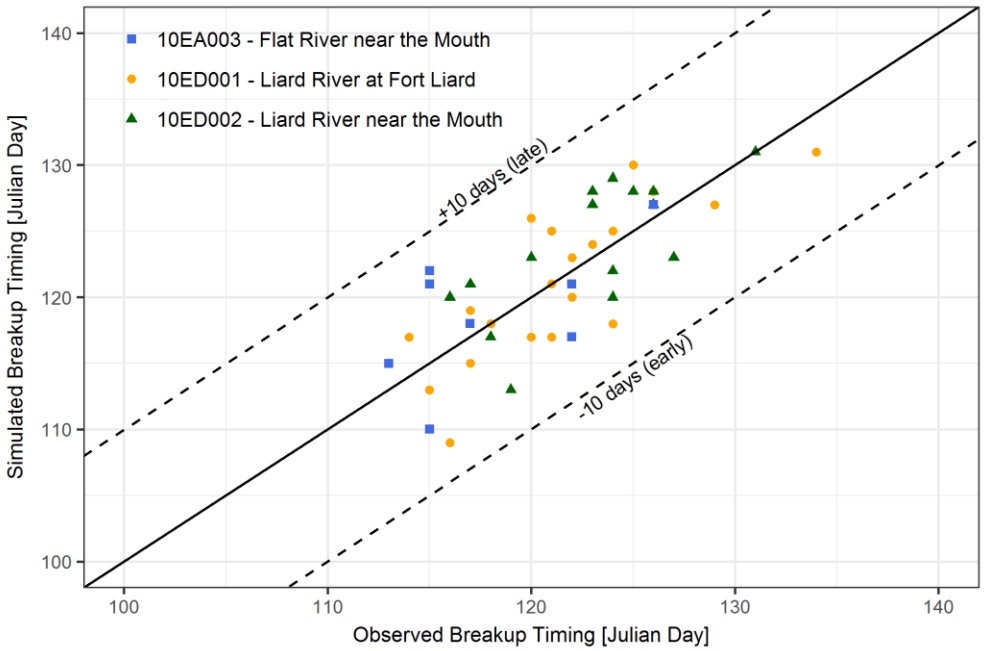

Figure 5.7. Comparison of simulated and observed breakup timing for three gauges within the Liard basin

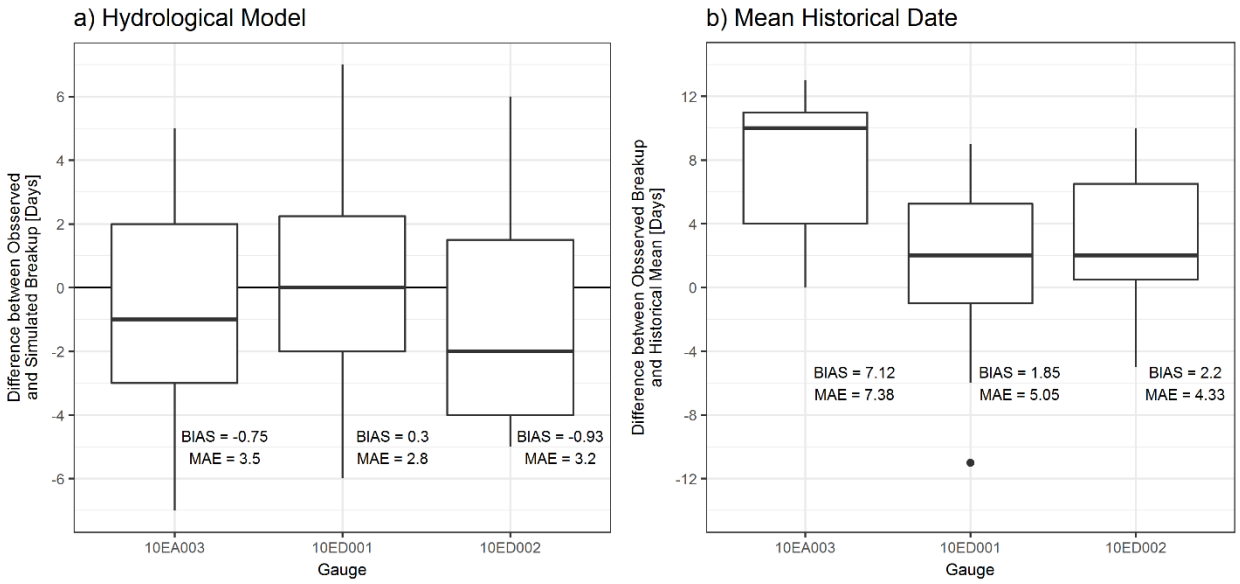

Figure 5.8 Spread between observed and simulated breakup timing for breakup dates simulated by a) the hydrological model and b) the mean historical breakup date

Other tools from the literature for predicting breakup severity either ignore predicting the timing of breakup (White, 1996), rely on the historical mean breakup date (Mahabir et al., 2002, 2006), are calculated based on water temperature (Morales-Marin et al., 2019) or are determined when the ice thickness completely melts (Ma et al., 2001). In general, tools from the literature which

can predict breakup timing do so within ten days of the observed breakup timing, making the methodology using the hydrological model comparable.

To further validate the hydrological model methodology, the results were compared to using the mean historical breakup date. Other tools which use this method, are based on historical breakup occurring over a small time period. For example at Fort McMurray, Alberta 75% of historical breakup dates are known to occur within one week of the mean historical date (Mahabir et al., 2006). There is similar variation on the Liard River as shown in Figure 5.8b. On the Liard River at Fort Liard (10ED001) and Fort Simpson (10ED002) at least 80% of break up occurs within one week of the mean historical breakup date. However, on the Flat River only 37% of breakup occurs within a week of the mean historical breakup date.

Although breakup occurs at a fairly consistent time on the Liard, using the methodology to predict the timing of breakup based on simulating the rise in the hydrograph does provide better results than using the mean historical date as summarized by the bias and mean absolute error in Table 5.5.

Table 5.5: Comparison of simulating breakup timing using the hydrological model and the mean historical breakup date

Gauge	Hydrograph Rise		Mean Historical Breakup Date	
	Bias [d]	MAE [d]	Bias [d]	MAE [d]
10ED001	0.30	2.8	1.9	5.1
10ED002	-0.93	3.2	2.2	4.3
10EA003	-0.75	3.5	7.1	7.4
Overall	-0.32	3	3.0	5.2

Simulating the breakup timing could be incrementally improved by reducing the bias of the early rise in the hydrograph in the hydrological model. Possible reasons for the early rise in the hydrograph include the snowmelt simulation used in the model and the routing parameters. Changing the snowmelt model from the HBV model to a more physically based model, like an energy balance method could improve the timing of when melt is first occurring within the basin which strongly influences the rise in the hydrograph. Additionally, since an increasing lag is seen closer to the outlet within the model, improved routing (definition of the channel geometry and routing parameterization) could potentially improve the model function. Routing within the model was not a focus of the calibration process therefore, it is expected that some improvement could be seen by focusing on these parameters.

5.3.2 Breakup Severity

The methodology outlined in Chapter 3 for predicting breakup severity based on the flow, cumulative shortwave radiation and ice thickness at the initiation of breakup was applied using the hydrological model simulations of flow and breakup timing. In evaluation, it is desirable that forecasting models are biased towards false positives rather than false negatives, with high magnitude false negatives being particularly problematic. The prediction results at Fort Liard and Fort Simpson are shown in Figure 5.9 and Figure 5.10 and summarized in Table 5.6.

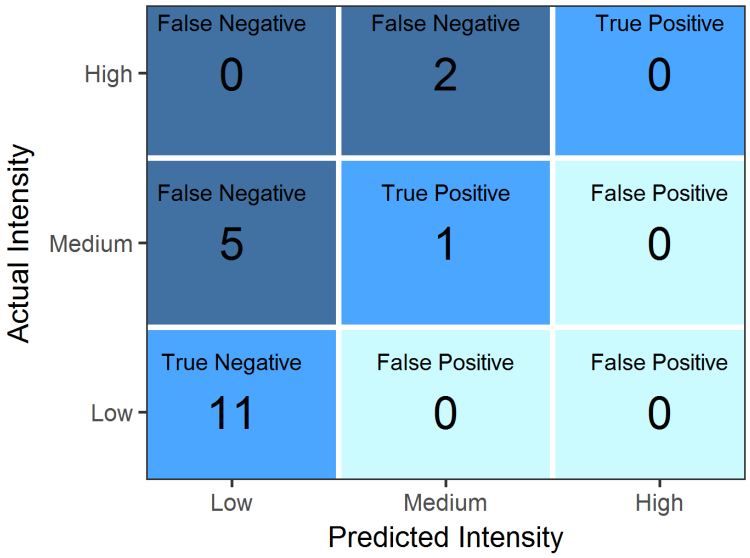

Figure 5.9: Prediction results at Fort Liard using the hydrological model simulation outputs

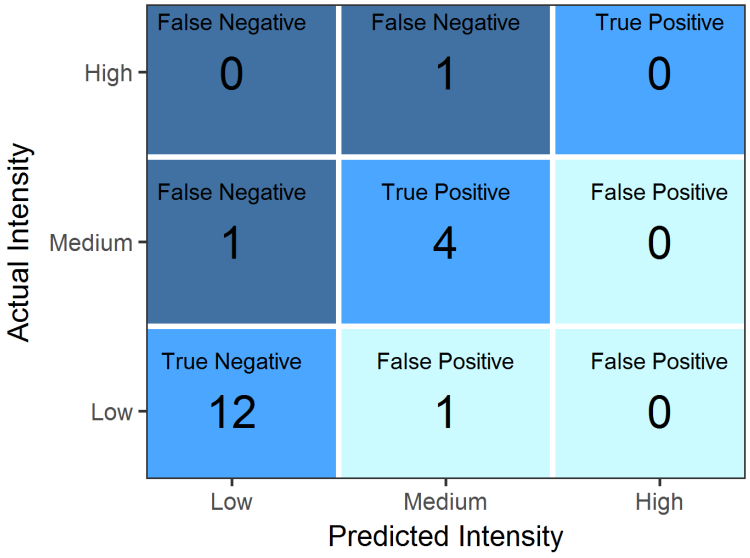

Figure 5.10: Prediction results at Fort Simpson using the hydrological model simulation outputs

Table 5.6: Summary of false predictions using measured flow and simulated flows

Location	Real Time Measured Flow		Simulated Flows	
	False Negatives	False Positives	False Negatives	False Positives
Fort Liard	0%	15%	36%	0%
Fort Simpson	0%	15%	5%	10%

When using the simulated flows, the prediction tends to underestimate the severity of events, with all high severity events classified as medium severity. Additionally, at Fort Liard most medium severity events were classified as low severity. Upon examination of the simulated flow and cumulative shortwave radiation plots at Fort Liard and Fort Simpson (Figure 5.11 and Figure 5.12), the model tends to underestimate the rate of rise in the hydrograph resulting in the increased rate of false negatives.

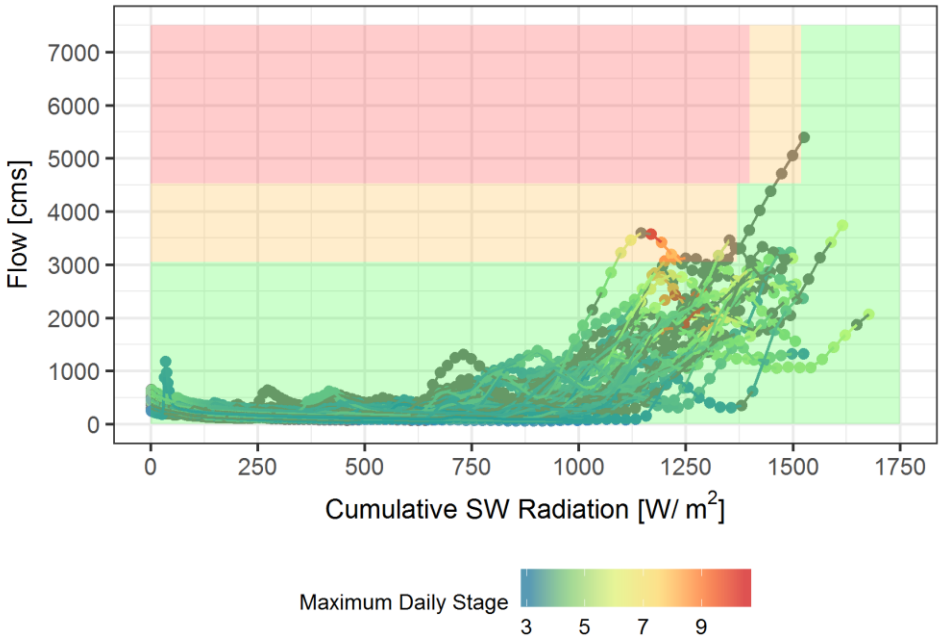

Figure 5.11: Cumulative shortwave radiation and simulated flow at Fort Liard

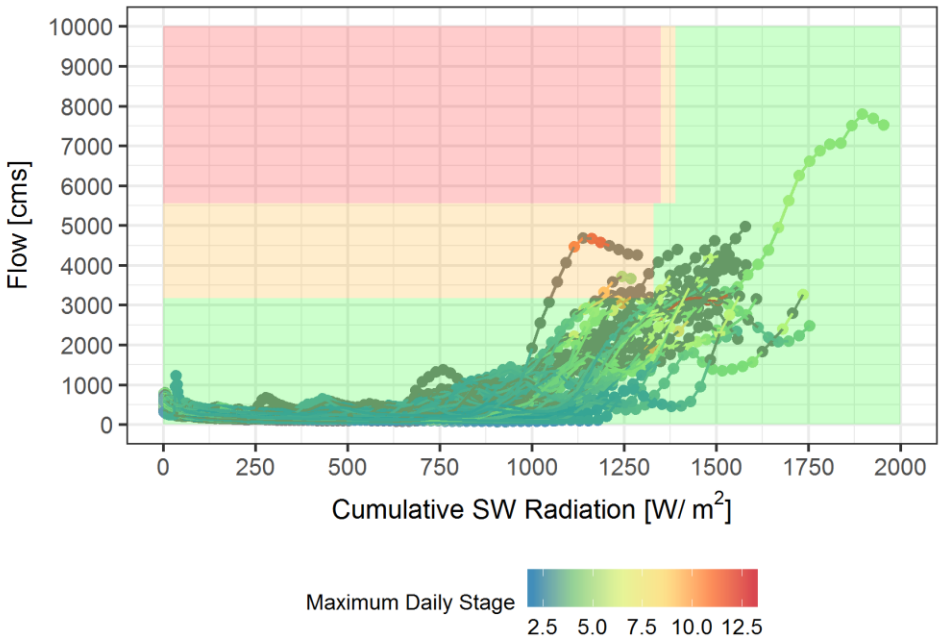

Figure 5.12: Cumulative shortwave radiation and flow at Fort Simpson

Although the model can generally simulate the timing and slope of the full rising limb well, as shown previously in Figure 4.11, it is the initial rise that is more important for this prediction methodology to work. There are some possible solutions for further improving the model simulation during this period that may improve the predictive capabilities. During the calibration process, ice affected values were not included in the calculation of calibration metrics or automatic calibration procedure. This initial rise in the hydrograph would have all been considered ice affected values. The explicit inclusion of this portion of the hydrograph during the calibration procedure could improve results. Furthermore, different snow melt modules could be examined to see if the timing of snowmelt can be improved. The timing of snowmelt is the main driver of the rising limb of the hydrograph and therefore critical in achieving good predictions.

The ongoing collection of data, such as ice thickness and documenting the severity of breakup each year would help improve the understanding of when severe breakup will occur within the basin and subsequent prediction.

5.4 Independent Verification

One criticism of breakup forecasting methodologies is that they are highly site specific. Although the methodology proved to be adequate at the two locations with the Liard basin, as third site located outside the basin was used as additional verification of the methodology. Hay River, NWT is a small town located at the confluence of the Hay River and Great Slave Lake, as shown in Figure 5.13.

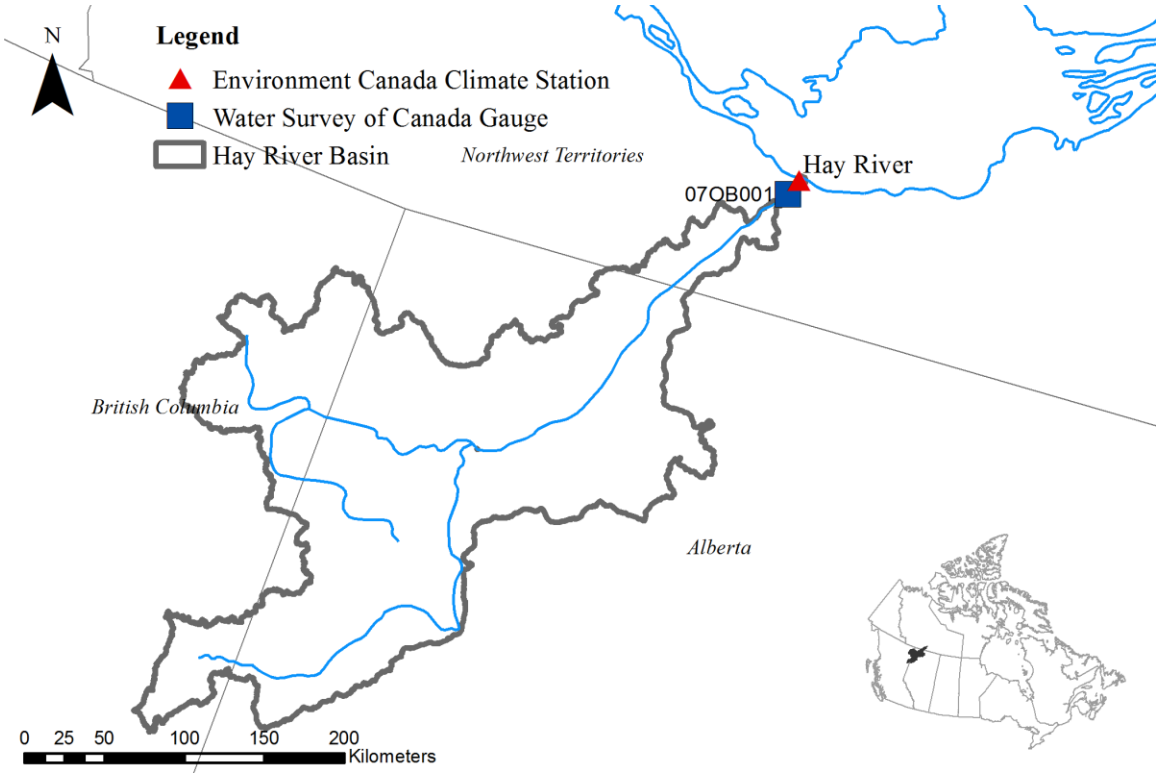

Figure 5.13: Overview of the Hay River basin

The Hay River catchment area is approximately 51,700 km^2. The headwaters of the basin start in the foothills of the Northern Rocky Mountains and transitions into low relief plains of the Hay River lowlands. The hydrograph at Hay River typically begins to rise in April as a result of the freshet reaching peak values of around 400 cms in May.

Hay River has a long history of ice jam flooding with significant research efforts being put into documenting and understanding breakup (Brayall & Hicks, 2012; De Coste et al., 2017; Hicks et al., 1992; Kovachis, 2011; Stanley & Gerard, 1992; Watson et al., 2009b). As a result, there are long records documenting the timing and severity of breakup. Kovachis (2011) summarized the severity and timing of breakup from 1868 to 2010. Breakup timing and severity was determined

from observations from researchers, historical mission records, community groups, and newspaper articles. Breakup severity was classified based on significant flooding, minor flooding, some flooding and no flooding. This record of breakup timing and severity was used instead of extracting breakup timing from the raw stage data and interpolating breakup severity based on stage data.

A simple Raven model was built for the town of Hay River to simulate the forcing data required as inputs for the ice thickness simulations in MATLAB. The model is not a full hydrological model of the Hay River basin which simulates flow, but simply generates the required inputs (shortwave radiation, snow water equivalent, temperature). Instead of simulating flow, flow data from a nearby water survey of Canada gauge (07OB001) was used instead. Climate data from a nearby Environment Canada station was used to force the Raven model. The model is based on a simulation period from 1964 to 2010.

Freeze up timing was simulated using the logistic regression developed for the Liard Basin, with the regression parameters manually calibrated to correlate to freeze up timing for Hay River from the CID database. The timing of observed versus modelled freeze up timing is shown in Figure 5.14. The modelled data has a bias of 1 day and a mean absolute error of 5.2 days, which is generally comparable to results from the Liard basin.

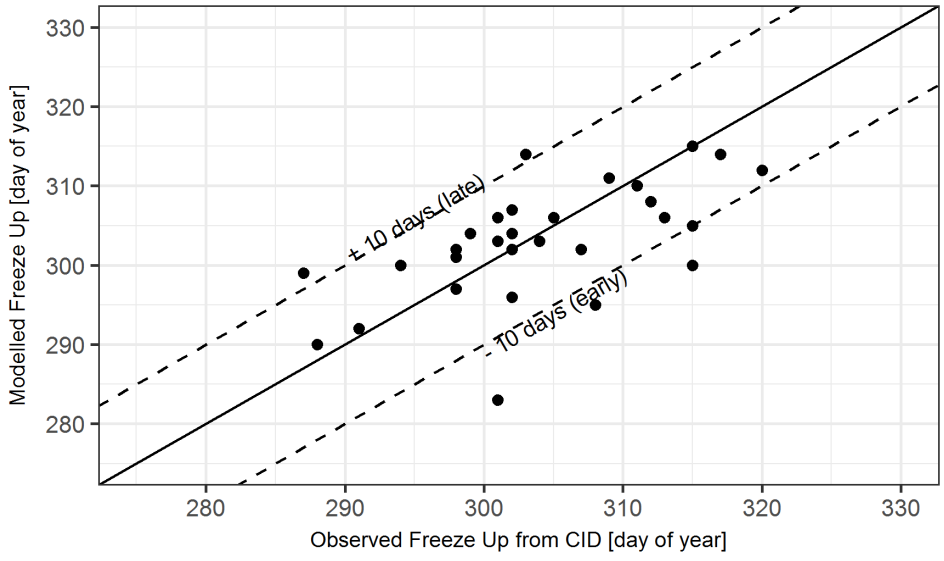

Figure 5.14: Comparison of modelled and observed freeze up timing at Hay River

Maximum ice thickness for each season was also compared to measured values within the CID database. Figure 5.15 shows the modelled and measured thickness for years where data was available. The modelled maximum ice thickness does not correlate well to the measured ice thickness with a R^2 value of 0.02. There is some uncertainty related to the timing of the measured values as previously described. Additionally, the Raven model has not been thoroughly calibrated therefore a bias related to snow accumulation and melt could exist which would impact the simulation of ice thickness.

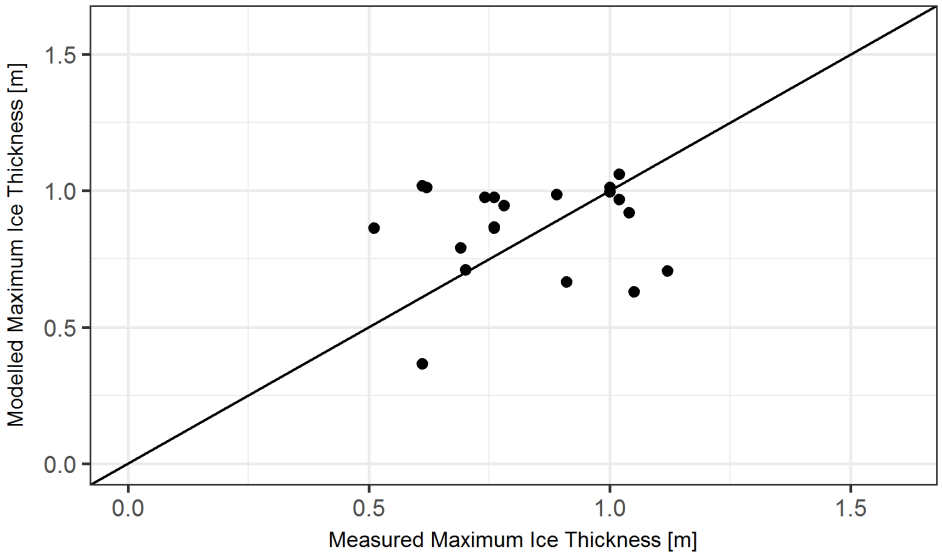

Figure 5.15: Comparison of measured and modelled maximum ice thickness at Hay River

Since flow is not being explicitly modelled, breakup timing was not predicted but observed breakup dates were used instead. The timing of breakup is still strongly correlated with the rise in the hydrograph limb, with breakup occurring on average one week after the initial rise (Figure 5.16).

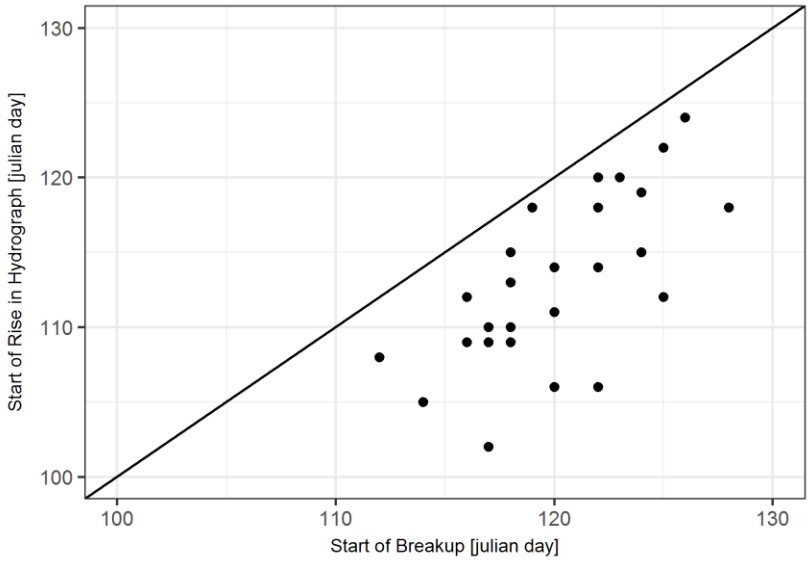

Figure 5.16: Relationship between the rise in the hydrograph and start of breakup at Hay River

Similar to the locations within the Liard, the thresholds for flow, cumulative shortwave radiation and ice thickness were determined using the PADDS algorithm. Figure 5.17 shows the trade off between the false positive and false negative predictions at Hay River with the selected point indicated.

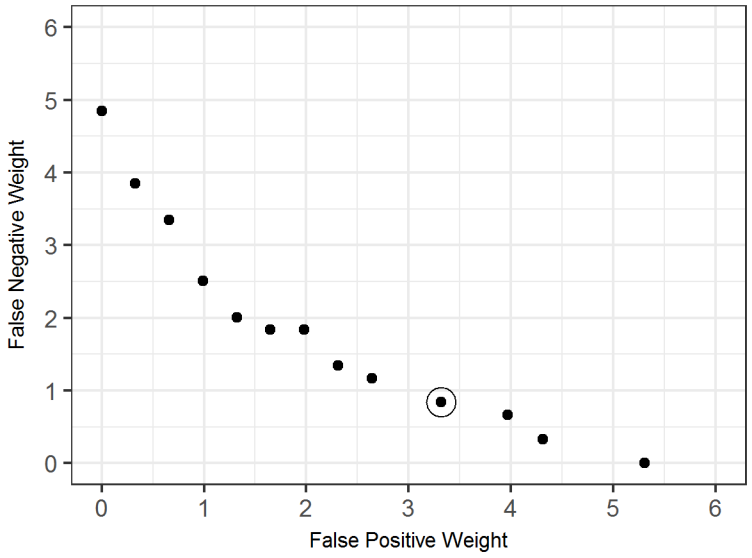

Figure 5.17: Pareto curve for Hay River showing trade off between false negative and false positive predictions

The corresponding ice thickness, flow and cumulative shortwave radiation, and prediction result figures are shown in Figure 5.18 through Figure 5.20.

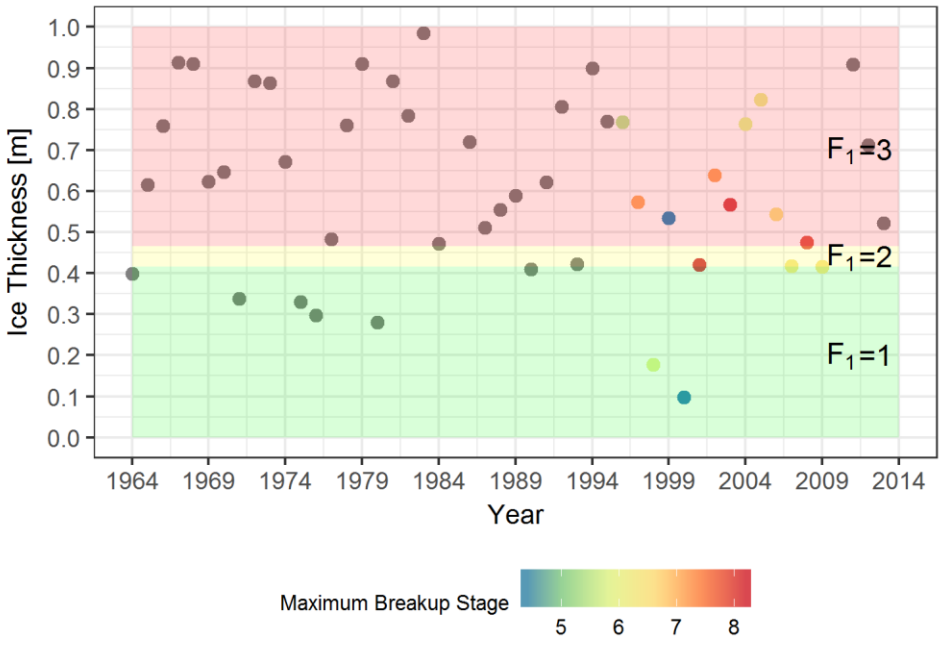

Figure 5.18: Ice thickness thresholds for Hay River

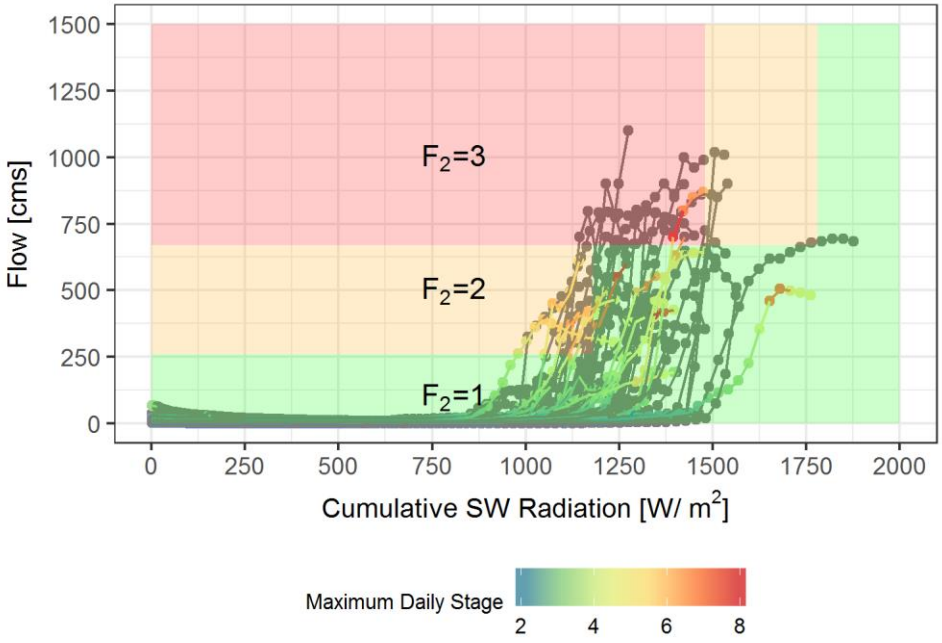

Figure 5.19: Flow and cumulative shortwave radiation thresholds for Hay River

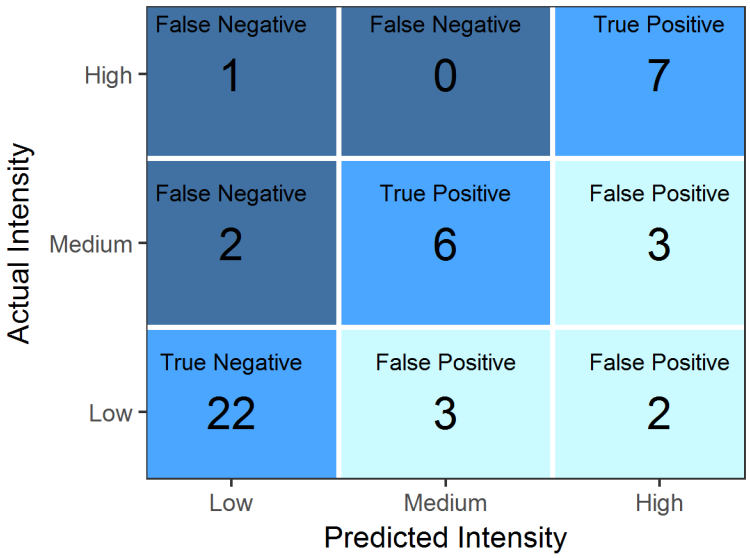

Figure 5.20: Prediction results at Hay River

The performance of the predictive model at Hay River is similar to the performance at Fort Liard and Fort Simpson, as indicated in Table 5.7. However, there is a larger rate of false negatives at Hay River.

Table 5.7: Comparison of false positive and negative rates at Hay River to Fort Liard and Fort Simpson

Location	False Negative	False Positive
Hay River	6.5%	17%
Fort Liard	0%	15%
Fort Simpson	0%	15%

Upon closer examination of the flow and cumulative shortwave radiation plots, years which resulted in significant flooding do not show the same relationship seen at the two locations in the Liard Basin, where significant flooding was associated with high flow and low cumulative shortwave radiation. Instead, the significant flooding appears to occur on years which had higher flows but not necessarily less shortwave radiation (Figure 5.21).

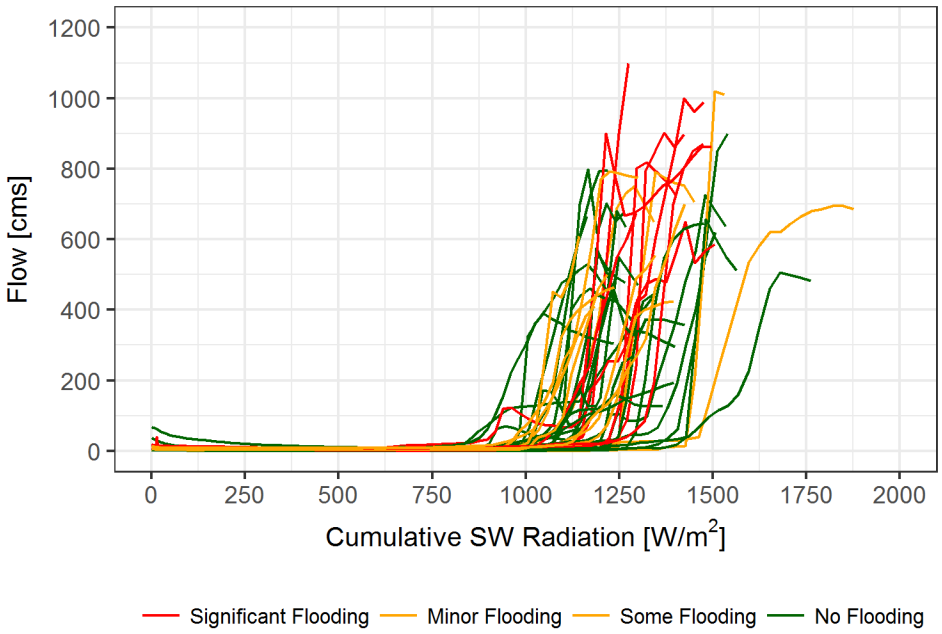

Figure 5.21: Flow and cumulative shortwave radiation at Hay River showing historical breakup intensity

The author found only one other breakup prediction methodology that had been specifically tested for transferability between locations. The fuzzy and neuro-fuzzy logic models built for the Athabasca River at Fort McMurray were tested at Hay River by Mahabir et al. (2007). The fuzzy and neuro-fuzzy models were originally based on the measured SWE from satellite, an index of antecedent basin moisture conditions (cumulative precipitation of previous summer), an index of the severity of winter (cumulative negative degree days), and an early indicator of the spring runoff (measured change in groundwater levels). Due to a lack of data at Hay River, the measured groundwater levels were not included in the tested fuzzy and neuro-fuzzy models. The same rule base was tested between each location, however the membership functions for the input and output data were redefined. The model was tested for 24 years of historical flooding. Differentiation between false positives and false negatives were not reported, however the percentage of true and false predictions were compared to the results from the hydrological model methodology.

Table 5.8: Comparison of Hay River model predictions to other prediction models

Model	Source	True Predictions	False Predictions
Fuzzy Model	(Mahabir et al., 2007)	54%	46%
Neuro Fuzzy Model		42%	58%
Hydrological Model	This Work	76%	24%

The hydrological based predictive model used here does perform better than the transferred fuzzy and neuro-fuzzy models of Mahabir et al. (2007). The hydrological modelling methodology can employ more direct indicators of the driving and resisting factors related to breakup. The comparison also highlights the potential role for hydrological models to play different forecasting methodologies, as input data to the forecast does not need to rely on site specific measurements but can be simulated through a hydrological model.

Chapter 6
Conclusions

The primary objective of this thesis was to demonstrate how hydrological models can be used to predict river ice breakup. The focus of the application was to data sparse regions, where long historical records may not exist to apply existing predictive models. In support of this objective, the secondary objective of the thesis was the development of a hydrological model of the Liard basin in northern Canada.

Chapter 4 outlines the development and performance of the hydrological model of the Liard basin. Given the application of the hydrological model, an emphasis was placed on developing a model that provides realistic results at all time periods and scales within the model. A thorough calibration procedure was used to achieve a high performing model. The calibration procedure was based on a multi-objective approach which included the calibration of the model structure and internal processes.

The methodology behind predicting river ice breakup including the coupled 1D river ice model is outlined in Chapter 3, with results from predicting breakup with the hydrological model outputs discussed in Chapter 5. The forecasting methodology is based on correctly simulating the timing in the rise of the hydrograph to determine breakup timing. The hydrological model did have a slight early bias; however, in general the model could forecast breakup timing within a one week period and was an improvement over using the mean historical breakup date. Breakup severity is determined using thresholds for flow, ice thickness, and cumulative shortwave radiation. The forecasting methodology results in comparable performance to other predictive models when using historical flows. The simulated flow values underestimate the rate of rise in the hydrograph resulting in a larger number of false negative events.

The prediction methodology was transferred to an independent site as a verification step. Although the prediction performance decreased when transferred to the independent site it was still an improvement when compared to other methodologies that tested transferability.

This thesis has demonstrated that hydrological models can be a useful tool in predicting breakup timing and severity. Instead of relying on large historical data sets of point measurements, the hydrological model can simulate many of the variables of interest in forecasting breakup making

them especially useful in data sparse regions. Several improvements could still be made to the development and calibration of a hydrological model for this purpose. In the case of the Liard model, calibration of the routing parameters and examination of different snow melt models could potentially improve the timing and initial rise in the hydrograph. Additionally, the explicit inclusion of these portions of the hydrograph in the calibration and validation period is likely warranted even though there is some uncertainty related to the flow measurements.

6.1 Contributions to Literature

This thesis presents two main contributions to literature. First, is the development and calibration procedure of the hydrological model of the Liard basin. Notably, the model structure was explicitly considered during calibration and the calibration process made use of multiple objectives and multiple gauges. This level of thoroughness is typically not considered in hydrological model calibration making the procedure unique in literature.

The second contribution is the use of a hydrological model to develop a forecast for breakup timing and severity. Two other studies have used hydrological models to predict breakup timing (Ma & Fukushima, 2002; Morales-Marin et al., 2019). However, the explicit modelling of both timing and severity using a hydrological model is novel within the literature. In addition to this, the unique procedure of using a multi-objective algorithm to minimize the false predictions has not been attempted before in river ice literature.

6.2 Future Opportunities

This thesis has demonstrated that hydrological models can be a useful tool for predicting breakup in regions where data is relatively sparse. Although the predictive methodology demonstrated in this thesis had adequate results, the application of hydrological models for forecasting river ice breakup does not necessarily need to be limited to this method. The benefit of using hydrological models is that variables which are of interest during breakup, and that are a result of the complex relationships between climate and hydrology, can easily be simulated. This makes hydrological models especially useful in areas where long term observations are not necessarily available. The hydrological model outputs could easily be applied to a variety of predictive methodologies which already exist in literature.

Another opportunity related to this work is the full integration of a river ice model into a hydrological model. Since Raven is a flexible modelling framework, the river ice model could be integrated directly into Raven. The only other known combined river ice and hydrological model was completed by Ma and Fukushima (2002). The integration of the ice model fully into a hydrological model would allow for numerous applications in cold region basins, especially since the ice model developed by Ashton (2011) was intended to be used for both rivers and lakes. Applying the ice model in a location with additional data (ice thickness, snow thickness, timing of decay) would help further validate the model. Furthermore, a more physically based model of freeze up timing (e.g. water temperature based) may be useful for applications to different locations. The inclusion of a water temperature component would also allow for other 1D ice models to be applied within the modelling framework.

Finally, there are further opportunities related to improving the hydrological model performance during the breakup period. With reference to the Liard basin model, additional calibration of routing parameters and the examination of different snow melt models should be explored. Additionally, the inclusion of ice affected flows during the breakup period may benefit the model performance.

References

Abbott, M. B., Bathurst, J. C., Cunge, J. A., O'Connell, P. E., & Rasmussen, J. (1986). An Introduction to the European Hydrological System "SHE": Structure of a physically-based, distributed Modelling System. *Journal of Hydrology*, *87*, 61–77.

Allen, R. G., Trezza, R., & Tasumi, M. (2006). Analytical integrated functions for daily solar radiation on slopes. *Agricultrual and Forest Meteorology*, *139*, 55–73. https://doi.org/10.1016/j.agrformet.2006.05.012

Anderton, S., Latron, J., & Gallart, F. (2002). Sensitivity analysis and multi-response, multi-criteria evaluation of a physically based distributed model. *Hydrological Processes*, *16*, 333–353. https://doi.org/10.1002/hyp.336

Andreadis, K. M., Schumann, G. J. P., & Pavelsky, T. (2013). A simple global river bankfull width and depth database. *Water Resources Research*, *49*(10), 7164–7168. https://doi.org/10.1002/wrcr.20440

Asadzadeh, M., & Tolson, B. A. (2009). A new multi-objective algorithm, pareto archived DDS. *Proceedings of the 11th Annual Conference on Genetic and Evolutionary Computation Conference*, 1963–1966. https://doi.org/10.1145/1570256.1570259

Ashton, G. D. (1986). *River and Lake Ice Engineering*. Chelsea, Michigan, USA: Water Resources Publications.

Ashton, G. D. (2011). River and lake ice thickening, thinning, and snow ice formation. *Cold Regions Science and Technology*, *68*, 3–19. https://doi.org/10.1016/j.coldregions.2011.05.004

Assel, R. A. (1976). *St. Lawrence River Freeze-Up Forecast Procedure. NOAA Technical Memorandum ERL GLERL-6.* Ann Arbour, Michigan.

Beaton, A., Sanden, J. Van Der, Corston, K., Deschamps, A., & Tolszczuk-Leclerc, S. (2017). Near Real-Time Monitoring of Ice Breakup in the Far North of Ontario Using RADARSAT-2 in Support of Provincial Flood Forecasting and Warning. *19th Workshop on the Hydraulics of Ice Covered Rivers*. Retrieved from http://cripe.ca/docs/proceedings/19/Beaton-et-al-2017.pdf

Beltaos, S. (1990a). Fracture and breakup of river ice cover. *Canadian Journal of Civil Engineering*, *17*, 173–183. https://doi.org/10.1139/l90-022

Beltaos, S. (1990b). Guidelines for Extraction of Ice Break Up Data From Hydrometric Station Records. In S. Beltaos, R. Gerard, S. Petryk, & T. D. Prowse (Eds.), *Working Group on River Ice Jams: Field Studies and Research Needs* (pp. 37–70). National Hydrology Research Institute.

Beltaos, S. (1997). Onset of river ice breakup. *Cold Regions Science and Technology*, *25*(3), 183–196. https://doi.org/10.1016/S0165-232X(96)00011-0

Beltaos, S. (2003). Threshold between mechanical and thermal breakup of river ice cover. *Cold Regions Science and Technology*, *37*(1), 1–13. https://doi.org/10.1016/S0165-

232X(03)00010-7

Beltaos, S. (2008). Onset of Breakup. In S. Beltaos (Ed.), *River-Ice Breakup* (pp. 167–207). Highlands Ranch: Water Resources Publications, LLC.

Beltaos, S., & Burrell, B. C. (2002). Extreme ice jam floods along the Saint John River, New Brunswick, Canada. *The Extremes of the Extremes: Extraordinary Floods*, 9–14. Reykajavik, Iceland: IAHS Publ, no 271.

Beltaos, S., & Krishnappan, B. G. (1982). Surges from ice jam releases: a case study. *Canadian Journal of Civil Engineering*, *9*, 276–284. https://doi.org/10.1139/l82-029

Beltaos, S., Prowse, T., & Carter, T. (2006). Ice regime of the lower Peace River and ice-jam flooding of the Peace Athabasca Delta. *Hydrological Processes*, *20*, 4009–4029.

Beltaos, S., Tang, P., & Rowsell, R. (2012). Ice jam modelling and field data collection for flood forecasting in the Saint John River, Canada. *Hydrological Processes*, *26*, 2535–2545. https://doi.org/10.1002/hyp.9293

Bergstrom, S., & Forsman, A. (1973). Development of a conceptual deterministic rainfall-runoff model. *Nordic Hydrology*, *4*(3), 147–170.

Bergstrom, S., Lindstrom, G., & Pettersson, A. (2002). Multi-variable parameter estimation to increase confidence in hydrological modelling. *Hydrological Processes*, *16*(2), 413–421. https://doi.org/10.1002/hyp.332

Beven, K. J. (2000). Uniqueness of place and process representations in hydrological modelling. *Hydrology and Earth System Sciences Discussion, European Geosciences Union*, *4*(2), 203–213. https://doi.org/10.5194/hess-4-203-2000

Beven, K. J. (2006). A manifesto for the equifinality thesis. *Journal of Hydrology*, *320*, 18–36. https://doi.org/10.1016/j.jhydrol.2005.07.007

Beven, K. J., Kirkby, M. J., Schofield, N., & Tagg, A. F. (1984). Testing a Physically-Based Flood Forecasting Model (TOPMODEL) for Three U.K Catchments. *Journal of Hydrology*, *69*, 119–143. https://doi.org/10.1016/0022-1694(84)90159-8

Bilello, M. A. (1964). Method for Predicting River and Lake Ice Formation. *Journal of Applied Meteorology*, *3*, 38–44.

Blackburn, J., & Hicks, F. (2003). Suitability of Dynamic Modeling for Flood Forecasting during Ice Jam Release Surge Events. *Journal of Cold Regions Engineering*, *17*(1), 18–36. https://doi.org/10.1061/(ASCE)0887-381X(2003)17:1(18)

Bonsal, B. R., Prowse, T. D., Duguay, C. R., & Lacroix, M. P. (2006). Impacts of large-scale teleconnections on freshwater-ice break/freeze-up dates over Canada. *Journal of Hydrology*, *330*, 340–353. https://doi.org/10.1016/j.jhydrol.2006.03.022

Brayall, M., & Hicks, F. E. (2012). Applicability of 2-D modeling for forecasting ice jam flood levels in the Hay River Delta, Canada. *Canadian Journal of Civil Engineering*, *39*, 701–712. https://doi.org/10.1139/l2012-056

Brook, G. A., & Ford, D. C. (1980). Hydrology of the Nahanni karst, northern Canada, and the

importance of extreme summer storms. *Journal of Hydrology*, *46*, 103–121. https://doi.org/10.1016/0022-1694(80)90038-4

Burn, D. H. (1994). Hydrologic effects of climatic change in west-central Canada. *Journal of Hydrology*, *160*, 53–70. https://doi.org/10.1016/0022-1694(94)90033-7

Campolo, M., Andreussi, P., & Soldati, A. (1999). River flood forecasting with a neural network model. *Water Resources Research*, *35*(4), 1191–1197. https://doi.org/10.1029/1998WR900086

Cao, W., Bowden, W. B., Davie, T., & Fenemor, A. (2006). Multi-variable and multi-site calibration and validation of SWAT in a large mountainous catchment with high spatial variability. *Hydrological Processes*, *20*, 1057–1073. https://doi.org/10.1002/hyp.5933

Cayan, D.R., Kammerdiener, S.A., Dettinger, M.D., Caprio, J.M., & Peterson, D.H. (2001). Changes in the Onset of Spring in the Western United States. *Bulletin of the American Meteorological Society*, *82*(3), 399–415.

Chlumsky, R., & Craig, J. R. (2019). *RavenR: Raven Hydrological Modelling Framework R Support and Analysis*. Retrieved from https://github.com/rchlumsk/RavenR%0A

Clark, M. P., Kavetski, D., & Fenicia, F. (2011). Pursuing the method of multiple working hypotheses for hydrological modeling. *Water Resources Research*, *47*(9), 1–16. https://doi.org/10.1029/2010WR009827

Cloke, H. L., & Pappenberger, F. (2009). Ensemble flood forecasting: A review. *Journal of Hydrology*, *375*, 613–626. https://doi.org/10.1016/j.jhydrol.2009.06.005

Connon, R. F., Quinton, W. L., Craig, J. R., Hanisch, J., & Sonnentag, O. (2015). The hydrology of interconnected bog complexes in discontinuous permafrost terrains. *Hydrological Processes*, *29*, 3831–3847. https://doi.org/10.1002/hyp.10604

Craig, J. R., & Raven Development Team. (2018). *Raven user's and developer's manual (Version 2.8)*. Retrieved from http://www.civil.uwaterloo.ca/jrcraig/Raven/Main.html

Das, A., Rokaya, P., & Lindenschmidt, K. E. (2017). Assessing the impacts of climate change on ice jams along the Athabasca River at Fort McMurray, Alberta, Canada. *19th Workshop on the Hydraulics of Ice Covered Rivers. Whitehorse, Yukon, Canada, July 9 -12, 2017*.

De Coste, M., She, Y., & Blackburn, J. (2017). Incorporating the effects of upstream ice jam release in the prediction of flood levels in the Hay River Delta, Canada. *Canadian Journal of Civil Engineering*, *44*, 643–651. https://doi.org/10.1139/cjce-2017-0123

de Rham, L. P. (2006). *Spatial and Temporal Variations of River-ice Break-up, Mackenzie River Basin, Canada*. Univserity of Victoria.

de Rham, L. P., Prowse, T. D., & Bonsal, B. R. (2008). Temporal variations in river-ice break-up over the Mackenzie River Basin, Canada. *Journal of Hydrology*, *349*, 441–454. https://doi.org/10.1016/j.jhydrol.2007.11.018

Dingman, S. L. (2015). *Physical Hydrology*. Long Grove, IL: Waveland Press Inc.

Fenicia, F., Kavetski, D., & Savenije, H. H. G. (2011). Elements of a flexible approach for

conceptual hydrological modeling: 1. Motivation and theoretical development. *Water Resources Research*, *47*(11), 1–13. https://doi.org/10.1029/2010WR010174

Fenicia, F., Savenije, H. H. G., Matgen, P., & Pfister, L. (2008). Understanding catchment behavior through stepwise model concept improvement. *Water Resources Research*, *44*(1), 1–13. https://doi.org/10.1029/2006WR005563

Freer, J. E., & Beven, K. J. (2001). Equifinality, data assimilation, and uncertainty estimation in mechanistic modelling of complex environmental systems using the GLUE methodology. *Journal of Hydrology*, *249*, 11–29. https://doi.org/10.1016/S0022-1694(01)00421-8

Galbraith, P. W. (1981). On estimating the likelihood of ice jams in the Saint John River using meterological variables. *Porceedings of the 5th Canadian Hydrotechnical Conference, Fredericton, N.B., May 26-27, 1981*, 219–237. Montreal, Quebec: Canadian Society for Civil Engineering.

Goulding, H. L., Prowse, T. D., & Bonsal, B. (2009). Hydroclimatic controls on the occurrence of break-up and ice-jam flooding in the Mackenzie Delta, NWT, Canada. *Journal of Hydrology*, *379*, 251–267. https://doi.org/10.1016/j.jhydrol.2009.10.006

Greene, G. M. (1983). *Forecasting Ice-Cover Freeze-up, Growth, and Breakup on the St.Marys River. NOAA Technical Memorandum ERL GLERL-47.* Ann Arbor, Michigan.

Greene, G. M., & Outcalt, S. I. (1985). A simulation model of river ice cover thermodynamics. *Cold Regions Science and Technology*, *10*(3), 251–262. https://doi.org/10.1016/0165-232X(85)90036-9

Gupta, H. V., Kling, H., Yilmaz, K. K., & Martinez, G. F. (2009). Decomposition of the mean squared error and NSE performance criteria: Implications for improving hydrological modelling. *Journal of Hydrology*, *377*(1–2), 80–91. https://doi.org/10.1016/j.jhydrol.2009.08.003

Hamilton, A. S., Hutchinson, D. G., & Moore, R. D. (2001). Estimation of winter streamflow using a conceptual hydrological model: a case study, Wolf Creek, Yukon Territory. *Proceedings of the 11th Workshop on the Hydraulics of Ice Covered Rivers*. Retrieved from http://cripe.civil.ualberta.ca/Downloads/11th_Workshop/Hamilton-et-al-2001.pdf

Hamlet of Fort Liard. (2017). Emergency Services: Spring Break-Up. Retrieved August 27, 2019, from https://www.fortliard.com/copy-of-emergency-services

Hartmann, A., Wagener, T., Rimmer, A., Lange, J., Brielmann, H., & Weiler, M. (2013). Testing the realism of model structures to identify karst system processes using water quality and quantity signatures. *Water Resources Research*, *49*, 3345–3358. https://doi.org/10.1002/wrcr.20229

Hicks, F. E., Steffler, P. M., & Gerard, R. (1992). Finite element modeling of surge propagation and an application to the Hay River, N.W.T. *Canadian J. Civil Engineering*, *19*(3), 454–462. https://doi.org/10.1139/l92-055

Hicks, F., McKay, K., & Shabayek, S. (1997). Modelling an ice jam release surge on the Saint John River New Brunswick. *The 9th Workshop on River Ice*, 303–314. Fredericton, N.B.

Hutchison, T. K., & Hicks, F. E. (2007). Observations of ice jam release waves on the Athabasca River near Fort McMurray, Alberta. *Canadian Journal of Civil Engineering*, *34*, 473–484. https://doi.org/10.1139/l06-144

Jasek, M. (2003). Ice jam release surges, ice runs, and breaking fronts: field measurements, physical descriptions, and research needs. *Canadian Journal of Civil Engineering*, *30*, 949–950. https://doi.org/10.1139/l03-085

Kirchner, J. W. (2006). Getting the right answers for the right reasons: Linking measurements, analyses, and models to advance the science of hydrology. *Water Resources Research*, *42*(3), 1–5. https://doi.org/10.1029/2005WR004362

Klemes, V. (1986). Operational testing of hydrological simulation models. *Hydrological Sciences Journal*, *31*(1), 13–24. https://doi.org/10.1080/02626668609491024

Kouwen, N., Soulis, E. D., Pietroniro, A., Donald, J., & Harrington, R. A. (1993). Grouped response units for distributed hydrologic modelling. *Journal of Water Resources Planning and Management*, *119*(3), 289–305.

Kovachis, N. (2011). *Patterns of River Breakup Timing and Sequencing, Hay River, NWT*. University of Alberta.

Krause, P., Boyle, D. P., & Bäse, F. (2005). Comparison of different efficiency criteria for hydrological model assessment. *Advances in Geosciences*, *5*, 89–97. https://doi.org/10.5194/adgeo-5-89-2005

Lai, A. M. W., Shen, H. T., Lal, A. M. W., & Shen, H. T. (1991). Mathematical Model for River Ice Processes. *Journal of Hydraulic Engineering*, *117*(7), 851–867.

Lenormand, F., Duguay, C. R., & Gauthier, R. (2002). Development of a historical ice database for the study of climate change in Canada. *Hydrological Processes*, *16*, 3707–3722. https://doi.org/10.1002/hyp.1235

Lindenschmidt, K. E. (2017). RIVICE-A non-proprietary, open-source, one-dimensional river-ice model. *Water (Switzerland)*. https://doi.org/10.3390/w9050314

Lindsey, S., & Johnson, C. (2017). Alaska Pacific River Forecast Center Operations. *Committee on River Ice Processes and the Environment 19th Workshop on the Hydraulics of Ice Covered Rivers*. Retrieved from http://aprfc.arh.noaa.gov/general/brkup.html

List, R. J. (1951). *Smithsonian Meterological Tables, 6th rev. ed*. Washington, D.C.: Smithsonian Institution.

Luo, C., Gardner, T., & Campbell, D. (2015). Evaluation of the CLEVER Model – A Real-time Flood Forecast Model for Large-Scale Watersheds in British Columbia. *Proceedings of CWRA BC Branch Conference, Vancouver, BC, Canada 18-25 November, 2015.*

Ma, X., & Fukushima, Y. (2002). *A numerical model of the river freezing process and its application to the Lena River*. *2140*(February 2001), 2131–2140. https://doi.org/10.1002/hyp.1146

Ma, X., Fukushima, Y., & Ohata, T. (2001). Hydrological modelling of river ice processes in

cold regions. In A. J. Dolman, A. J. Hall, M. L. Kavvas, T. Oki, & J. W. Pomeroy (Eds.), *Soil-Vegetation Atmosphere Transfer Schemes and Large Scale Hydrological Models. IAHS Publication no. 270.* (pp. 327–332). https://doi.org/10.1002/hyp.1146

Mahabir, C., Hicks, F. E., & Fayek, A. R. (2007). Transferability of a neuro-fuzzy river ice jam flood forecasting model. *Cold Regions Science and Technology*, *48*(3), 188–201. https://doi.org/10.1016/j.coldregions.2006.12.004

Mahabir, C, Hicks, F. E., & Fayek, A. R. (2002). Forecasting ice jam risk at Fort McMurray, AB, using fuzzy logic. *Ice in the Environment: Proceedings of the 16th IAH International Symposium on Ice*, (December), 91–98. Dunedin, New Zealand: International Association of Hydraulic Engineering and Research.

Mahabir, C, Hicks, F. E., Robichaud, C., & Fayek, A. R. (2006). Forecasting breakup water levels at Fort McMurray, Alberta, using multiple linear regression. *Canadian Journal of Civil Engineering*, *33*, 1227–1238. https://doi.org/10.1139/l06-067

Mahabir, Chandra, Hicks, F., & Fayek, A. R. (2006). Neuro-fuzzy river ice breakup forecasting system. *Cold Regions Science and Technology*, *46*(2), 100–112. https://doi.org/10.1016/j.coldregions.2006.08.009

Massie, D. D., White, K. D., Daly, S. F., & McDonald, R. (2002). Predicting Ice Jams With Neural Networks. *Proceedings of OMAE'02 21st International Conference on Offshore Mechanics and Arctic Engineering. June 23- 28, 2002.* https://doi.org/10.1115/omae2002-28551

Mekis, É., & Vincent, L. A. (2011). An overview of the second generation adjusted daily precipitation dataset for trend analysis in Canada. *Atmosphere-Ocean*, *49*(2), 163–177. https://doi.org/10.1080/07055900.2011.583910

Ménard, P., Duguay, C. R., Flato, G. M., & Rouse, W. R. (2002). Simulation of ice phenology on Great Slave Lake, Northwest Territories, Canada. *Hydrological Processes*, *16*(18), 3691–3706. https://doi.org/10.1002/hyp.1230

Morales-Marin, L. A., Sanyal, P. R. R., Kadowaki, H., Li, Z., Rokaya, P., & Lindenshmidt, K. E. (2019). A hydrological and water temperature modelling framework to simulate the timing of river freeze-up and ice-cover breakup in large-scale catchments. *Environmental Modelling and Software*, *114*, 49–63. https://doi.org/10.1016/j.envsoft.2019.01.009

Morrill, J. C., Bales, R. C., & Conklin, M. H. (2004). Estimating Stream Temperature from Air Temperature: Implications for Future Water Quality. *Journal of Environmental Engineering*, *131*(1), 139–146.

Nash, E., & Sutcliffe, V. (1970). River Flow Forecasting through Conceptual Models: Part I - A Discussion of Principles. *Journal of Hydrology*, *10*, 282–290.

Natural Resources Canada. (2013). *Canadian Digital Elevation Model*. Sherbrooke, Canada.

Natural Resources Canada. (2015). *Canadian Land Cover, circa 2000, Geobase Series*. Sherbrooke, Canada.

Natural Resources Canada. (2019). *CanVec*. Sherbrooke, Canada.

Parajka, J., & Blöschl, G. (2008). The value of MODIS snow cover data in validating and calibrating conceptual hydrologic models. *Journal of Hydrology*, *358*, 240–258. https://doi.org/10.1016/j.jhydrol.2008.06.006

Pietroniro, A., Fortin, V., Kouwen, N., Neal, C., Turcotte, R., Davison, B., … Pellerin, P. (2007). Development of the MESH modelling system for hydrological ensemble forecasting of the Laurentian Great Lakes at the regional scale. *Hydrology and Earth System Sciences*, *11*(4), 1279–1294. https://doi.org/10.5194/hess-11-1279-2007

Prowse, T. D. (1986). Ice jam characteristics, Liard–Mackenzie rivers confluence. *Canadian Journal of Civil Engineering*, *13*, 653–665. https://doi.org/10.1139/l88-037

Prowse, T. D. (1995). River Ice Processes. In Spyros Beltaos (Ed.), *River Ice Jams* (pp. 29–68). Highlands Ranch, Colorado: Water Resources Publications, LLC.

Prowse, T. D., Chew, H. A. M., & Demuth, M. N. (1990). The deterioration of freshwater ice due to radiation decay. *Journal of Hydraulic Research*, *28*(6), 685–697. https://doi.org/10.1080/00221689009499019

Prowse, T. D., & Marsh, P. (1989). Thermal budget of river ice covers during breakup. *Canadian Journal of Civil Engineering*, *16*, 62–71. https://doi.org/10.1139/l89-008

Quinton, W., Berg, A., Braverman, M., Carpino, O., Chasmer, L., Connon, R., … Sonnentag, O. (2019). A synthesis of three decades of hydrological research at Scotty Creek, NWT, Canada. *Hydrology and Earth System Sciences*, *23*(4), 2015–2039. https://doi.org/10.5194/hess-23-2015-2019

Quinton, W. L., Hayashi, M., Blais, K. E., Wright, N., & Peitroniro, A. (2004). The water balance of wetland-dominated permafrost basins. *Northern Research Basins Water Balance*, 186–194. Victoria, Canada: IAHS Publ. 290.

Quinton, W. L., Hayashi, M., & Chasmer, L. E. (2009). Peatland Hydrology of Discontinuous Permafrost in the Northwest Territories: Overview and Synthesis. *Canadian Water Resources Journal*, *34*(4), 311–328. https://doi.org/10.4296/cwrj3404311

Rango, A., & Martinec, J. (1995). Revisiting the Degree-Day Method for Snowmelt Computations. *JAWRA Journal of the American Water Resources Association*, *31*(4), 657–669. https://doi.org/10.1111/j.1752-1688.1995.tb03392.x

Rokaya, P., Das, A., & Lindenshmidt, K. E. (2017). Exploring flow operation schemes for sustainable ice-jam flood management along the Peace River in western Canada. *19th Workshop on the Hydraulics of Ice Covered Rivers. Whitehorse, Yukon, Canada, July 9 -12, 2017*.

Rokaya, P., Wheater, H., & Lindenschmidt, K.-E. (2019). Promoting Sustainable Ice-Jam Flood Management along the Peace River and Peace-Athabasca Delta. *Journal of Water Resource Planning and Management*, *145*(1). https://doi.org/10.1061/(ASCE)WR.1943-5452.0001021.

Shaw, J. K. E., Lavender, S. T., Stephen, D., & Jamieson, K. (2013). Ice Jam Flood Risk Forecasting at the Kashechewan FN Community on the North Albany River. *Proceedings of the 17th Workshop on River Ice. Edmonton, Alberta. July 21-24, 2013.*

She, Y., & Hicks, F. (2006). Modeling ice jam release waves with consideration for ice effects. *Cold Regions Science and Technology*, *45*(3), 137–147. https://doi.org/10.1016/j.coldregions.2006.05.004

She, Yuntong, Hicks, F., & Andrishak, R. (2012). The role of hydro-peaking in freeze-up consolidation events on regulated rivers. *Cold Regions Science and Technology*, *73*, 41–49. https://doi.org/10.1016/j.coldregions.2012.01.001

Shen, H. T. (2010). Mathematical modeling of river ice processes. *Cold Regions Science and Technology*, *62*(1), 3–13. https://doi.org/10.1016/j.coldregions.2010.02.007

Shen, H. T., & Chiang, L.-A. (1984a). Simulation of Formation, Growth and Decay of River Ice Cover. *Journal of Hydraulic Engineering*, *110*(7), 958–971. https://doi.org/10.1061/(ASCE)0733-9429(1984)110:7(958)

Shen, H. T., & Chiang, L.-A. (1984b). Simulation of growth and decay of river ice cover. *Journal of Hydraulic Engineering*, *110*(7), 958–971.

Shen, H. T., Foltyn, E. P., & Daly, S. F. (1984). *Forecasting water temperature decline and freeze-up in rivers. CRREL Report 84-19*. Hanover, NH.

Shen, H. T., & Yapa, P. D. (1985). A unified degree-day method for river ice cover thickness simulation. *Canadian Journal of Civil Engineering*, *12*, 54–62.

Shulyakovskii, L. G. (1963). *Manual of forecasting ice formation for rivers and inland lakes.* Jerusalem, Israel.

Stanley, S. J., & Gerard, R. (1992). Ice jam flood forecasting: Hay River, N.W.T. *Canadian Journal of Civil Engineering*, *19*, 212–223. https://doi.org/10.1139/l92-027

Tang, P., & Beltaos, S. (2008). Modeling of River Ice Jams for Flood Forecasting in New Brunswick. *65th Eastern Snow Conference*, 167–178. Fairlee (Lake Morey), Vermont.

Theriault, I., Saucet, J.-P., & Taha, W. (2010). Validation of the Mike-Ice model simulating river flows in presence of ice and forecast of changes to the ice regime of the Romaine river due to hydroelectric project. *Proceedings of the 20th IAHR Symposium on Ice*.

Thompson, R. (2008). Liard River Floods Two Homes. *Northern News Services*.

Thorne, R. (2011). Uncertainty in the impacts of projected climate change on the hydrology of a subarctic environment: Liard River Basin. *Hydrology and Earth System Sciences*, (15), 1483–1492. https://doi.org/10.5194/hess-15-1483-2011

Thorne, R., & Woo, M. K. (2006). Efficacy of a hydrologic model in simulating discharge from a large mountainous catchment. *Journal of Hydrology*, *330*, 301–312. https://doi.org/10.1016/j.jhydrol.2006.03.031

Timalsina, N. P., Alfredsen, K. T., & Killingtveit, A. (2015). Impact of climate change on ice regime in a river regulated for hydopower. *Canadian Journal of Civil Engineering*, *42*, 634–644.

Tolson, B. A., & Shoemaker, C. A. (2007). Dynamically dimensioned search algorithm for computationally efficient watershed model calibration. *Water Resources Research*, *43*(1),

1–16. https://doi.org/10.1029/2005WR004723

Toth, E., Brath, A., & Montanari, A. (2000). Comparison of short-term rainfall prediction models for real-time flood forecasting. *Journal of Hydrology*, *239*, 132–147. https://doi.org/10.1016/S0022-1694(00)00344-9

Turcotte, B., & Morse, B. (2013). A global river ice classification model. *Journal of Hydrology*, *507*, 134–148. https://doi.org/10.1016/j.jhydrol.2013.10.032

Turcotte, B., & Morse, B. (2015). River ice breakup forecast and annual risk distribution in a climate change perspective. *18th Workshop on the Hydraulics of Ice Covered Rivers.* Quebec City, QC.

van der Linden, S., & Woo, M. (2003a). Application of hydrological models with increasing complexity to subarctic catchments. *Journal of Hydrology*, *270*, 145–157.

van der Linden, S., & Woo, M. (2003b). Transferability of hydrological model parameters between basins in data-sparse areas, subarctic Canada. *Journal of Hydrology*, *270*, 182–194.

Warren, S., Puestow, T., Richard, M., & Khan, A. A. (2017). Near Real-time Ice-Related Flood Hazard Assessment of the Exploits River in Newfoundland , Canada. *CGU HS Committee on River Ice Processes and the Environment 19th Workshop on the Hydraulics of Ice Covered Rivers*. Retrieved from http://cripe.ca/docs/proceedings/19/Warren-et-al-2017.pdf

Watson, D., Hicks, F., & Andrishak, R. (2009). Analysis of Observed 2008 Ice Jam Release Events on the Hay River, NWT. *Proceedings of the 15th CRIPE Workshop on River Ice, St. John's*, 316–330.

Webb, B. W., Clack, P. D., & Walling, D. E. (2003). Water-air temperature relationships in a Devon river system and the role of flow. *Hydrological Processes*, *17*, 3069–3084. https://doi.org/10.1002/hyp.1280

White, K. D. (1996). Predicting Breakup Ice Jams Using Logistic Regression. *Journal of Cold Regions Engineering*, *10*(4), 178–189.

White, K. D. (2003). Review of prediction methods for breakup ice jams. *Canadian Journal of Civil Engineering*, *30*, 89–100. https://doi.org/10.1139/l02-047

White, K. D., & Daly, S. F. (2002). Prediciting Ice Jams with Discriminant Function Analysis. *Proceedings of 21st International Conference on Offshore Mechanics and Arctic Engineering*, 8. Osolo, Norway.

Wood, E. F., Lettenmaier, D. P., & Zartarian, V. G. (1992). A land-surface hydrology parameterization with subgrid variability for general circulation models. *Journal of Geophysical Research*, *97*(D3), 2717–2728. https://doi.org/10.1029/91JD01786

Wood, E. F., Sivapalan, M., Beven, K., & Band, L. (1988). Effects of Spatial Variability and Scale with Implications to Hydrologic Modeling. *Journal of Hydrology*, *102*, 29–47. https://doi.org/http://dx.doi.org/10.1016/0022-1694(88)90090-X

Wuebben, J. L., & Gagnon, J. J. (1995). *Ice Jam Flooding on the Missouri River Near Williston, North Dakota. CRREL Report 95-19.*

Zhang, X., David Harvey, K., Hogg, W. D., & Yuzyk, T. R. (2001). Trends in Canadian streamflow. *Water Resources Research*, *37*(4), 987–998. https://doi.org/10.1029/2000WR900357

Appendix A – Raven Input File

```
#------------------------------------------------------------------------
# Simulation parameters

:StartDate          1985-10-01 00:00:00
:Duration           7305 00:00:00
:TimeStep           24:00:00

#------------------------------------------------------------------------
# Model options
:Method              ORDERED_SERIES
:Interpolation       INTERP_NEAREST_NEIGHBOR

:Routing             ROUTE_DIFFUSIVE_WAVE
:CatchmentRoute      ROUTE_TRI_CONVOLUTION

:Evaporation         PET_HARGREAVES_1985
:OW_Evaporation      PET_HARGREAVES_1985
:SWRadiationMethod   SW_RAD_DEFAULT
:SWCloudCorrect      SW_CLOUD_CORR_NONE
:SWCanopyCorrect     SW_CANOPY_CORR_NONE
:LWRadiationMethod   LW_RAD_DEFAULT
:RainSnowFraction    RAINSNOW_HBV
:PotentialMeltMethod POTMELT_HBV
:OroTempCorrect      OROCORR_HBV
:OroPrecipCorrect    OROCORR_SIMPLELAPSE
:OroPETCorrect       OROCORR_HBV
:CloudCoverMethod    CLOUDCOV_NONE
:PrecipIceptFract    PRECIP_ICEPT_USER

:SoilModel           SOIL_MULTILAYER 4

#------------------------------------------------------------------------
# Soil Layer Alias Definitions
:Alias       VADOSE_RESERVOIR      SOIL[1]
:Alias       FAST_RESERVOIR        SOIL[2]
:Alias       SLOW_RESERVOIR        SOIL[3]

#Wetland, Upland Groups
:DefineHRUGroups WetlandHRUs, UplandHRUs,FlushWetlands, NahanniHRUs,
:DefineHRUGroups ForestHRUs, BarrenHRUs, ShrublandHRUs

#------------------------------------------------------------------------
# Hydrologic process order for modified HBV-EC model of the Liard Basin

:HydrologicProcesses
  :SnowRefreeze          FREEZE_DEGREE_DAY  SNOW_LIQ        SNOW
  :Precipitation         PRECIP_RAVEN       ATMOS_PRECIP    MULTIPLE
  :CanopyEvaporation     CANEVP_ALL         CANOPY          ATMOSPHERE
  :CanopySnowEvap        CANEVP_ALL         CANOPY_SNOW     ATMOSPHERE
  :SnowBalance           SNOBAL_SIMPLE_MELT SNOW            SNOW_LIQ
    :-->Overflow         RAVEN_DEFAULT      SNOW_LIQ        PONDED_WATER
  :Flush                 RAVEN_DEFAULT      PONDED_WATER    GLACIER
    :-->Conditional HRU_TYPE IS GLACIER
  :Flush                 RAVEN_DEFAULT      SOIL[0]         GLACIER
      :-->Conditional HRU_TYPE IS GLACIER
  :GlacierMelt           GMELT_HBV          GLACIER_ICE     GLACIER
  :GlacierRelease        GRELEASE_HBV_EC    GLACIER         SURFACE_WATER
  :Flush                 RAVEN_DEFAULT      PONDED_WATER    DEPRESSION
    :-->Conditional HRU_TYPE IS WETLAND
  :DepressionOverflow    DFLOW_THRESHPOW    DEPRESSION      SURFACE_WATER
  :Seepage               SEEP_LINEAR        DEPRESSION      FAST_RESERVOIR
  :OpenWaterEvaporation  OPEN_WATER_EVAP    DEPRESSION      ATMOSPHERE
  :Infiltration          INF_HBV            PONDED_WATER    MULTIPLE
```

```
  :LateralFlush          RAVEN_DEFAULT UplandHRUs SURFACE_WATER To FlushWetlands
DEPRESSION
  :LakeEvaporation       LAKE_EVAP_BASIC    SURFACE_WATER   ATMOSPHERE
    :-->Conditional HRU_TYPE IS LAKE
  :Flush                 RAVEN_DEFAULT      SURFACE_WATER   FAST_RESERVOIR
    :-->Conditional HRU_TYPE IS_NOT GLACIER
       :-->Conditional HRU_TYPE IS_NOT LAKE
       :-->Conditional HRU_TYPE IS_NOT WETLAND
       :-->Conditional HRU_GROUP IS_NOT UplandHRUs
       :-->Conditional HRU_GROUP IS_NOT NahanniHRUs
  :SoilEvaporation       SOILEVAP_HBV       SOIL[0]         ATMOSPHERE
  :Percolation           PERC_GAWSER        SOIL[0]         VADOSE_RESERVOIR
    :-->Conditional HRU_GROUP IS NahanniHRUs
  :Baseflow             BASE_THRESH_POWER    SOIL[0]        SURFACE_WATER
    :-->Conditional HRU_GROUP IS NahanniHRUs
  :Flush                 RAVEN_DEFAULT      SURFACE_WATER   VADOSE_RESERVOIR
    :-->Conditional HRU_GROUP IS NahanniHRUs
  :Split RAVEN_DEFAULT VADOSE_RESERVOIR FAST_RESERVOIR SLOW_RESERVOIR 6.5-01
    :-->Conditional HRU_GROUP IS NahanniHRUs
  :CapillaryRise         RISE_HBV           FAST_RESERVOIR  SOIL[0]
  :Percolation           PERC_CONSTANT      FAST_RESERVOIR  SLOW_RESERVOIR
    :-->Conditional HRU_GROUP IS_NOT NahanniHRUs
  :Baseflow              BASE_POWER_LAW     FAST_RESERVOIR  SURFACE_WATER
  :Baseflow              BASE_LINEAR        SLOW_RESERVOIR  SURFACE_WATER
:EndHydrologicProcesses
```

Appendix B - Automatic Calibration Parameters

Table B.1: Parameters targeted during automatic calibration and their associated acceptable range

Parameter Name	Units	Initial Value	Low	High
Adiabatic Lapse Rate	°C/km	5.1	4	6
Precipitation Lapse Rate	mm/d/m	1.02	1	2
Porosity	-	0.2	0.1	0.35
HBV Beta	-	0.7	0.5	0.8
Field Capacity	-	0.8	0.7	0.9
Maximum Percolation Rate	mm/d	2.1	1	3
Fast Reservoir - Baseflow Coefficient	1/d	0.05	0.03	0.07
Slow Reservoir - Baseflow Coefficient	1/d	0.02	0.01	0.03
Fast Reservoir - Baseflow N	-	1.2	1	2
Melt Factor (Default)	mm/d/°K	1.5	1	2
Melt Factor (Forest)	mm/d/°K	1.5	1	2
Melt Factor (Glacier)	mm/d/°K	1.5	1	2
Melt Factor (Barren)	mm/d/°K	1.8	1	2
Melt Factor (Shrubland)	mm/d/°K	2.8	2	3
Min Melt Factor (Default)	mm/d/°K	2.9	1.5	3.5
Min Melt Factor (Forest)	mm/d/°K	2.9	1.5	3.5
Min Melt Factor (Glacier)	mm/d/°K	2.9	1.5	3.5
Min Melt Factor (Barren)	mm/d/°K	2	1.7	2.3
Min Melt Factor (Shrubland)	mm/d/°K	3.5	2.7	3.8
HBV Melt Apsect Correction (Default)	-	0.4	0.3	0.5
HBV Melt Aspect Correction (Forest)	-	0.5	0.4	0.6
HBV Melt Forest Correction (Default)	-	0.45	0.3	0.5
HBV Melt Forest Correction (Forest)	-	0.3	0.2	0.4
HBV Melt Forest Correction (Glacier)	-	0.6	0.5	0.7
HBV Melt Forest Correction (Barren)	-	0.45	0.3	0.5
HBV Melt Forest Correction (Shrubland)	-	0.45	0.3	0.5